



A Modern Look at Spiropyrans: From Single Molecules to Smart Materials

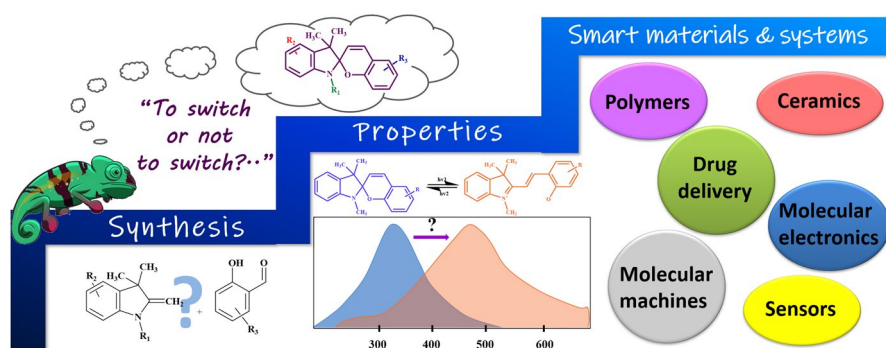
Anastasia S. Kozlenko¹ · Ilya V. Ozhogin¹ · Artem D. Pugachev¹ · Maria B. Lukyanova¹ · Islam M. El-Sewify^{1,2} · Boris S. Lukyanov¹

Received: 17 May 2022 / Accepted: 30 November 2022 / Published online: 10 January 2023
© The Author(s), under exclusive licence to Springer Nature Switzerland AG 2023

Abstract

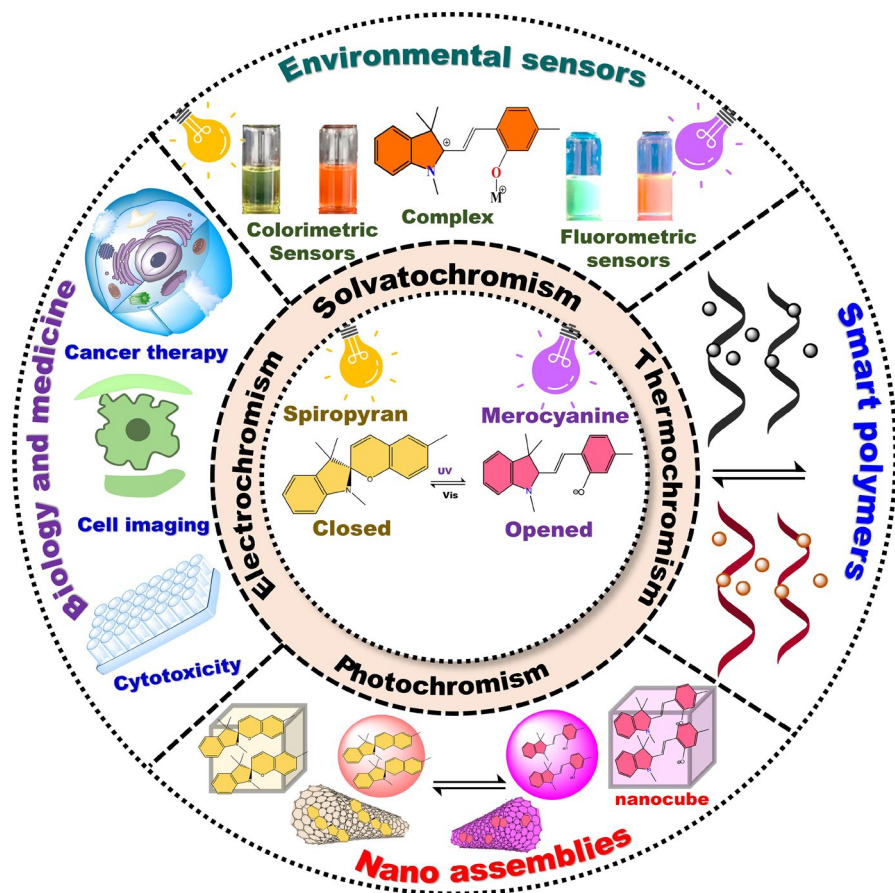
Photochromic compounds of the spiropyran family have two main isomers capable of inter-switching with UV or visible light. In the current review, we discuss recent advances in the synthesis, investigation of properties, and applications of spiropyran derivatives. Spiropyrans of the indoline series are in focus as the most promising representatives of multi-sensitive spirocyclic compounds, which can be switched by a number of external stimuli, including light, temperature, pH, presence of metal ions, and mechanical stress. Particular attention is paid to the structural features of molecules, their influence on photochromic properties, and the reactions taking place during isomerization, as the understanding of the structure–property relationships will rationalize the synthesis of compounds with predetermined characteristics. The main prospects for applications of spiropyrans in such fields as smart material production, molecular electronics and nanomachinery, sensing of environmental and biological molecules, and photopharmacology are also discussed.

Graphical Abstract



Keywords Spiropyran · Photochromism · Multi-sensitivity · Molecular switch · Smart materials · Indoline

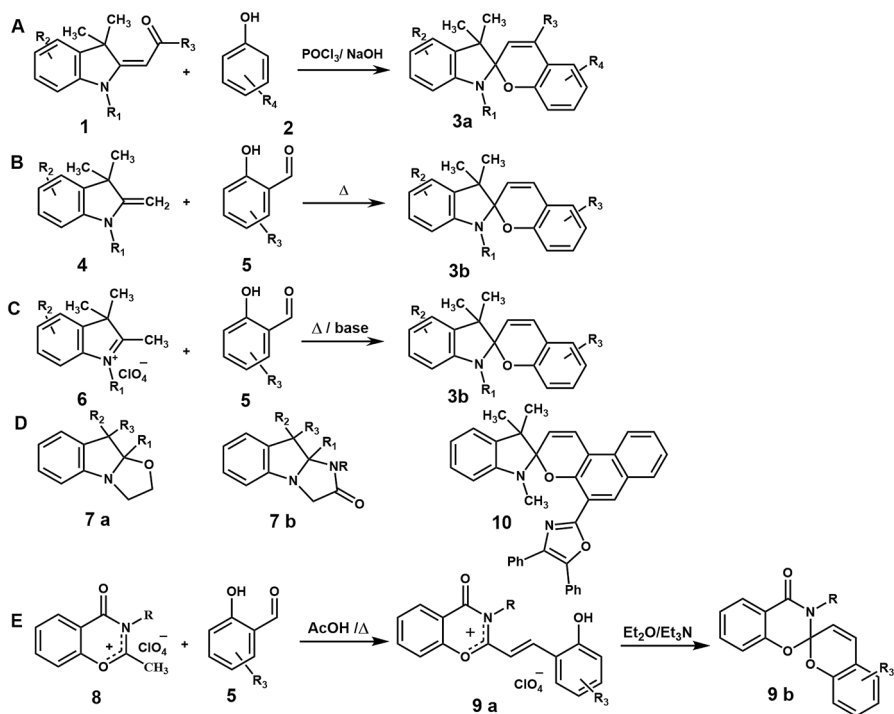
Extended author information available on the last page of the article



Scheme 1 Basic properties and application areas of spiropyrans

1 Introduction

Spiropyrans represent one of the most promising classes among the many known reversible photochromic compounds [1–3]. The attractive properties of spiropyrans include the simplicity in preparation and modification, and the ability to tune the properties via even insignificant changes in the molecular structure. Transformation of spiropyran molecules from the cyclic (SP) to the opened merocyanine (MC) form can be initiated by electromagnetic irradiation and changes in temperature, pH, redox potential, and polarity of a medium, and even by mechanical stress (Scheme 1). Moreover, the presence of many metal cations, several nucleophilic anions, and some organic species can also induce their isomerization. Thus, spiropyran-like systems meet the basic requirements for multi-functionality and sensitivity that make them promising building blocks for the creation of various dynamic materials [4]. Special requirements are put forward for the fabrication of spiropyran

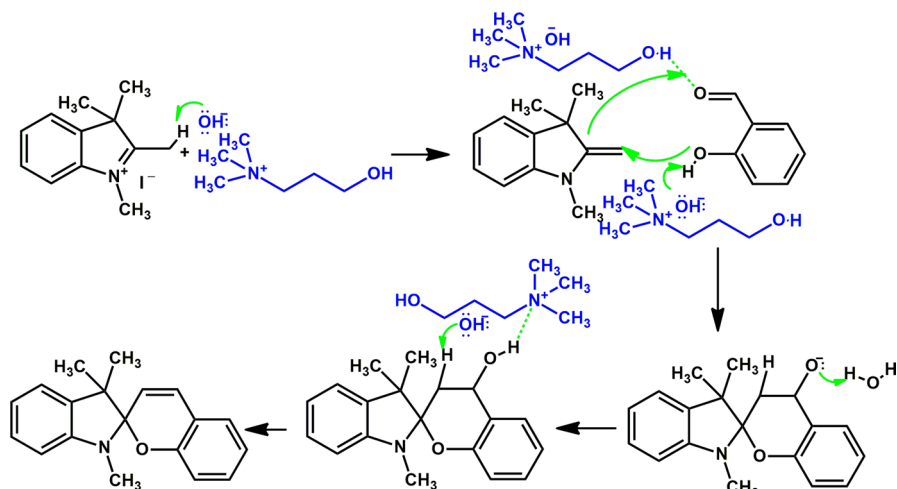


Scheme 2 Synthetic approaches and structures of some initial compounds

molecules. Depending on the applications, the suggested fragments providing the system with the necessary properties can be integrated into the structure during molecular design. In the current review, we intend to shed light on the general approaches and current trends in synthesis, the structure–property relationships, and the main prospects for application of spiroopyrans in the twenty-first century.

2 Current Trends in Synthesis

The basic techniques for the synthesis of indoline spiroopyrans **3 (a, b)** were developed in the mid-1950s and have not been significantly modified since then. The main approaches are based on the condensation of substituted (indolin-2-ylidene)ketones **1** with phenols **2** [5] or of 1,3-substituted 2-methyleneindoles **4** [6] and their salt forms **6** [7] with corresponding *o*-hydroxyaldehydes **5**. In some cases, cyclo-condensed derivatives **7 (a, b)** can be used instead of corresponding Fisher bases [8–10]. In contrast to indoline spiroopyrans, most of their analogues based on other heterocycles require a two-stage technique consisting of condensation and deprotonation stages (Scheme 2E). For example, spiroopyrans of 1,3-benzoxazin-4-one series **9b** can be obtained from 4*H*-1,3-benzoxazin-4-onium perchlorate **8** [11, 12]. The need to obtain styryl salt **9a** at the first stage arises from the instability of 3-methyl-2-methylidene-1,3-benzoxazin-4-one. There are few examples of the use of this



Scheme 3 Possible mechanism of spiropyran formation in the presence of choline hydroxide

technique for synthesis of indoline derivatives. Thus, compound **10** was obtained with intermediate isolation of the styryl salt and its further cyclization using ammonia as a base, in contrast to the commonly used triethylamine or piperidine [13, 14]. However, such a procedure is more time-consuming due to lower nucleophilicity of the methyl group in the salt compared to the methylene group of Fischer's base **4** and is rarely used.

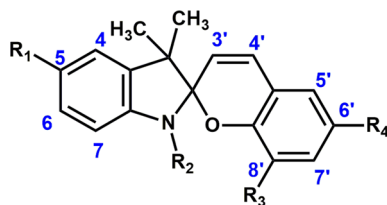
The replacement of standard bases and solvents with choline hydroxide, illustrated in Scheme 3, can be considered as an innovative alternative [15]. This approach made the synthesis more eco-friendly due to reactions passing in the aqueous medium. Moreover, the researchers noted a significant increase in the yields of reaction products in comparison with the use of other organic bases. The main reason is based on the catalytic role of choline hydroxide, which consists in increasing the water solubility of the starting aldehydes. The synthetic procedure can be modified by the use of microwave radiation, which greatly reduces the reaction times as well [16]. For instance, this method was carried out to obtain spiropyrans based on 1,2,3-trimethylindole variously substituted at position 3.

In general, the synthesis of currently known indoline spiropyrans is somehow reduced to one of the three methods described above in Scheme 2. The key improvements include minimizing the number of stages [17], introducing the active functional groups and fragments to the structure, and obtaining derivatives with a predetermined set of properties.

2.1 Derivatives Containing Active Functional Groups: Synthesis and Modification

Spiropyran bearing active functional groups are of great interest due to the possibility of using them as ready-made building blocks for further modifications that can greatly facilitate the construction of new materials or systems with an

Fig. 1 Scheme of substitution positions numbering in the structure of common indoline spiropyran



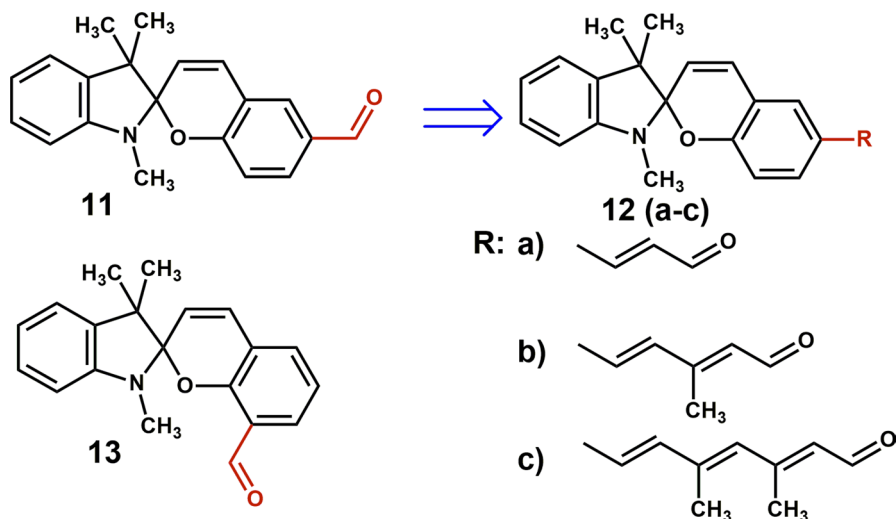
extended set of properties. Active substituents are usually introduced to one of a few positions of the target molecule as the components of corresponding aldehydes and indoles (see Scheme 2B, C). The most important positions of the indoline spiropyran molecule are substituted by “ R_n ” as shown in Fig. 1.

Recently, a series of spiropyrans with carbonyl-like substituents were described by Laptev et al. [18]. Formyl- and carboxyl-containing spiropyran derivatives are the most interesting molecules among them. Spiropyran derivatives **12(a–c)** (Scheme 4) with the aldehyde groups, which are not directly linked to the benzopyran moiety, were obtained using the carbon chain extension method [19] based on compound **11**. Spiropyrans containing formylcoumarin fragments were obtained by Nikolaeva et al. [20]. The same research group obtained a series of spirocyclic derivatives with ketovinyl and azomethine substituents using the reactivity of the formyl group of spiropyran **13** [21]. It should be noted that all of the above-discussed compounds were synthesized starting from corresponding diformylphenols.

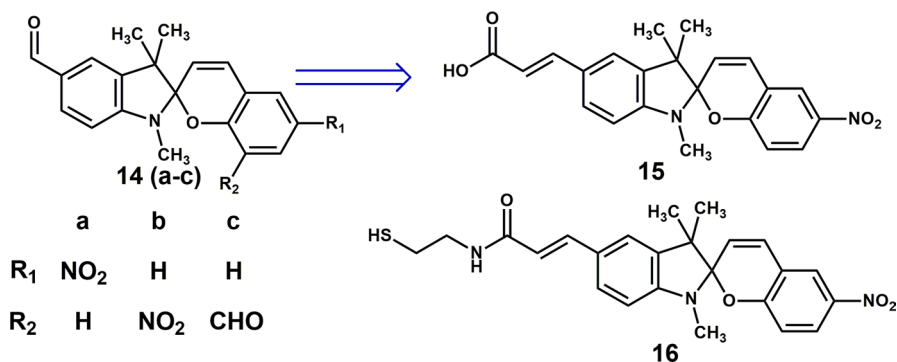
A modified Duff method for the regioselective introduction of a formyl group into position 5 was developed by Laptev et al. [22]. For these 5-formyl-substituted compounds, carbon chain extension is also possible [23] as far as several other reactions. For instance, multistage modification of compound **14** based on Horner–Emmons olefination was described (Scheme 5). It was initiated by the synthesis and isolation of the carboxyl-containing derivative **15** and followed by its interaction with *N*-(2-mercaptoethyl)-amide [24], leading to the formation of target compound **16**. It is worth noting that the one-stage Knoevenagel–Doebner olefination procedure unexpectedly resulted in a lower yield of the product.

Derivatives with fullerene [25], rhodamine [26, 27], uracil [28], and other functional molecular fragments were obtained via imine or hydrazone [29, 30] bond formation based on 5-formyl-substituted spiropyrans. Other azomethine derivatives **17–23** were synthesized from 6'-aminospiropyran [31–33], while compound **24** was obtained by a one-step procedure starting from 5-amino-substituted Fisher's base [34] (Fig. 2). Zhao et al. developed a method for the synthesis of spiropyrans on solid substrates using aminoindole as a starting material [35].

Spiropyrans bearing carboxylic groups can be synthesized by typical methods [18, 36, 37] and also provide simple ways of modification based on reactions with alcohols and amines to obtain the corresponding esters and amides [38–41]. This technique can be used to combine several fragments with different modalities in one molecule, as well as to fix spiropyran molecules on the surface of nanoparticles or polymer materials. Spiropyrans containing sulfonic acid groups are also of interest



Scheme 4 Formyl-substituted spiropyrans



Scheme 5 Modifications of spiropyrans containing reactive formyl groups

because of their increased water solubility [42–44]. Interestingly, no cases of direct spiropyran sulfonation were observed, while the nitration reaction with nitric acid occurs under mild conditions at position 5 of indole core and gives compound **25** instead of the protonated salt form as shown in Scheme 6 [45]. More often such substituents are introduced in the structure of parent indoles or aldehydes.

The linking of a hydroxy- (**26**) or a sulfo-group (**27**) to the indoline nitrogen atom is usually realized using 2-bromoethanol [46] or propanesultone [47] (Fig. 3). Hydroxy group can also be introduced to the benzopyran moiety to give compound **28** by utilization of dihydroxylated aromatic aldehydes [48–50]. Furthermore, several spiropyran containing potentially active groups [37, 50–52], such as 3-substituted derivatives [16, 53] and halogen-containing spiropyran, have become in high demand due to their applicability in cross-coupling reactions [54].

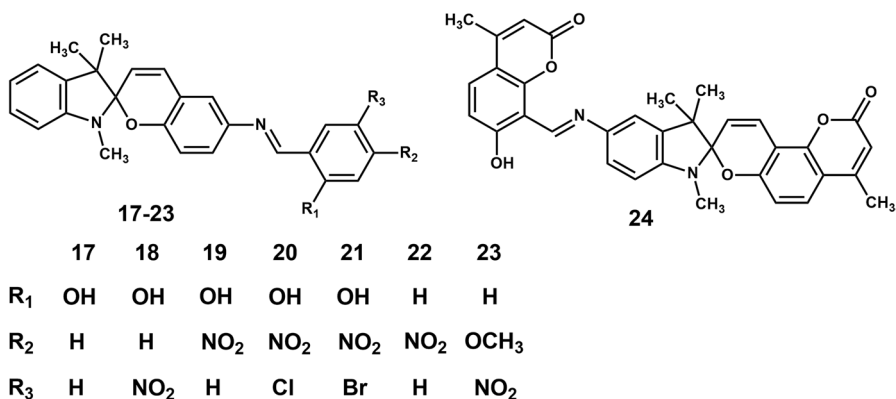
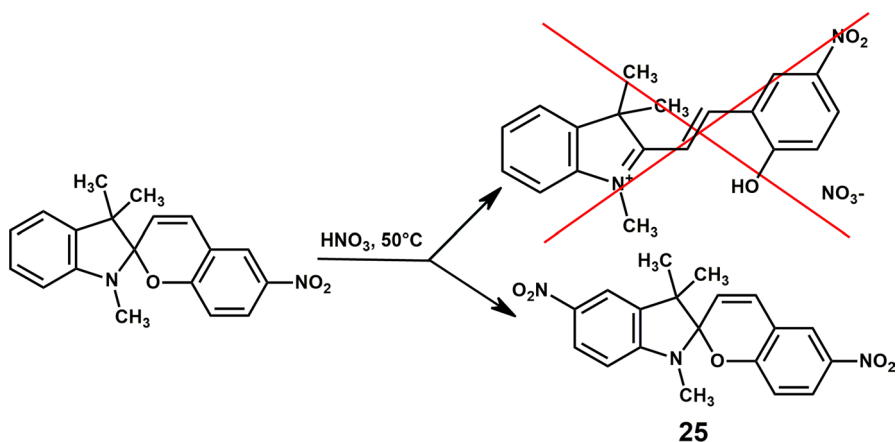


Fig. 2 Spiropyran-derived imines



Scheme 6 Direct nitration of indoline spiropyran

Finally, it should be noted that the introduction of active functional groups can lead to less evident ways of structure modification. For instance, Kleiziene et al. [9] showed the capability of spiropyran **29** bearing an acetamide fragment to isomerize with the formation of racemic benzoxazepinoindoles by boiling in alkali solutions (Fig. 3B).

2.2 Bis-Spiroyrans and Dyads

To enhance the properties of spiroyrans, novel structures containing two spirocenters (bis-spiroyrans) and fragments bringing additional significant properties (spiropyran-based photochromic dyads) were created. Bis-spiroyrans **30** and **31** with two hetarene fragments connected by common benzobipyran moiety were synthesized

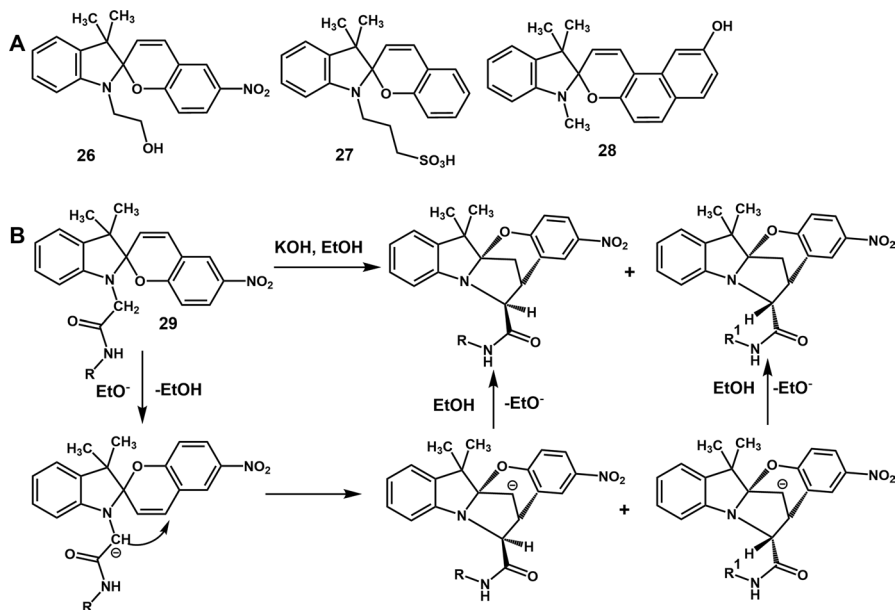


Fig. 3 Spiropyrans with active functional groups (A); the formation of racemic benzoxazepinoindoles (B)

from diformylresorcinol derivatives [51, 55–60] (Fig. 4). The condensed bis-indoline Fisher bases were used to obtain compounds **32**, **33** with common central hetarene fragments [61, 62].

Another way to realize the synthesis of bis-spiropyrans with non-conjugated photoactive centers is to link them via a single bond, as in compound **34** [63, 64], or by other functional fragments (**35**) [36, 59, 63, 65–69]. The synthesis of such derivatives often involves different variations of Sonogashira or Suzuki–Miyaura cross-coupling reactions [70, 71]. Similar methods are also used for attaching molecules to the surface of materials [72, 73] and within the concept of “click chemistry” gaining great popularity in recent years [70, 74]. A method for the preparation of bis-spiropyran **34** (Scheme 7) was proposed using the oxidative electrochemical dimerization of well-known nitro-BIPS [75–77]. A similar process was described by Natali et al. in the presence of copper perchlorate [78]. Considerable attention has been focused on photochromic dyads demonstrating strong fluorescence [79–84]. In this case, the fluorophores were added into the structure during the synthesis of initial reagents or due to cross-coupling, esterification, and other reactions with ready-made spiropyrans.

2.3 Cationic and Anionic Derivatives

The first representatives of cationic spiropyrans were described by Kawanishi et al. [85] in a study dedicated to the effects of substituents on the spectral and kinetic

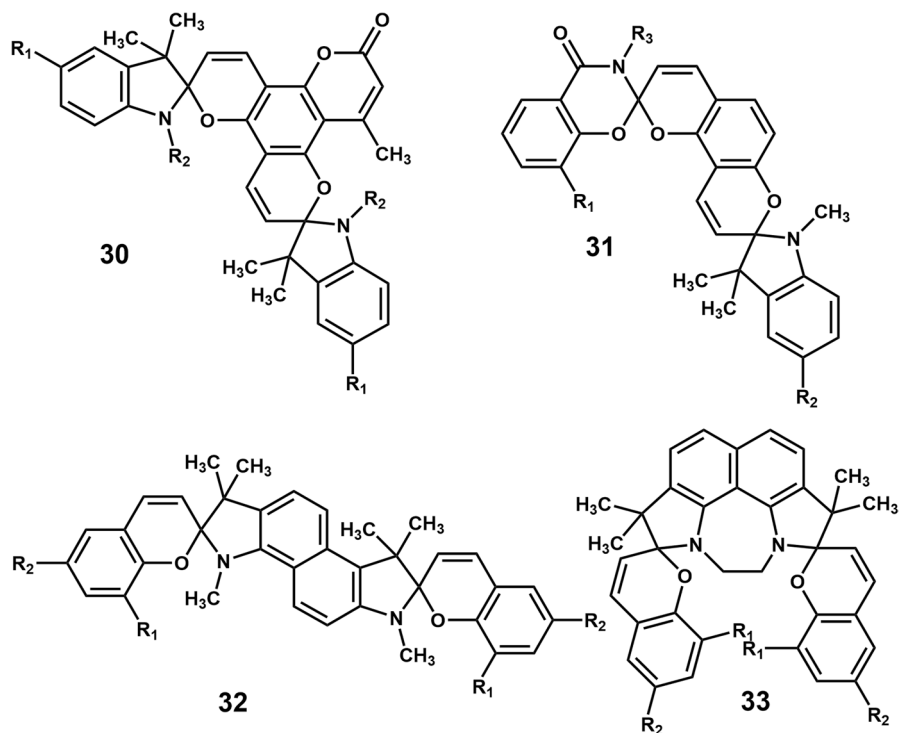


Fig. 4 Representatives of bis-spiropyrans with different types of fused fragments

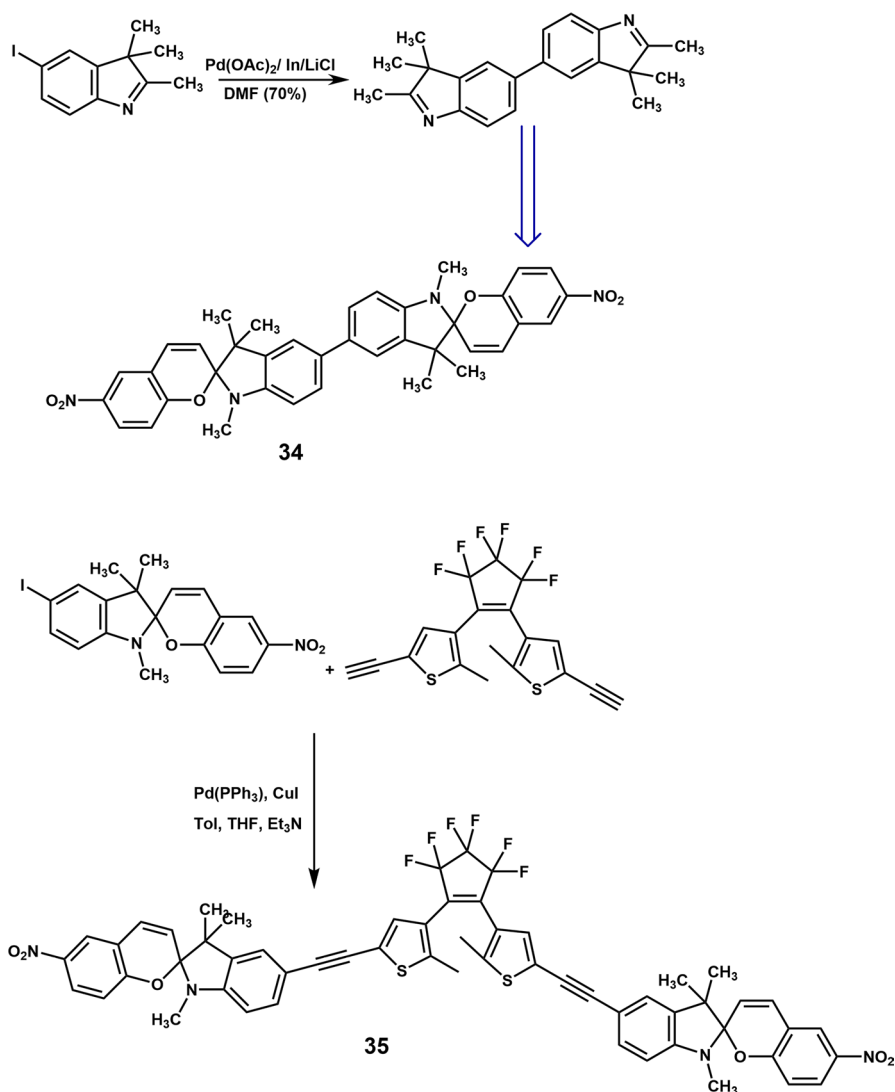
properties. The cationic fragment was introduced in the structure of **36** via the intercalation of triethylamine to the C–Cl bond to form salt **37** (Scheme 8). A range of cationic spiropyrans **38–41** was obtained by a typical technique from corresponding aldehydes [86–88]. The cationic fragment of compound **39** was added into the structure during Fischer base synthesis [89], while compound **41** was obtained from different aminospiropyrans and pyrilium salts [90].

Bérnard et al. proposed the synthesis of pyridinium-type derivatives **43** by methylation of spiropyran **42** as shown in Scheme 9 [91]. Similar compounds [92–94] including cationic bis-spiropyran **44** [69] have been described. Afterwards, compound **45** was bonded with polyphosphate chains to produce compound **46** by the aldehyde fragment exchange [95], and the condensation reaction was reversible [96].

The condensation of aromatic *o*-hydroxydialdehydes with two equivalents of indolium perchlorate led to spiropyrans containing conjugated cationic *3H*-indolium fragments **47** and **48** (Scheme 10) [97–106].

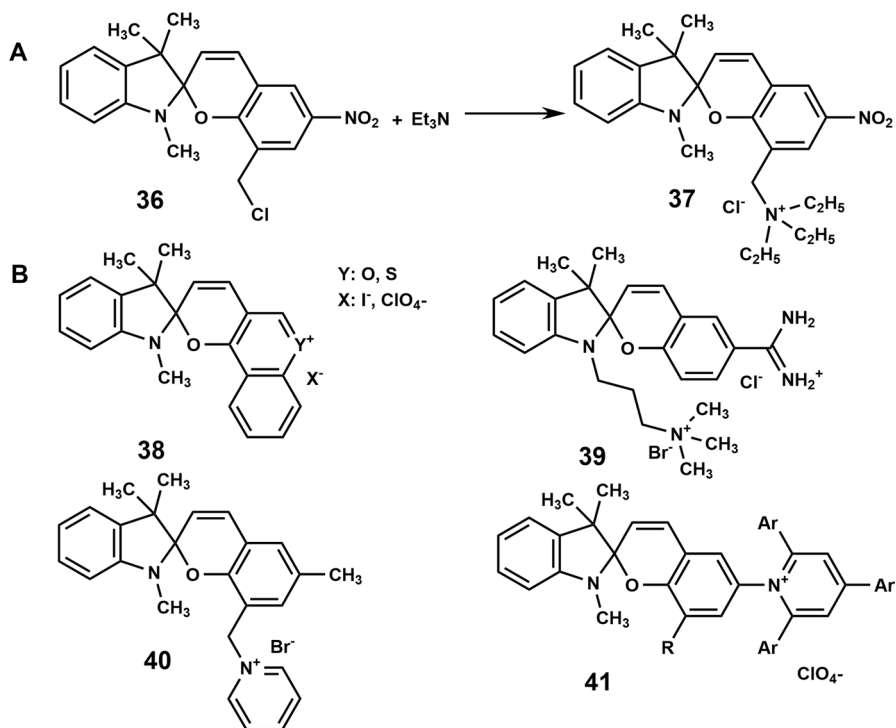
Anionic derivatives can be produced by the interaction between sulfo- [107, 108] and carboxy-substituted spiropyrans [109] with alkali solutions [42, 110]. Most of them demonstrate increased solubility in water and negative photochromic properties.

Thus, the strategy for the synthesis of spiropyrans is always based on molecular design principles, taking into account the desired properties of the target compound. If



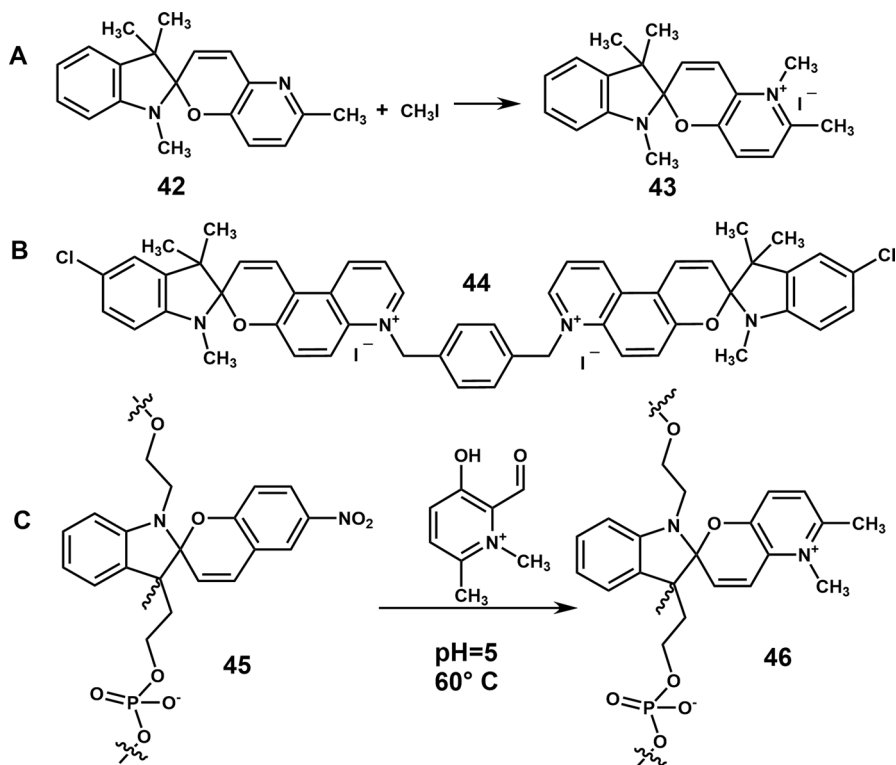
Scheme 7 Bis-spiropyrans with separate indoline moieties

some strict requirements for the properties of compounds are put forward (longer MC lifetime, absorption maxima position, etc.) general patterns of structure–property correlations can be used (see Sect. 2 for more detail). However, it should be noted that such property prediction methods are not sufficiently accurate. To access the spiropyran-containing materials, it is necessary to understand what reactive substituents spiropyran should contain in its structure for further modifications and to introduce them into the molecules of initial derivatives of indoline or another heterocycle and hydroxyaromatic aldehydes **5**. At the next stage, an appropriate synthesis method must be chosen



Scheme 8 Cationic spiropyrans synthesis (A) and representatives (B)

(Scheme 2) to ensure maximum yields of target compounds. Method **B** from Scheme 2 is usually suitable for most spiropyrans containing ordinary substituents (methoxy-, nitro-, carboxy group, etc.). To obtain salt spiropyrans **47**, **48** with a conjugated cationic fragment, it is necessary to use method **C**. In other cases, everything depends on the characteristics of the reaction and the properties of the final product. Sometimes it becomes impossible to modify the structure of spirocyclic compounds by chemical reactions under convenient conditions due to their susceptibility to hydrolysis and degradation upon heating, which requires the use of special media or ultrasound instead of heating. However, in some cases the presence of reactive substituents makes it possible to modify spiropyrans and obtain various molecular dyads containing, for example, fluorescent moiety, another photochromic center (compound **35**), or chelating fragment. Undoubtedly, an increase in the structural diversity of spirocyclic compounds is the basis for imparting new and unique properties to them, allowing the search for new applications for this class of organic photochromes and creating useful smart materials.

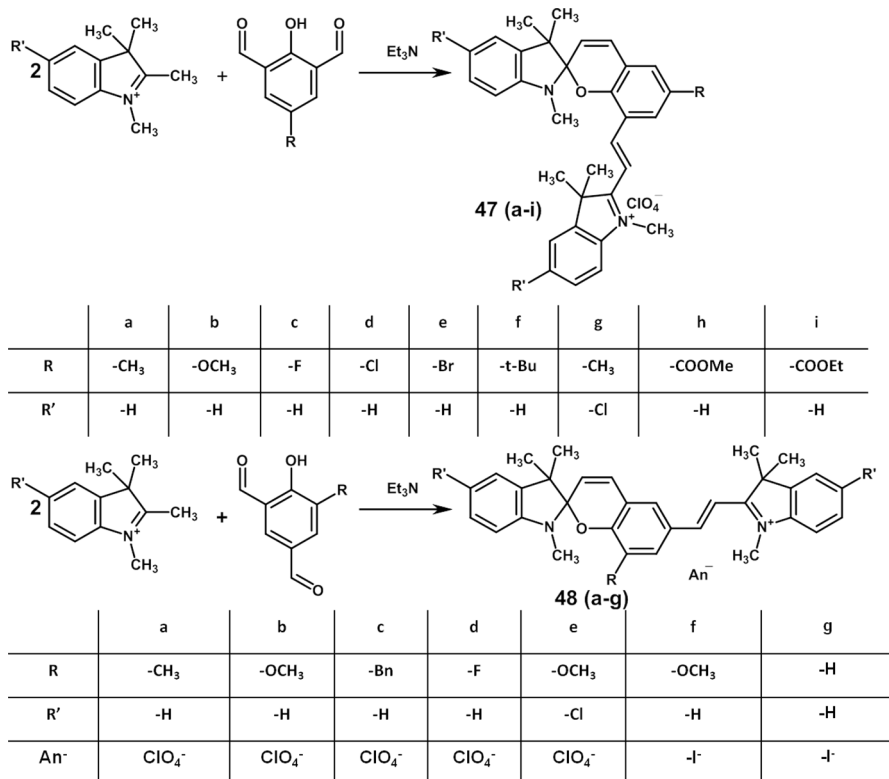


Scheme 9 Formation of cationic spiropyran by direct methylation (A), cationic bis-spiropyran structure (B) and process of aldehyde fragment exchange (C)

3 Variety of Spiropyran Properties

3.1 The Mechanism of Spiropyran Ring Opening-Closure

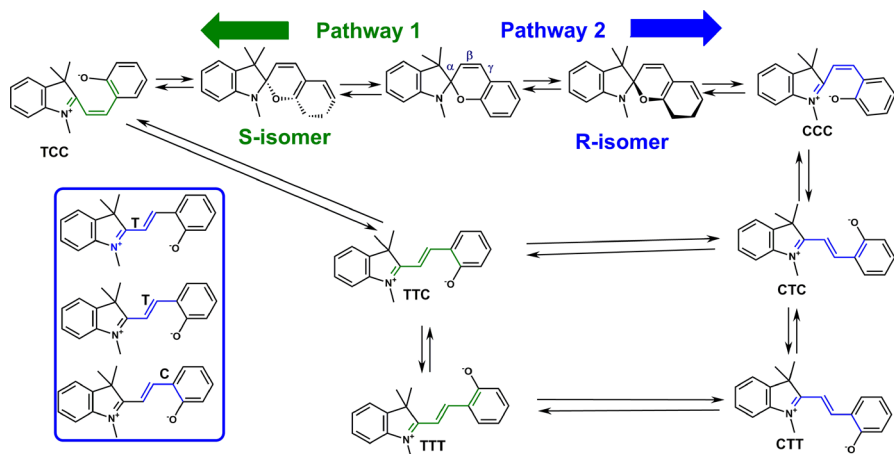
As mentioned above, the main advantage of spiropyrans is their multi-sensitivity. The transformation between spirocyclic (SP) and several merocyanine (MC) forms can be initiated by many factors. The variety of triggers was comprehensively discussed in a recent review by Kortekaas and Browne [111]. Light-induced isomerization was firstly described by Hirshberg and Fischer in 1952 [112]. Later, the ability to isomerize upon heating, changing the solvent [113], and under the influence of many other factors, which will be discussed below, was postulated. The variation in spiropyran optical properties in all these cases is owing to the changes in the molecular structure. According to the classical theory of color, the bathochromic shift of the MC form absorption wavelength in comparison with the SP is caused by the increase in the conjugation chain length in the molecule [114, 115]. Investigation of the isomerization process is still vital for predicting and modeling the properties of the spiropyran system.



Scheme 10 Synthesis of spiropyrans containing conjugated 3H-indolium fragment

According to modern ideas, several isomeric forms can be distinguished depending on the geometric configuration of spirocyclic fragment bonds involved in the isomerization process, as shown in Scheme 11. The structure of various isomers was confirmed by X-ray diffraction data or using a tandem of experimental and theoretical methods [116–120]. Under ambient conditions, most spiropyrans exist in their SP form in both solid and solution. However, several examples are known when the MC form is fully or partially stabilized [54, 102, 121–123]. In the latter case, compounds can demonstrate both positive and negative photochromism and, thus, are of particular interest [106, 122, 123]. Such systems are called “photochromic balances.” Their peculiarity lies in the fact that the type of exhibited photochromism can change under irradiation with light of different wavelengths. This circumstance enables the realization of a bipolar absorption switch with three states.

The ring-opening reaction can be induced by UV [112] and X-ray irradiation [124] or electron bombardment [125]. In most cases, the isomerization of spiropyrans proceeds through the singlet excited states in the same way with 2*H*-chromene molecules. Therefore, it is often utilized to simulate the



Scheme 11 Possible pathways of spiropyran isomerization

opening-closure process of spirocyclic compounds [126–128]. Exceptions include some nitro-substituted derivatives (**49–51** in Fig. 5) with preferable triplet excited states [129–131]. However, they are exceedingly short-lived due to effective quenching in an oxygen atmosphere.

The mechanism of the pyran moiety opening is not completely investigated because of the individual features for each compound. Studies of spiropyran isomerization reaction have been carried out in greater detail using quantum-chemical simulations [132–144], 2D electron spectroscopy [120], and super-resolution fluorescence microscopy [145]. Isomerization of spiropyrans can be considered as a process that occurs in the ground singlet state S_0 with the overcoming of a certain activation barrier [132], with vertical excitation to one of the excited states (S_1 , S_2 , and S_3) [133], or at a conical intersection of potential energy surfaces (PESs) [134, 135].

In general, the process of spiropyran isomerization begins with a heterolytic cleavage of the $C_{\text{spiro}}-O$ bond followed by changes in the valence angles of the bonds as highlighted in Scheme 11. In some recent studies, the length of the $C_{\text{spiro}}-O$ bond was considered as an indicator of its strength [133, 136, 137, 146]. Also, the bond length alteration parameter is used to describe the degree of electron density delocalization in the MC form [130, 138]. Depending on the degree

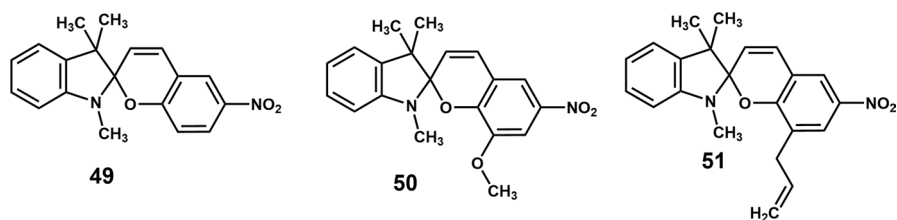


Fig. 5 Spiropyrans with preferable triplet excited states

of electron density delocalization, the MC structure can be represented as a zwitterionic or quinoidal form (Fig. 6A). Most often, it is closer to the second option, despite the presence of centers of positive and negative charge localization [139] (Fig. 6B).

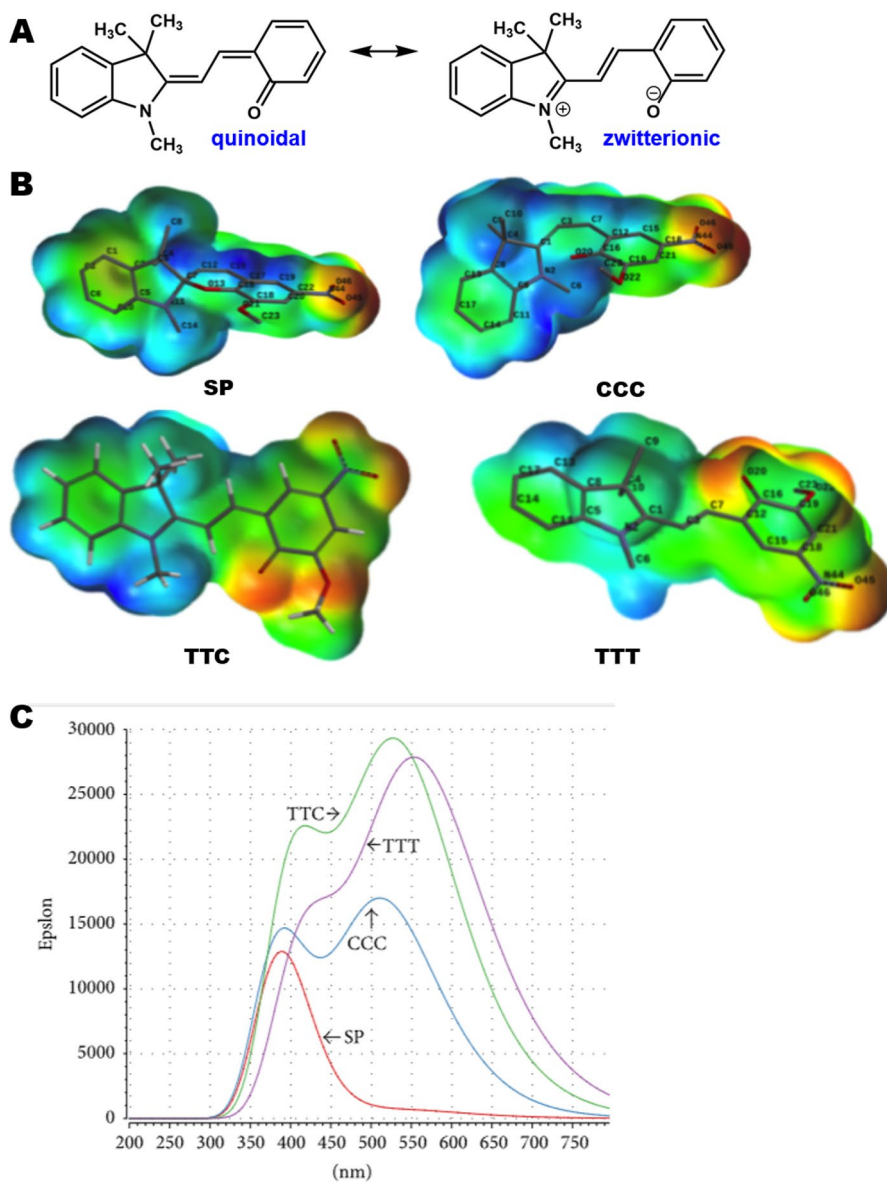


Fig. 6 Quinoidal and zwitterionic representation of MC (A), changes in ESP distribution for different isomeric forms (B), and calculated positions of different isomers absorption maxima (C). [139] Adapted from Ref.

Liu et al. [140, 141] showed that the energy of the system gradually increases with an increase in the length of the $C_{\text{spiro}}\text{-O}$ bond in the range of about 1.7–2.2 Å, approaching the energy of the $\pi \rightarrow \pi^*$ transition corresponding to the SP^* state. This is followed by a transition to the state $\pi \rightarrow \sigma^*$ of the $C_{\text{spiro}}\text{-O}$ bond, in which the configuration of other bonds around the C_{spiro} atom is flattened (the $sp^3 \rightarrow sp^2$ transition), and the subsequent breaking of the $C_{\text{spiro}}\text{-O}$ bond with active rotation along bond α leading to the MC. In this case, the presence of a previously unrecorded movement of hydrogen out-of-plane of the molecule (HOOP) was noted. The authors assumed that this movement was the real driving force of further isomerization. Similar results were obtained in several subsequent studies [142–144]. More recently, experimental evidence of flattened MC existence in the krypton matrix at 15 K was obtained by Nunes et al. [147]. Thus, despite the rather extensive amount of accumulated knowledge, the subtle effects of the spiro-pyran isomerization process are still largely hidden from researchers.

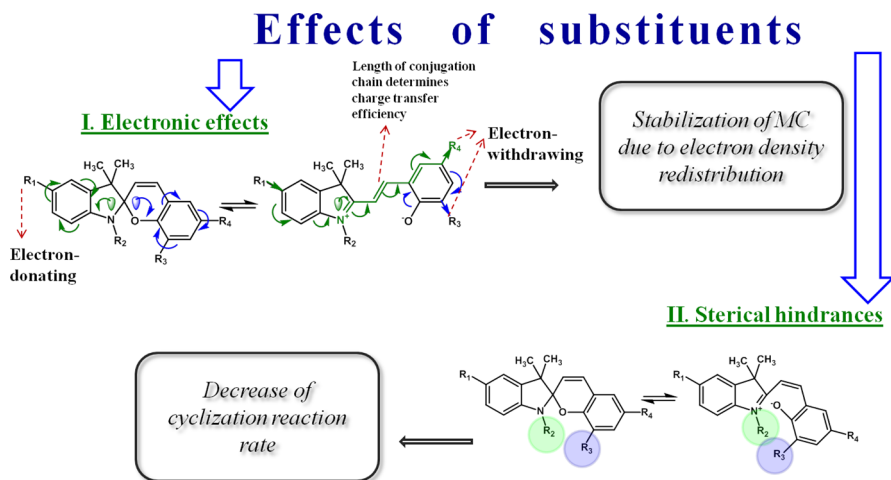
The ring-opening can be carried out by one of the two pathways depending on the spatial configuration of the initial molecule [132, 148, 149] (Scheme 11). Since all possible isomers are related to each other, photoisomerization in some cases can lead to the racemization of the compound. Among the possible isomers of the merocyanines, the most stable structures are transoid with respect to the central β -bond *E*-forms (CTC, TTC, and TTT). If the intermediate cisoid *Z*-forms are compared, then it is worth highlighting the CCC and TCT [130, 132, 145, 150, 151]. Interesting insight on the stability of different forms was recently offered by Menzonatto et al. [152]. The authors carefully investigated intramolecular non-covalent interactions in several MC isomers and postulated that steric hindrances play the key role in destabilization of CXX-like structures. This effect could be the main one causing the impossibility of experimental detection of the CTC isomer. At the same time, the TTC-isomer is additionally stabilized by the $C(3')\text{-H}\cdots\text{O}$ hydrogen bond with the phenolic oxygen atom; however, the TTT isomer can also make a significant contribution in some cases [101, 119, 120, 145, 151, 153]. The difference in absorption maxima wavelengths of TTC and TTT is usually about 50–60 nm (Fig. 6C) [139, 145], which makes it challenging to isolate the individual components of the absorption spectrum corresponding to each of the forms.

In most experimental studies, the UV-light sources are generally used to carry out photoinduced transformations of spiro-pyrans. However, of special practical interest is the possibility of using near-infrared (NIR) irradiation based on two-photon absorption phenomena [153, 154]. The variations in energy and sequence of the pump-pulse can also allow additional tuning of the system characteristics due to the prevalence of one or another isomeric form and thus prevent photodegradation of compound [128, 149, 155].

3.2 Photochromic Properties

3.2.1 The Effects of Molecular Structure on Photochromic Properties

For many years, 6-nitroBIPS **49** has been a standard for photochromic behavior evaluation of spiro-pyrans. According to the data obtained by Song et al. [156], spiro-pyran **49** demonstrates absorption bands with maxima at 336 nm ($\epsilon = 0.8 \times 10^4 \text{ M}^{-1} \text{ cm}^{-1}$)



Scheme 12 Determinants of MC stability

for SP and 555 nm ($\epsilon = 3.5 \times 10^4 \text{ M}^{-1} \text{ cm}^{-1}$) for MC form in acetonitrile solution at room temperature. One of the most prominent advantages of spiropyrans is the possibility to fine-tune their characteristics by varying the substituents. Even a small structural change can lead to a strong variation in dark reaction rate and mutual stability of SP and MC forms [157–159]. The main factors affecting the MC lifetime are (i) electronic effects of substituents and (ii) the possibility of a steric hindrance as shown in Scheme 12.

Generally, a lowering of the ring-opening energy barrier is promoted by electron-donating substituents in the indoline and electron-withdrawing ones in the 2*H*-chromene moiety [133, 154, 155, 159]. The compensation of corresponding partial charges in MC form is considered as the main cause, as shown in Scheme 12. The most tangible impacts come from the groups located in *para*-positions towards the charge localized centers, i.e. in positions 5 and 6' (see Scheme 12). The proportional dependence of the SP and MC mutual stability on the nature of substituent electronic effects has been confirmed by both experimental [37, 160–162] and theoretical data [133, 163]. The 8'-substituted derivatives are usually characterized by an increase in the MC stability, especially in the case of acceptor substituents [163]. In addition to the optical characteristics of spiropyrans, the electronic contribution of the substituents can affect their sensing (e.g. selectivity or sensitivity) [164, 165] and mechanochromic properties [166].

The lifetime can be considered as a stability criterion of photoinduced forms. Thus, the electron-withdrawing effect of substituents in position 5 leads to a decrease in MC lifetime [26, 159, 167, 168], and at the same time an increase in the photocoloration rate [122]. The hindered rotation around the β -bond plays a key role together with additional MC stabilization due to strong conjugation. The significance of these factors has been confirmed by the investigation of 1',3,3',4'-tetrahydrospiro[chromene-2,2'-indoles] [169]. Conjugated fragments significantly increase the MC lifetime by enhancing the degree of electron density

delocalization. The range of thiophene-containing spiropyrans **52–55**, derivatives with conjugated neutral **56** [167, 170], and cationic heterocyclic fragments **47, 48** [100, 102] were used as models for this effect (Fig. 7). It was shown that the addition of each new thiophene unit to the structure **53** doubles the lifetime of the photoinduced form (from 293 to 1100 s). At the same time, the second spiro moiety in **55** slightly increases the lifetime due to the competition of two quinoid parts of the MC form for electron density [71]. In addition, the presence of additional heteroatoms allows for a reduction of the photoinduced transformation reaction barrier because of the lower-lying molecular orbital contribution [167]. A more obvious effect of the introduction of electron-withdrawing substituents together with elongation of the conjugation chain is an increase in the wavelength of the absorption maximum of compounds in both the SP and the MC form [100, 102, 168]. In the case of retinal-like substituted spiropyrans **12 (b, c)**, this is probably not observed due to the hyperconjugation effect of methyl groups. This is one of the marvelous examples of spiropyran sensitivity to the substituent electronic effects.

Substituents at the indoline nitrogen atom in most cases have no significant influence on the relative stability of forms, unlike those located in the hetarene moiety aromatic ring [167, 171]. However, bulky neopentyl substituent may be an exception, leading to the stabilization of the MC isomer [172]. The lifetime of the MC in the case of compounds **58c** and **59c** increases 2.4–2.6-fold in comparison with

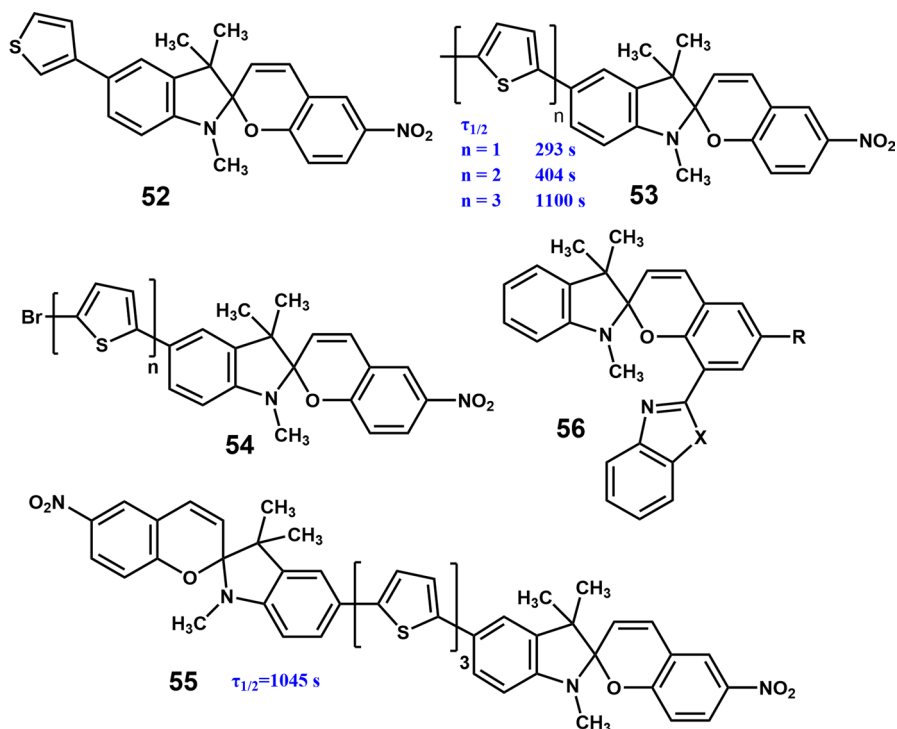


Fig. 7 Spiropyrans containing thiophene and other heterocyclic fragments

N–Me-substituted analogues (Table 1). At the same time, a decrease in the photoinduced MC stability for N–Bn spiropyrans possibly indicates the significance of the contribution of the methyl group rotational degrees of freedom to the steric hindrance effect. At the same time, benzyl substituent does not induce any important changes due to the rigidity and planar configuration, in contrast to the neopentyl with its movable methyl groups. Recently detailed theoretical insight on the N-bound substituent effect of the stability of different MCs has been reported using non-covalent interactions analysis (NCI) [152]. Zanoni et al. [158] described another interesting effect. The rate constants of thermal relaxation of compounds **60** (**a**, **b**) differing by just one methylene group in the substituent at the indoline nitrogen atom are 5.9×10^{-3} and $8.3 \times 10^{-3} \text{ s}^{-1}$, respectively, at 298 K. The activation energy of this process is ca. 25% lower for compound **60a** compared with **60b**. The authors associate this effect with the possibility of intramolecular π – π interactions between thiophene and 2*H*-chromene moieties due to the increased degrees of freedom in the substituent (Fig. 8). The replacement of the naphthalene fragment with quinoline and benzofuran in structures **57**–**59** resulted in the reinforcement of the photochromic properties owing to the lone electron pair density contribution of heteroatoms to the aromatic system (Fig. 8).

The negative photochromism phenomenon can be observed in the case of the greater thermodynamical stability of the MC form. Such compounds are much less common than those characterized by positive photochromism. Generally, negatively photochromic spiropyrans contain two electron-withdrawing substituents in the benzopyran moiety. The most widely known are the dinitro-BIPS **61a** [119] and bromonitro-BIPS **62** (Fig. 9) [163]. Interestingly, compound **61b** with a similar structure has no similar properties [173].

The MC forms of spiropyrans **48(b, d)**, **61a**, **62**, and **63**–**66** have been detected in the crystalline state [174, 175] (Fig. 10). They are usually stabilized by hydrogen bonds with solvent (**48b**, **62**, **65**) or with another MC molecule (compound **66**). X-ray analysis data revealed that some merocyanines had a TTT configuration, while the TTC form had long been considered the most stable.

Thus, substituents in both parts of the molecule have a significant effect on the lifetime of the photoinduced isomer and, in general, on the mutual stability of the

Table 1 Spectrokinetic characteristics of the MC forms of spiropyrans with annulated naphthalene, quinoline, and benzofuran fragments in ethanol

No.	λ_{max} (MC), nm	$\tau_{1/2}$ (MC), s
57a	573	0.7
57b	569	0.6
57c	578	0.5
58a	530, 562	0.7
58b	530, 565	0.3
58c	535, 569	1.7
59a	578, 586	3.1
59b	482, 596	0.69
59c	480, 600	8.1

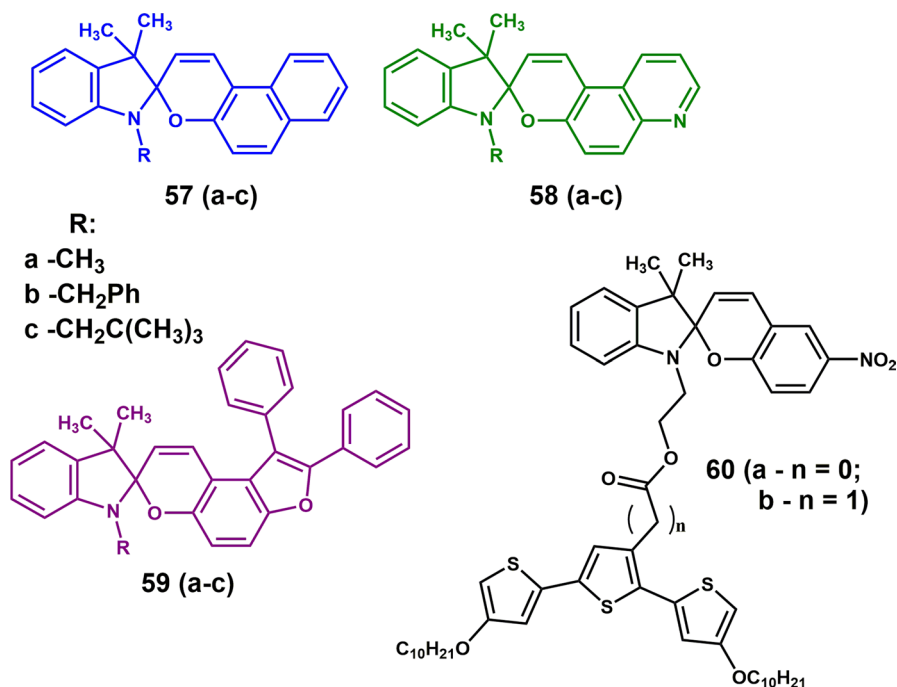


Fig. 8 Spiroyrans containing annulated naphthalene (**57**), quinoline (**58**), benzofuran fragments (**59**), and linked trithiophene moiety (**60**)

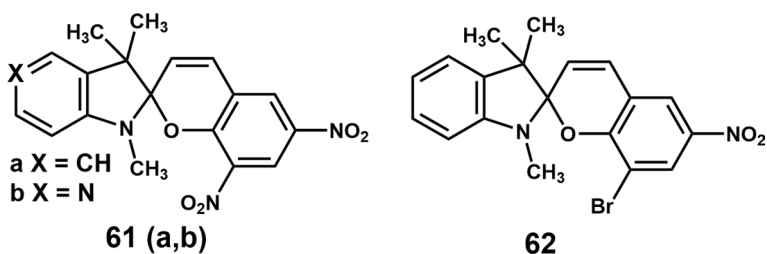
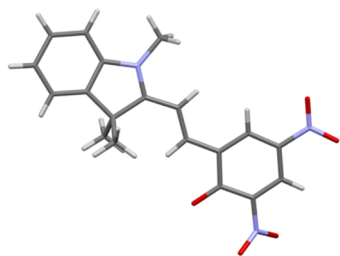
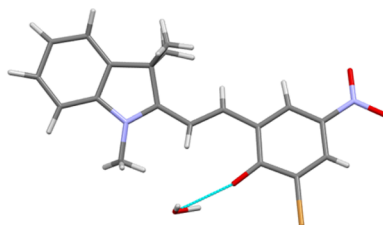


Fig. 9 Chemical structures of dinitro-BIPS, bromo-nitro-BIPS, and related compound

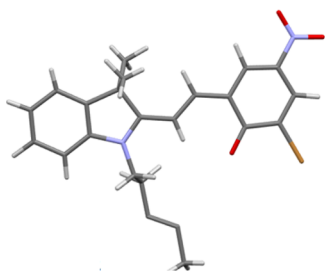
forms. At the same time, the dependence between substituents' electronic effects and the position of absorption maxima has a more complex nature. The general tendency is that electron-donating substituents in the indoline or *2H*-chromene moieties induce a bathochromic shift of the absorption maxima, while the presence of electron-withdrawing groups leads to a hypsochromic shift of the absorption band maxima of both SP and MC forms [2, 162]. In most cases, substituents in the indoline moiety have a less significant influence on the position of the absorption band than substituents in the *2H*-chromene fragment [170]. The exception is the nitro-group due to appearance of an additional charge-transfer band [162, 177].



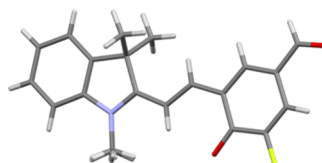
61a (BAPNAH)



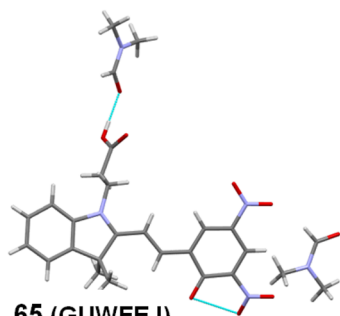
62 (BETGEM)



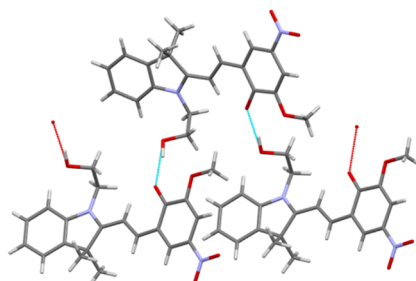
63 (FAFPOR)



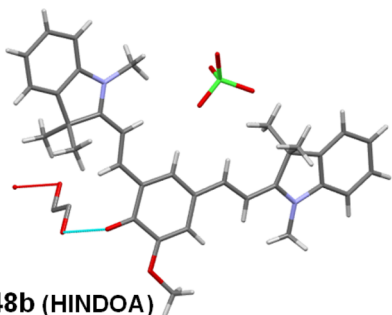
64 (TAGMIB)



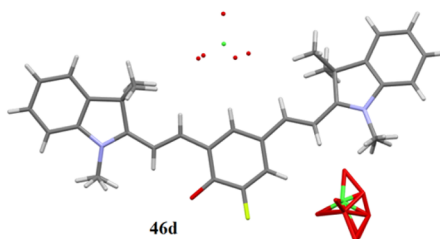
65 (GUWFEJ)



66 (YURHAV)

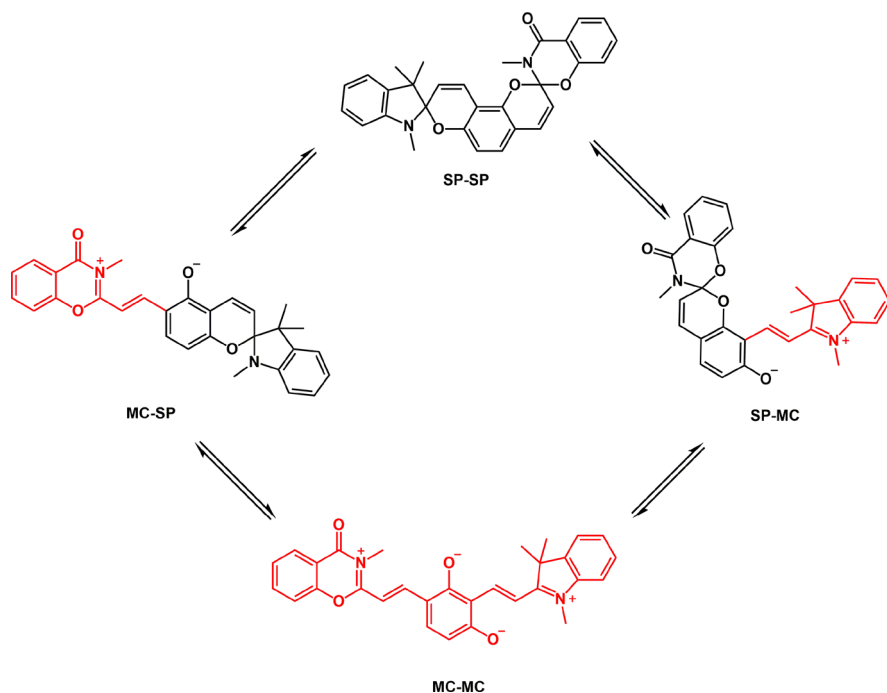


48b (HINDOA)



48d (TAFXIL)

Fig. 10 Structures of MC forms detected in solid state (performed using materials of CCDC [176]; the database identifiers of structures are provided in parentheses)

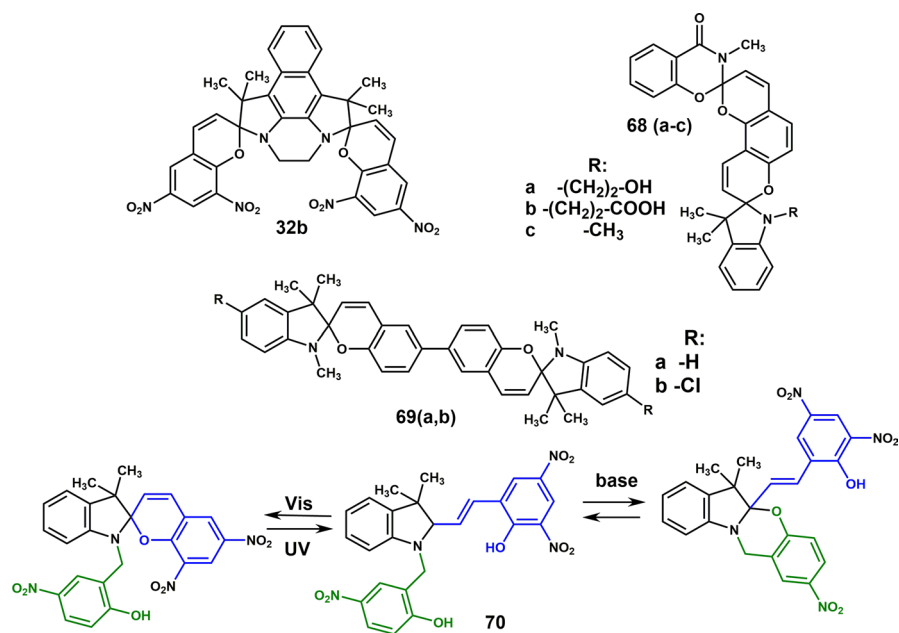


Scheme 13 Possible forms of unsymmetrical bis-spiropyran

3.2.2 Properties of Spiropyran-Based Multi-State Molecular Switches

Bis-spiroyrans have two photochromic centers in the structure; therefore, they can act as at least three-state molecular switches turning out between SP-SP, SP-MC, and MC-MC forms (Scheme 13). Most bis-spiroyrans can be opened only once, as their MC-SP or SP-MC forms are more stable than the MC-MC [58]. The first representative for which a stable MC-MC form was detected is compound **68c** (Scheme 14) [56, 178]. Usually, the MC-MC form is more convenient for derivatives with non-condensed benzopyran moieties as in compound **69** [179]. In this case, the bathochromic shift of MC-MC isomers ($\lambda_{\max} > 610$ nm) relative to the MC-SP forms (for example, for **32b** $\lambda_{\max} \approx 550$ nm [61]) was observed. The increase in the MC form stability is facilitated by the introduction of electron-withdrawing substituents into the benzopyran [59, 62] and electron-donating into the hetarene moiety [55, 59]. The presence of two strong acceptors in the 2*H*-chromene moiety of **32b** leads to negative photochromism [61, 62] as previously described in dinitro-BIPS **60**.

To stabilize the SP-MC isomer, various substituents were added to the indoline nitrogen atom of compounds **68(a–c)** [180]. The introduction of a hydroxyethyl group in compound **68a** increased the lifetime of the SP-MC fourfold in comparison with compound **68c**. In the case of compound **68b**, two parallel processes with different rates were observed under dark discoloration, which was assigned as cyclization of indoline or benzoxazine moiety. According to the simulation results, the

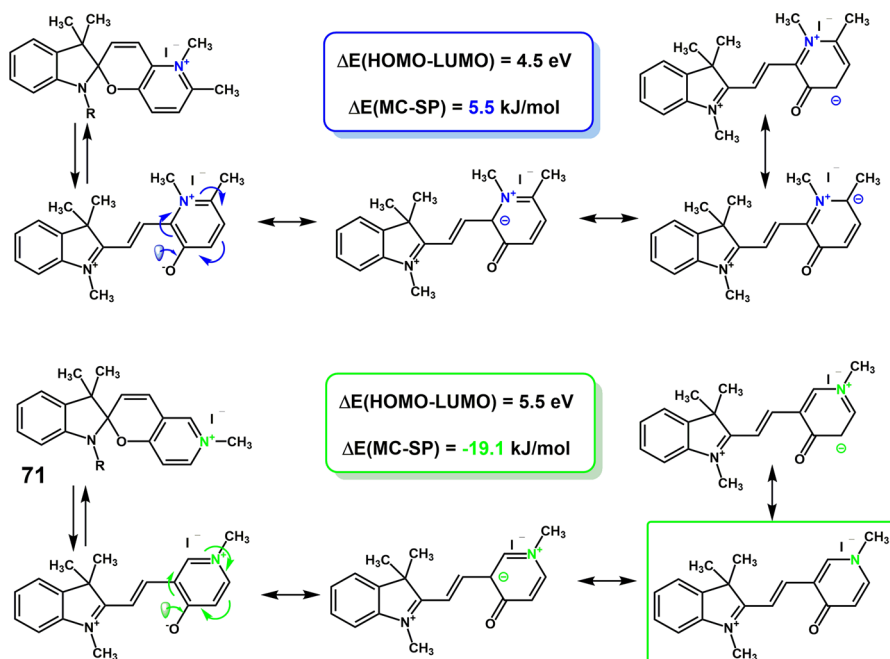


Scheme 14 Various types of bis-spiropyrans and three-state molecular switch **70**

carboxyethyl group of the indoline fragment is not involved in the process. Therefore, this phenomenon may be attributed to various energies of $\text{C}_{\text{spiro}}\text{-O}$ bonds, which was indirectly confirmed by XRD data of bond length in **68c** (1.427(3) Å for indoline and 1.472(3) Å for benzoxazine fragment) [180]. The introduction of electron-donating groups in the benzoxazinone fragment of relative bis-spiropyrans **31** [58] and bulky benzyl substituent to the oxazinic nitrogen atom also led to the stabilization of the once-opened SP-MC isomers. The other interesting three-state molecular switch is spiropyran **70**, described by Liu et al. [181].

3.2.3 Peculiarities of Cationic Derivatives

The fused cationic heterocyclic fragment in the benzopyran moiety leads to stabilization of the MC form. By comparison with neutral analogies, the efficiency of oxygen lone pair charge compensation increases in the presence of positively charged nitrogen [91]. The high MC stabilization in the case of the nitrogen atom location in position 6' is due to the more efficient overlapping of the molecular orbitals in the pyranopyridinium fragment [182]. For example, compound **71** (Scheme 15) exhibits negative photochromic properties. The addition of a bulky isopropyl group to the indoline nitrogen atom increases the thermal discoloration reaction rate, unlike the non-cationic *N*-neopentyl derivative **58c** [92]. This effect can be caused by the absence of active rotation, which is characteristic of the methyl group near the $\text{C}_{\text{spiro}}\text{-O}$ bond.



Scheme 15 Electronic density distribution in the cationic spiropyran molecules

The possibility of tuning the properties by changing the anionic part is another important advantage of cationic spiropyrans. For example, the spiropyran derivative with $[\text{PtF}_6]^-$ was used to control the SP:MC ratio in crystals by changing its growth conditions or irradiation. The iodide-containing compound **71** forms crystals solely in MC form. The same organic fragment with $[\text{PtF}_6]^-$ anion tends to destabilize MC due to the weakness of interionic interactions compared with MC-I [182]. The prospects for obtaining hybrid materials with both active cationic and anionic counterparts are especially interesting; however, it is worth noting the anionic effect. For instance, ionic liquids were obtained by combining cationic spiropyrans with $\text{N}(\text{SO}_2\text{CF}_3)_2^-$ and $\text{N}(\text{SO}_2\text{F})_2^-$ [183]. The polyoxometalate anions led to multi-photochromic systems [184] and the introduction of $[\text{CrMn}(\text{C}_2\text{O}_4)_3]^{3-}$ to molecular photomagnets [185].

Spiropyrans containing a conjugated cationic *3H*-indolium fragment **47** (a–h) and **48** (a–g) show interesting characteristics [17, 97–103]. Their MC forms are close to a cyanine dye family structure and properties. Elongation of the conjugation chain compared with the most common non-cationic derivatives leads to bathochromic shifts of the absorption spectra maxima of both SP and MC isomers [102, 186] and the molar extinction coefficient from $0.5 \times 10^{-4} \text{ M}^{-1} \text{ cm}^{-1}$ (**72c**) to $1.47 \times 10^{-4} \text{ M}^{-1} \text{ cm}^{-1}$ (**47c**) [106]. The addition of cationic moiety can also induce a substantial increase in the MC lifetimes (more than 75 min in the case of **47** (h, i)) [102]. In all known cases, introduction of the cationic substituent leads to 75–115 nm absorption maxima wavelength growth in comparison with compounds

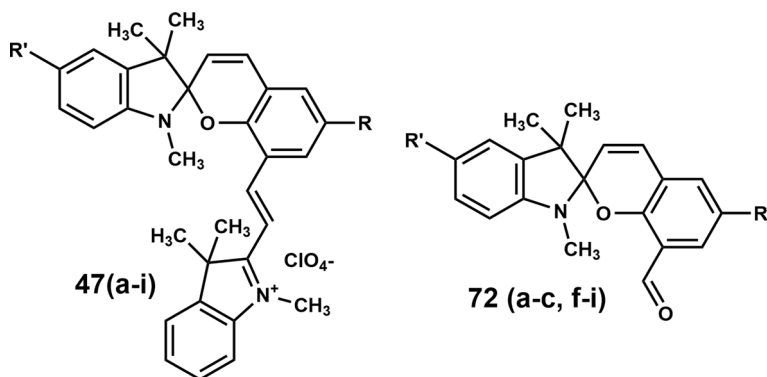


Fig. 11 The structures of spiroopyrans with conjugated 3*H*-indolium fragment and non-cationic related compounds

Table 2 The main characteristics of MC forms of spiroopyrans containing conjugated cationic fragments and related compounds

-R	-R'	Cationic derivatives			Formyl-containing spiroopyrans		
		No.	λ_{\max} MC, nm	$\tau_{1/2}$ MC, s	No.	λ_{\max} MC, nm	$\tau_{1/2}$ MC, s
-CH ₃	-H	47a	728	8.4	72a	621	10
-OCH ₃	-H	47b	Non-photochromic		72b	650	6.3
-F	-H	47c	738	27.8	72c	623	6
-Cl	-H	47d	709	189.5	72d	–	–
-Br	-H	47e	708	238.7	72e	–	–
- <i>t</i> -Bu	-H	47f	715	6.9	72f	615	12.2
-CH ₃	-Cl	47g	Non-photochromic		72g	627	15.7
-COOMe	-H	47h	642	4516.5	72h	566	1037.9
-COOEt	-H	47i	643	4250.3	72i	566	1130.5

72. The main spectral and kinetic characteristics of these compounds and related non-cationic spiroopyrans with formyl group **72** (Fig. 11) are summarized in Table 2.

Partial MC stabilization was observed in the case of 6'-cationic derivatives. Such compounds exist as an equilibrated mixture of SP and MC isomers in solution [175, 186] and in the MC form in the crystalline state [175]. The ester groups in **47** (**h**, **i**) are similar in their nature and strength of electronic effects on the cationic substituent; therefore, these compounds also exist in thermal equilibrium of isomeric forms. Recently, an interesting case of variable photochromic behavior was observed for the series of fluorine-substituted cationic spiroopyrans and their formyl-containing analogs [106]. Despite the strong electron-withdrawing effect of the fluorine atom, both 6'-fluoro-substituted derivatives **47c** and **72c** exist in the SP form and exhibit positive P- and T-type photochromism (Fig. 12A, C). At the same time, both 8'-fluoro-substituted spiroopyrans are in the SP:MC equilibrium but characterized by

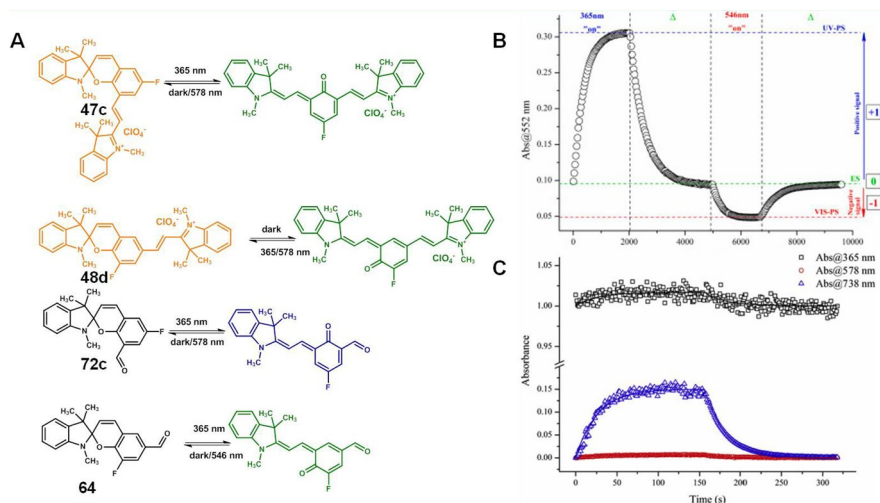


Fig. 12 Transformations of spiropyrans observed under different stimuli (A), kinetic profile of the bipolar absorption switch **64** (B), and absorbance changes of **47c** under successive UV–Vis light irradiation cycles. Adapted from Ref. [106] (Copyright 2022, with permission from Elsevier)

completely different properties. Cationic spiropyran **48d** is negatively photochromic and its cyclization reaction can be triggered by both UV and visible-light irradiation. Compound **64** transforms into the open form upon irradiation with UV light. However, after returning to the equilibrium state upon thermal relaxation, it can be further decolorized upon irradiation with visible light, demonstrating the properties of photochromic “balance” (Fig. 12B).

3.3 Solid-State Photochromism

Solid-state photochromism of spiropyrans is of great practical importance because of the solid nature of most materials the photochromic compounds can be introduced into. Many spiropyrans exhibit photochromic properties in powder or even in single crystals [93, 159, 187]. For instance, spiropyrans **73–75** (Fig. 13) have shown photoactivity in thin polydisperse films obtained by the thermal vacuum deposition technique [188, 189]. Photochromism of other compounds has been described for their pressed powders (in KBr pellets) [42] or thin films on the Bi(III) surface [190]. However, most of the spiropyrans (**49**, **76–78**) exhibit solid-state photochromism only at low temperatures due to the high rates of thermal discoloration reaction [191].

Due to the steric hindrances in the solid state, the transition from the SP to the structurally closest CCC-MC form is expected. However, Suzuki et al. achieved stable color in powder samples like that observed in ethanol solutions [192]. This phenomenon was attributed to the formation of the *trans*-isomer, and a new model of cooperative photochemical reactions was proposed [193] (see Fig. 14A).

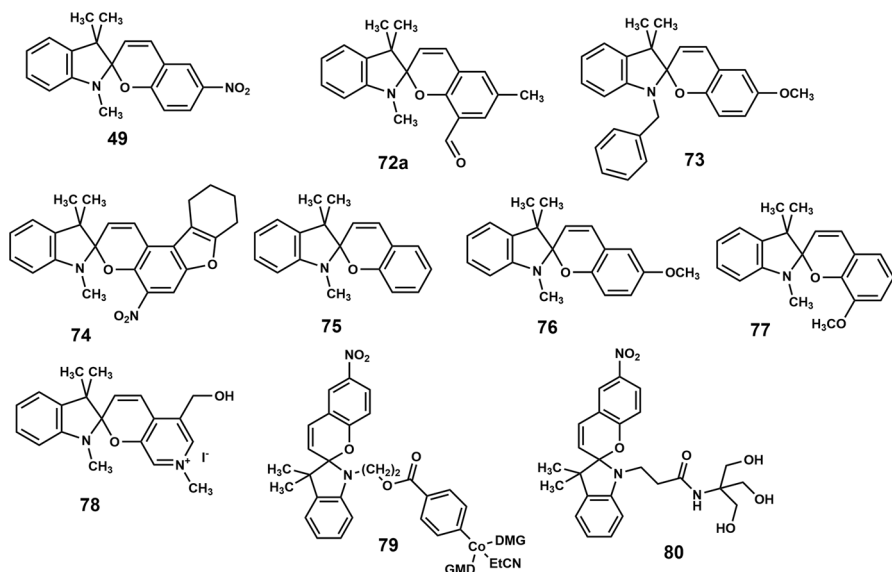


Fig. 13 Spiroirons exhibiting photochromism in solid state

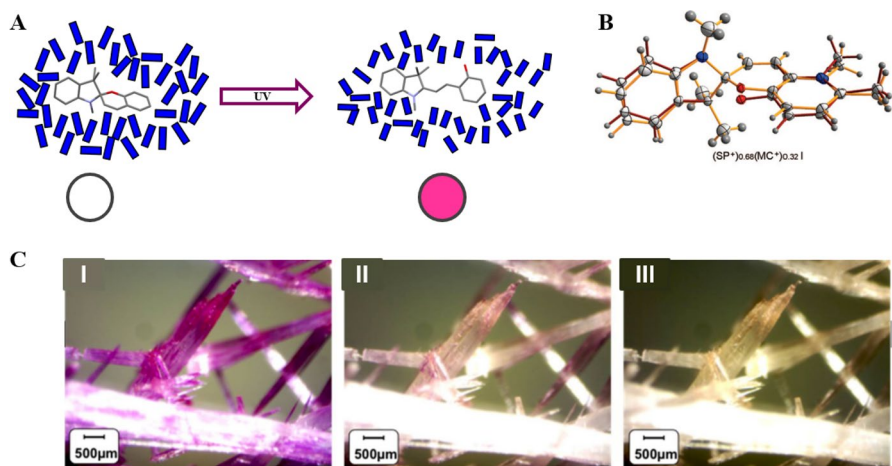


Fig. 14 Spiroiron photoisomerization in a flexible structure powder (A); ORTEP diagrams of SP and MC forms detected in a single crystal of **43** (B) [117]; photochromic performance in the crystalline state of norbornene-spiroiron under (i) UV irradiation for 1 min (merocyanine isomer), (ii) visible-light irradiation for 1 min (mixture of merocyanine and spiroiron isomers), (iii) visible-light irradiation for another 1 min (spiroiron isomer) (C). Adapted from Refs. [117, 200] with permission. Copyright 2008 American Chemical Society

According to this concept, the excitation increases the mobility of some areas in the crystal structure, making further isomerization possible. These processes seem to occur on the outer surface and are unlikely in the inner layers because of

crystal structure destruction, which was confirmed by Naumov et al. [117]. Single crystals of compounds **43** and **78** were obtained and their structure was investigated by X-ray diffraction (Fig. 14B). After irradiation, some of the molecules passed into the CCC-MC form, accompanied by the appearance of red coloration. The spirocyclic rupture tendency arises because of the looser molecular packing and the mutual repulsion between the quinoline moieties. Moreover, the elongation and the attendant weakening of the C_{spiro}-O bond is a result of the effect of the acceptor quinoline nitrogen atom.

The ability of spiropyrans to undergo photoinduced transformations in the solid state depends on the existence of adequate size cavities (Table 3) [194]. Thus, the main design strategies for solid-state photochromes are based on the addition of bulky motifs in their structure [195–198]. Yurieva et al. showed that cationic spiropyrans tend to exhibit photochromic properties, in contrast to their neutral analogues [93]. The formation of a looser crystal packing in the case of salt spiropyrans can be observed due to the mutual repulsion of like-charged ions in the structure. It was recently shown that the ability for solid-state phototransformation also strongly depends on the change in the strength of the interaction between counterions [194]. Sekine et al. investigated the possibility of controlling the volume of voids by visible-light irradiation [196]. The thermal bleaching rate increased significantly for the crystals exposed to visible light for 120 h followed by UV irradiation, which correlates with the surface void size. This theory is in agreement with various thermal relaxation rates observed for different polymorphic forms of compound **79** (Fig. 13). This indicates that the polymorphism of spiropyrans [199] can be used as an additional tool to tune the properties of crystalline materials.

Wu et al. [198] succeeded in obtaining spiropyran containing a methylene propionate group at the nitrogen atom of the indoline heterocycle exhibiting reversible photochromic properties in the crystalline state at room temperature without additional recrystallization, which is a very rare example of a neutral crystal of spiropyran. Crystallographic analysis showed that weak van der Waals forces were predominant in the crystal, which led to relatively loose packing and photochromic properties. This study is of great fundamental value for studying the relationship of molecular structure and packing mode with photochromic properties in the crystalline state. Also, as a result of research [200], norbornene-spiropyran derivatives were obtained, showing photochromism in the crystalline state at a temperature of 20 °C. The illustration of color transformations is shown in Fig. 14C. Thus, the presence of voids in the crystal [194], loose packing [198],

Table 3 Dependence between void size and anion type

Anion	V, Å ³	Anion	V, Å ³	Anion	V, Å ³
I ⁻	14.61; 11.95*	NO ₃ ⁻	8.91	PF ₆ ⁻	8.36
BPh ₄ ⁻	10.29	OTf ⁻	8.88	CF ₃ BF ₃ ⁻	8.06
SCN ⁻	9.60; 9.09*	ClO ₄ ⁻	8.60	BF ₄ ⁻	7.54

*Two independent parts are in the unit cell

and the absence of strong intermolecular interactions near the photochromic centers [199] play an important role in the manifestation of photochromism in the crystalline state.

The incorporation of spiropyran molecules into various porous structures and molecular architectures can be used to produce solid-state photo- and thermochromic materials. The notable examples are spiropyran-containing metal–organic frameworks (MOFs) [201, 202], wavelength orthogonal photodynamic networks [203], and polymeric or glass matrixes [204]. The additional polarization of spiropyran molecules, as well as an increase in material porosity and surface roughness, induced the tendency for solid-phase photochromism. The covalent bonding of initially passive compound **80** (Fig. 13) with polar polyoxometalate matrices allowed materials with pronounced photochromic properties to be obtained [40, 72, 184, 205].

3.4 Other Chromogenic Properties

3.4.1 Solvato-, Thermo-, Baro-, and Mechanochromism

To date, a large array of experimental data on the photochromic properties of spiropyrans has been collected. A significant characteristic known as solvatochromism is the potential to undergo isomerization depending on the polarity of the solvent [130, 206, 207] and its ability to form hydrogen bonds [135, 175, 208]. The enhancement in solvent polarity leads to stabilization of the MC form due to additional polarization and transition of MC to the zwitterionic-like rather than quinoidal form. This stabilization can be sufficient for switching the system from positively to negatively photochromic or vice versa [209]. Some spiropyrans that exist as SP:MC mixture in polar solvents can show bidirectional photochromism by equilibrium shift to individual SP or MC form under the different wavelength irradiation [102, 106, 122, 123]. In special cases, one can even observe a great influence of the solvent on the equilibrium of the two forms. Thus, in the case of 6'-formyl-8'-fluorine-substituted indoline spiropyran [106], the compound exists only as SP isomer in chloroform according to the results of nuclear magnetic resonance (NMR) spectroscopy. However, in acetonitrile solution an equilibrium of MC:SP forms with a ratio of 1:20 is observed, and during spectral-kinetic studies, behavior of the “photochromic balance” type was found.

It should be noted that changes in the solvent polarity and nature (protic or aprotic solvents) lead to a shift of the MC absorption maximum as well. For example, in a study carried out by Liu et al. [210], the absorption spectra of 6-nitro-substituted indoline spiropyran derivatives were compared in different solvents. It was shown that the strongest hypsochromic shift was typical for solutions in methanol ($\lambda_{\max} \approx 550$ nm), and the strongest bathochromic shift for solutions in ethyl acetate ($\lambda_{\max} \approx 590$ nm). The absorption maxima of compound solutions in ethanol, isopropanol, and acetone lay between these values. The current applicability of solvatochromism is based on silicon microcapillaries coated with spiropyran-containing

polymer bristles for solvent polarity detection [211], controlled self-organization of nanocrystals [212], and narrow-range temperature control [213].

The effect of temperature on energy exchange is considered the simplest way to effectively trigger spiropyran isomerization. For instance, thermochromism of compounds **26**, **49**, **50**, **57a** shown in Fig. 15 allowed thin films with optical memory effects to be obtained by rapid cooling of melts [214]. Also, thermosensitive polymer materials were obtained based on norbornene derivatives [215]. The MC form with additional stabilization due to the formation of hydrogen bonds in an aqueous medium (a mixture of water and alcohol) made it possible to use spiropyrans as temperature sensors [216]. In most cases, the recyclization reaction rate is expected to increase with increasing temperature. However, in the case of thiophene-substituted spiropyrans **67**, heating led to slowing of the thermal decolorization reaction [158]. Thermochromic silica-encapsulated spiropyrans were obtained and studied in a water/ethanol mixture by Iqbal et al. [217]. The thermal isomerization of SP to MC was a discontinuous process observed in a temperature range of 5–60 °C. The spiropyran derivatives, therefore, have potential application for colorimetric temperature indication.

Julià-López et al. [218] described a method of switching between photochromism types by thermal exposure in the solid state in the case of spirocyclic compounds **26** and **49** (Figs. 15, 16). At room temperature, these systems demonstrated positive photochromism, which is common for most spiropyrans. However, when heated to a temperature exceeding the melting point, negative photochromism was observed.

More recently, a research group headed by Metelitsa investigated the barochromic effect of indoline spiropyrans in the gas phase [219]. Barochromic and thermochromic or solvatochromic effects can have a different nature. On the one hand, color changes with increasing or decreasing pressure can be caused by a shift in the spectral holes [220]. However, in this case, the color changes will not be so pronounced and easily noticeable. In another case, barochromism may be the result of an isomerization reaction occurring when the pressure in the medium changes. This can be possible with an appropriate choice of the compound structure. In the article by Metelitsa et al. [219] it was shown that indoline spiropyrans with nitro- and

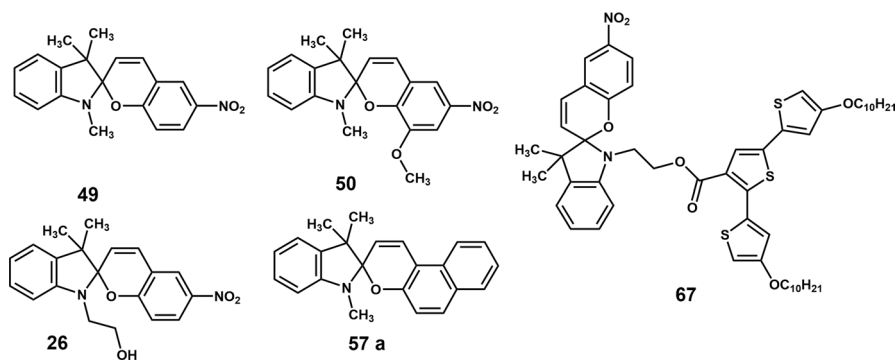


Fig. 15 Chemical structures of thermochromic spiropyrans

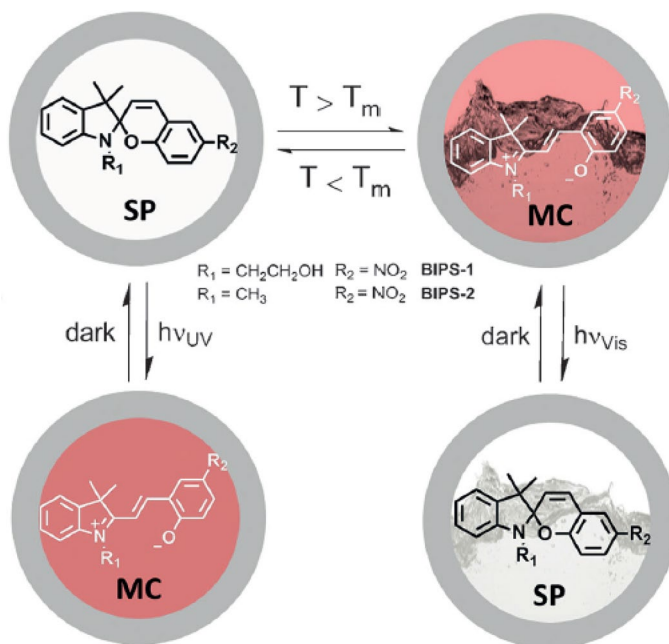


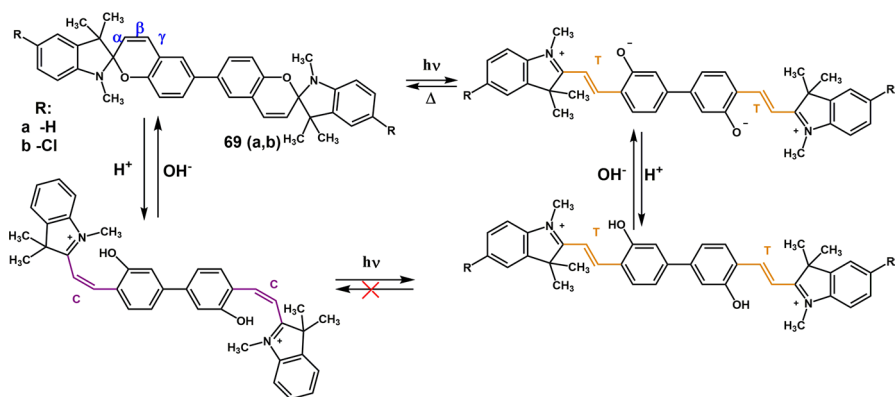
Fig. 16 Changes in photochromism type for indoline spiropyrans induced by temperature (T_m is the melting point). Reproduced from Ref. [218] by permission of John Wiley & Sons Ltd

formyl substituents in 6' and 8' positions of 2*H*-chromene moiety existed in spirocyclic form in the gas phase under pressure of 10^{-6} – 10^{-1} Torr. After the pressure increased to 760 Torr, isomerization to the merocyanine form occurred, resulting in sharp changes in the spectral properties. This transformation was probably possible due to the high stability of the MC isomer for these compounds at room temperature and normal atmospheric pressure.

Such experimental data without the use of activating radiation were obtained for the first time and are unique for this class of compounds. Although studies of the phototransformation of spiropyrans, including their protonated forms, were carried out earlier [221, 222], this will probably allow new applications to be found for spirocyclic compounds, for example, as gas-phase pressure sensors.

Mechanochromism is a general term that refers to changes in the color of a substance when it is crushed, ground, milled, rubbed (tribochromism), or sonicated, or after high pressure is applied (piezochromism) both in the solid state and in solution [223]. Unlike other methods of impact on a chromophore, with the mechanical method, a controlled gradual change in the spectral characteristics is possible, which is an important feature. A similar possibility of a controlled gradual color change under the application of different pressures was shown by Funasako et al. on a spiropyran-Nafion film [224].

It is important that over the past 10 years there has been a rapid increase in the number of research articles on this topic. These studies certainly opened up new possibilities for the application of spiropyrans in various fields of science and



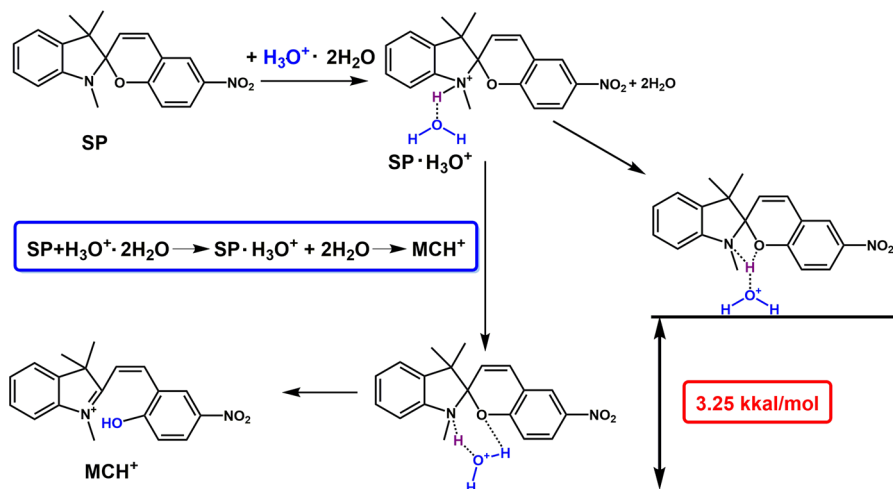
Scheme 16 Structures of protonated and non-protonated MC isomers of bis-spiropyran **69**

technology, including the use as sensors for damage, wear, or increased stresses in various constructions [225]. Another promising direction in the future may be the creation of materials capable of self-reinforcing and self-healing after the action of a destructive mechanical stress [226, 227].

3.4.2 pH-Sensitive Properties and Photoacidity

Spiropyrans tend to protonation due to the localization of lone electron pairs on the pyran oxygen atom [228]. The absorption spectra of protonated forms lie in the green-yellow range and predominantly have TTC configuration [229]. However, the authors admit the possibility of UV-controlled transitions into CCC or TTT forms. A stable protonated TTT-MC form was revealed [45] due to the absence of an intramolecular hydrogen bond $C(3')-H(3')\cdots O-C(9')$ registered for non-protonated forms [174], and following a lack in the stabilization of the TTC isomer. In the case of bis-spiropyrans **69** (a, b) the formation of XCX-configuration by protonation was detected. Under irradiation, it irreversibly transformed to XTX form as shown in Scheme 16 [179].

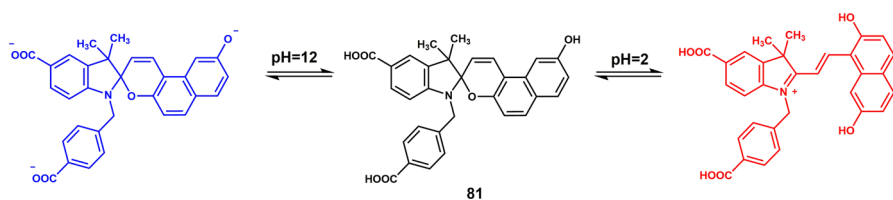
The properties of the absorption spectra character are somewhat dependent on the anionic type, while the strength of the acids significantly affects the protonation process, resulting in incomplete protonation by weak acids (organic or H_3PO_4) in aprotic solvents [229]. According to quantum-chemical simulations [230], the probable reason is a lowering of the protonation process barrier on account of proton transfer involving a polar protic solvent molecule (for instance, water) (Scheme 17). Moreover, protonation is facilitated by an increase in electronic density in the hetarene moiety. The protonation process mechanism at the first stage includes the formation of protonated spirocyclic form SPH^+ , which has been confirmed by computational methods [230, 231]. However, other researchers have questioned this mechanism, as it has not yet been possible to experimentally observe the SPH^+ isomer [228, 229].



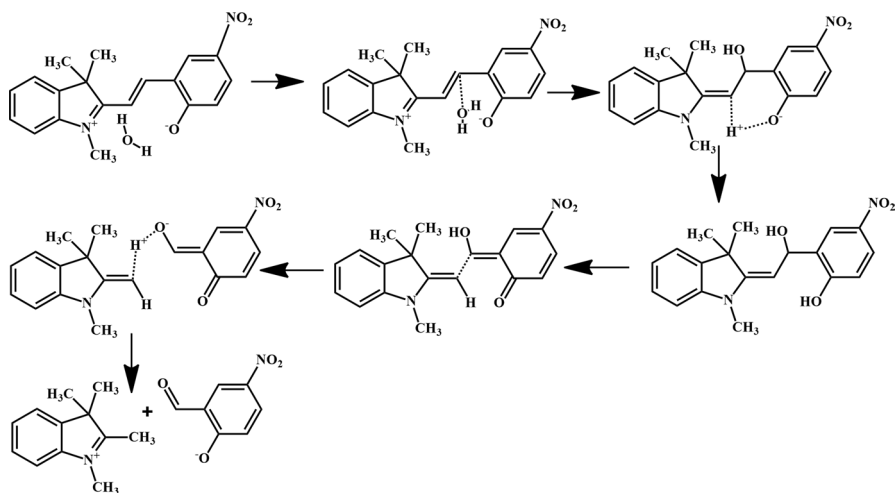
Scheme 17 Probable mechanism of spiropyran protonation in water

It seems obvious to expect that the nature of the substituents in the molecule also strongly affects the acidochromic properties of spiropyrans. Cui et al. [232] studied the effect of the substituent at position 7' of the *2H*-chromene moiety on the characteristics of the protonated isomer. All compounds considered were characterized by the absorption maximum of the protonated merocyanine form in a range from 410 (for the diethylamino group) to 446 nm (for the methoxy group). The pH value of the sudden color change point gradually increased passing from electron-withdrawing to donor substituents. The result was in agreement with the pK_a value from the experimental spectra.

Due to the acidochromic properties of spiropyrans, their solutions can serve as effective pH-sensors for detecting gaseous acids and bases [233, 234]. To increase the sensitivity of the system, compounds with pronounced fluorescence are often used [65, 77, 233]. The introduction of several centers susceptible to protonation/deprotonation into the molecule allows for accurate pH change detection. Wan et al. developed a pH-sensor based on compound **81** (Scheme 18) that was utilized in a pH range from 2 to 12 due to the presence of a hydroxy and several carboxyl groups [235].



Scheme 18 Schematic representation of pH-sensor performance



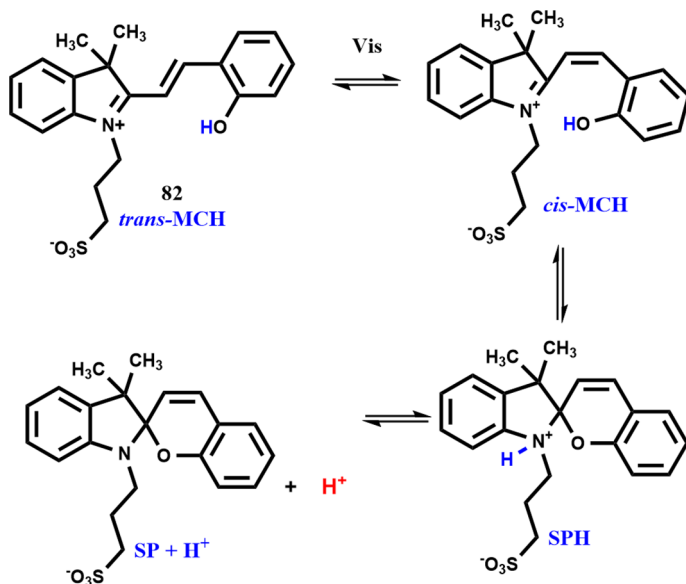
Scheme 19 Proposed mechanism of spiropyran hydrolysis

It should be noted that spiropyrans tend to undergo hydrolysis in water. The mechanism governing this process was proposed by Hammanson et al. and is shown in Scheme 19 [231]. The initial reversibility of the condensation reaction between indoles and aldehydes was investigated. The protonated forms usually are more stable in water solutions due to the lower activity of the phenolate oxygen atom at the first stage.

Over the past several years, special attention has been focused on self-protonated merocyanine forms (MCH) of spiropyrans which have potential as effective reversible photoacids—molecules capable of generating protons upon irradiation. As proton transfer is one of the most fundamental processes in nature, many applications have been reported in recent years in which photoacids are used to protonate materials for switching their properties, to catalyze bond formation and breaking, and to control ion-exchange processes [43, 44, 236–239].

In the case of spiropyrans, photoacidity becomes possible due to the isomerization of *trans*-merocyanine MCH to the meta-stable *cis*-merocyanine form, which undergoes cyclization to the SP isomer with proton release. This process is usually activated by visible-light irradiation, and some studies have shown that this can be used as a light source of low intensity, which is very important for potential biomedical applications.

Self-protonated merocyanine **82** (MCH) was obtained by Liao's group and became the first reported meta-stable photoacid [47]. It can be easily synthesized from salicylic aldehyde and alkylsulfonated 2,3,3-trimethylindoline and has a *trans*-MCH structure, which is stable in both aqueous and organic media without the addition of an external acid. Under irradiation with visible light, **82** (MCH) transforms into the meta-stable acidic *cis*-MCH form, which can produce protons or thermally revert to MCH [47] (Scheme 20). The thermal reaction rate strongly depends on the solvent type—the rate constant is 73.0, 1.6, and 0.035 $\text{M}^{-1}\cdot\text{s}^{-1}$, respectively, in



Scheme 20 The first representative of spiropyran photoacid

water, ethanol, and DMSO [43]. The half-life of the deprotonated form **82** (SP) in an aqueous solution is about 70 s and is significantly higher than the analogous parameter for the previously known polyaromatic hydroxy derivatives [240, 241]. At the same time, these properties allow for less susceptibility to hydrolysis in comparison with other spiropyrans [242]. Due to the attainable change in pH in an aqueous solution (about 2.2 a.u.), spiropyran **82** can be used as a photocontrollable catalyst in esterification reaction [47]. Berton et al. studied a light-switchable buffer system based on a relative protonated merocyanine photoacid [243]. It was found that para-substitution of the indolium moiety of its molecule with a methoxy group afforded a compound suitable for the creation of hydrolytically stable aqueous buffers whose pH could be switched between 7 and 4 with the help of green light irradiation

Table 4 The dependence of electronic effects of substituents on photoacid strength

Substituent	Increase of electron-donor effect			
	pK _a (R ₁)	pK _a (R ₂)	pK _a (R ₃)	pK _a (R ₄)
–NO ₂	–	–	–	4,72
–CF ₃	–	–	–	5,66
–CN	–	–	–	5,46
–F	6,20	5,72	6,12	5,90
–Cl	–	5,20	–	5,83
–Br	5,39	–	–	5,71
–OCH ₃	7,05	–	6,52	6,20

(500 nm). The possibility to control the complexation reactions according to the guest–host type in helix[6]arene was also considered [244]. Moreover, photoacids like **82** are of great interest for controlling the processes in biological systems (see Sect. 3.2.2).

Liu et al. investigated the properties of a wide range of monosubstituted spiro-pyran-based photoacids **83** (**a–n**) as shown in Table 4 [245]. In the case of 6'- and 8'-substituted compounds (the positions **R**₄ and **R**₂, respectively), the acidity significantly decreased by passing from electron-withdrawing to electron-donating substituents, which correlates with the previously described phenomena. This effect is slightly less pronounced for *meta*-substituted derivatives. In general, the introduction of substituents, except for 5- and 8'-methoxy-containing compounds, promoted an increase in the strength of the photoacid in comparison with the unsubstituted analogue **82** ($pK_a=6.23$).

The incorporation of propylsulfoxy-substituted photoacids into the *N*-isopropyl-polyamide matrix allows for their thermal control [246]. In general, photoacids are stable in polymers [238, 239]; however, the cycle closure process is hindered and can be initiated only in the presence of a base, which limits the scope of applications. The photochromic transformation ability was improved by mixing the compound into polyvinylpyrrolidone due to its basic properties [79].

The addition of quinoline fragment to molecule **84** allowed for controlling pH in a range from 3 to 7 due to intramolecular proton transfer (Fig. 17) [239]. It is suggested to use samples susceptible to intramolecular proton transfer for molecular machines working without accumulation of side products [247] and systems with pH-guided fluorescence [248]. The additional tuning of the optical properties is possible using mixtures of pH-responsive dyes (Fig. 17B) [249, 250], and a bathochromic shift of the absorption maximum was reached for highly conjugated spiro-pyran **85** (Fig. 17A) [251].

3.4.3 Complexation of Spiropyrans

Spiropyrans can be effective ligand systems due to the possibility of transforming into the MC form containing phenolate oxygen with lone electron pairs [252, 253]. Spiropyran complexes with metal cations often demonstrate pronounced coloration or fluorescence properties, which allows their use as chemosensors. The chelating fragments such as crown and azacrown ether [68, 254–257] or heterocyclic [165, 170, 258–261] substituents, methoxy [262, 263], carboxyl [264–267], imino group [30, 268], and others [26, 269, 270] were introduced into spiro-pyran molecules for efficient binding. Moreover, the metal cation chelation was facilitated in the presence of two active spaces [68, 252, 271, 272]. It is rather difficult to predict unambiguously which of the chelating centers will be involved in complexation. This aspect is practically obvious for the crown ether derivatives and compounds containing the methoxy group but remains uncertain in the case of polysubstituted spiro-pyrans. To investigate the structure of the complexes, single-crystal X-ray diffraction [176, 253] or in operando X-ray absorption spectroscopy (XAS) [165] was utilized. Therefore, Baldrighi et al. [263] showed that the copper, zinc, and magnesium cations in complexes with spiro-pyran **86a** are

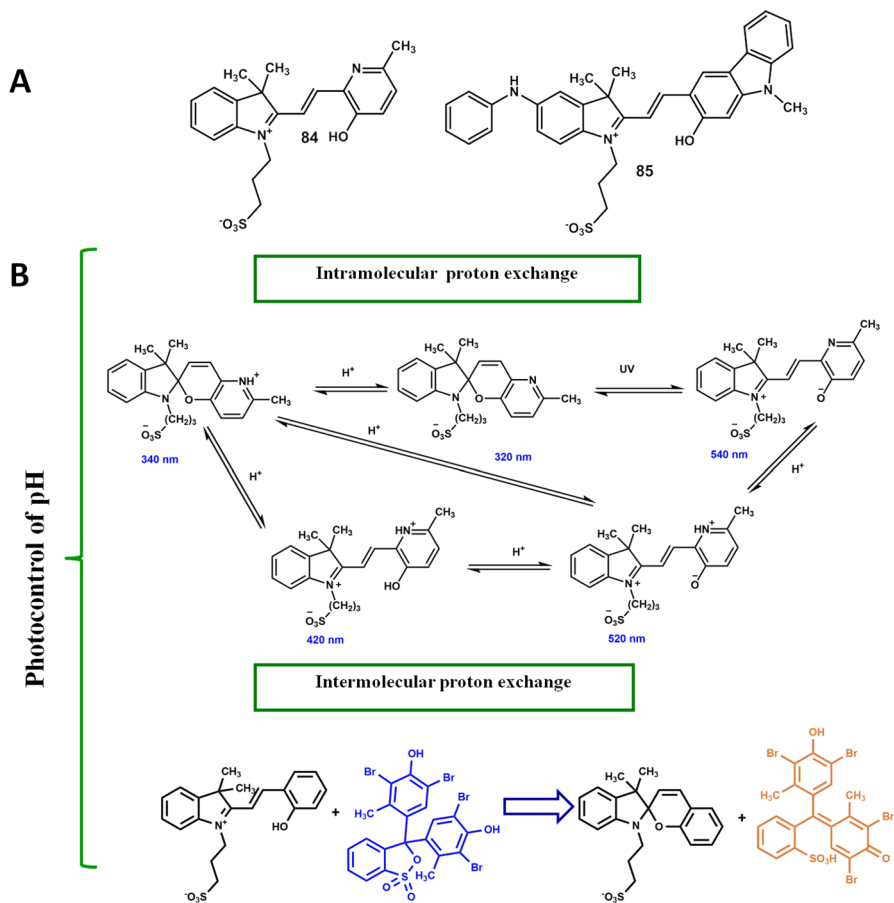


Fig. 17 Spiroyrans with heterocyclic fragments in the pyran moiety (**A**) and proton transfer in the systems containing spiroyrans-based photoacids (**B**)

bound by the phenolate oxygen atom and the methoxy group. The carboxyethyl substituent is not involved in complexation in this case, in contrast to many other compounds containing carboxylic groups (Fig. 18) [270, 271]. In general, the common molar ratio of cation to spiroyrans is 1:2, and multidentate ligands are required for trivalent metals [267]. In crystals, spiroyrans molecules are usually combined by metal cations into dimeric or linear patterns, which in turn form layers [270].

The introduction of some substituents (Fig. 19) allows selective binding of individual ions to be achieved [84, 263, 272–274] due to the correlation between the sizes of the cation and the ligand cavity. Moreover, the phenolate oxygen atom of the MC form stabilizes the complex. It is possible to detect relatively small cations such as lithium using azacrown ether derivatives **87** and **88** [68, 252]. On the contrary, spiroyrans compound **89** is capable of complexation only

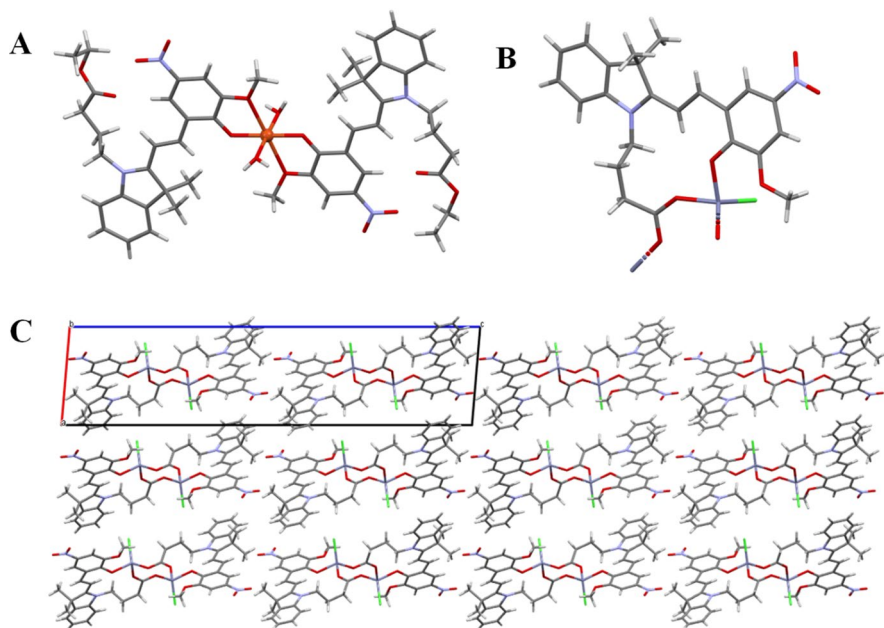


Fig. 18 Structures of spirocyan-metal complexes ISIVUD (A) and MACBID (B, C) in single crystals (received from CCDC)

in the cyclic state, since the photoinduced transformation increases the chelating cavity, resulting in a decrease in the efficiency of cation binding [68].

The sensitivity of spirocyan-based sensors can be significantly improved using their luminescent response. For example, the bifluorophoric [2]pseudo-rotaxane of the “host–guest” type exhibiting efficient ratiometric photoluminescence behavior via the Förster resonance energy transfer (FRET)-OFF process was proposed for monitoring ultratrace copper ion concentrations (0.53 μM) in living cells [275]. Spirocyan complexes **90**, **91** (a–c) with lanthanide cations [206, 276] also exhibited pronounced fluorescence.

Fluorescence is strongly influenced by substituents in the indoline moiety, and its intensity depends on the type of chelated cation. For example, the fluorescence intensity of complexes with lanthanide ions increased in the order $\text{Sm}^{3+} < \text{Eu}^{3+} < \text{Tb}^{3+}$. Changing the excitation wavelength made it possible to draw up individual luminescence maps with the effect of “fingerprints” to check the presence of cations and determine their type, as shown in Fig. 20 [206].

The ability of the complex to dissociate is considered an important parameter in the scope of spirocyan complexation and the creation of ionic transport systems [277]. Complexes with diamagnetic cations Cd^{2+} and Zn^{2+} turned out to be prone to photodissociation. The quantum yield of the process varied depending on the type of cation but was practically insensitive to the irradiation wavelength [261]. The CCC isomer was detected in solutions of spirocyan complexes **92** with dysprosium and yttrium cations as shown in Scheme 21 A. However, complex dissociation did not

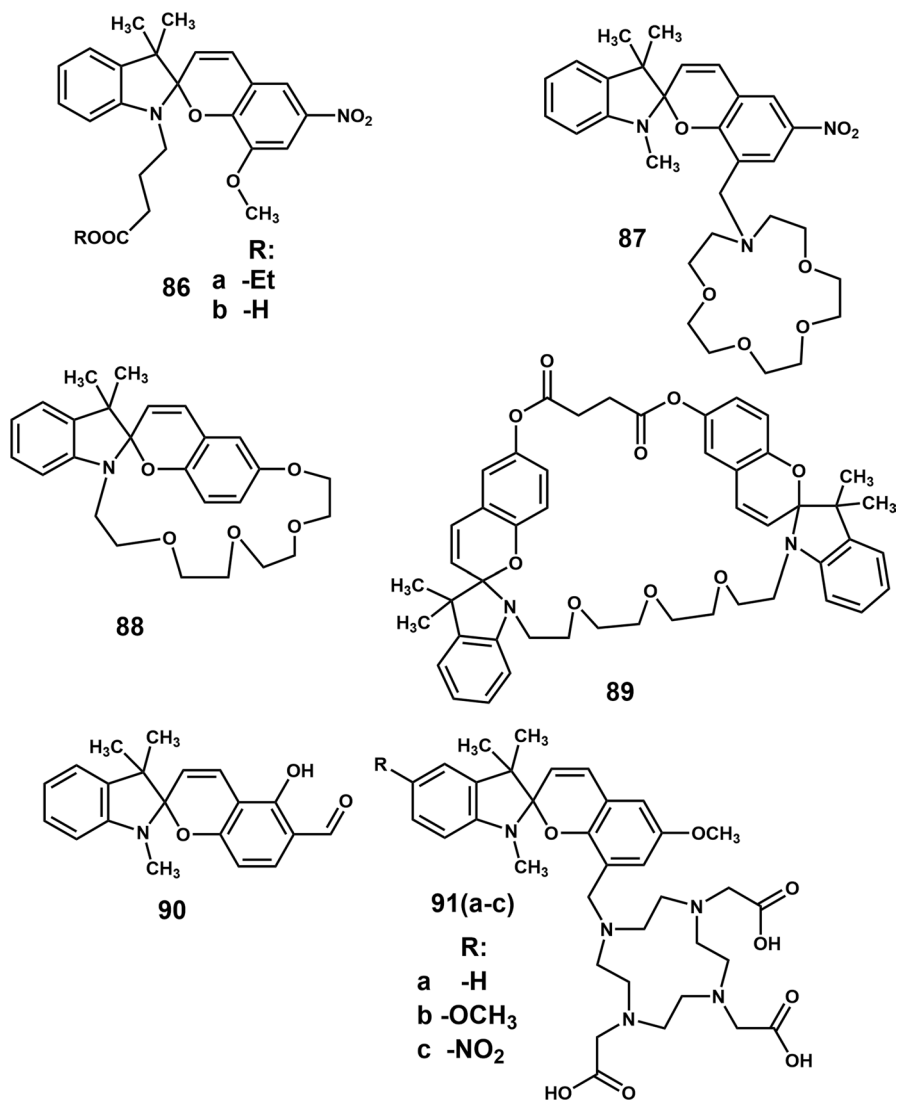


Fig. 19 Structures of spiropyrans with high complexation ability

occur [278]. Moreover, redox processes are possible along with the formation of complexes, leading to unexpected products. Such phenomena have been observed in the case of copper salts [30, 78]. Based on the structure similar to **92** with the same chelating fragment in position 6' instead of the nitro group, Zhao et al. proposed selective naked-eye detection of copper ions in aqueous media and on test paper strips [279]. Arjmanda et al. created a polymer nanocomposite containing spiropyrans which can be considered as a good alternative sensor due to its portability, high detection speed, and relatively low cost [280].

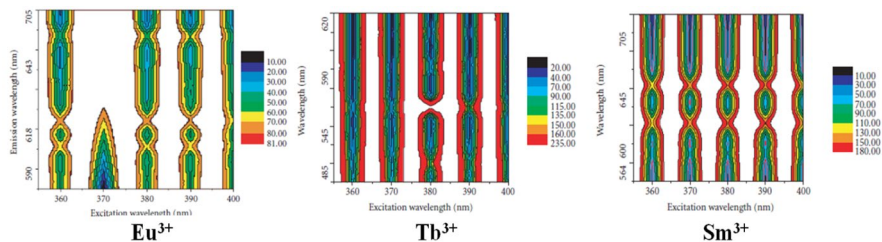
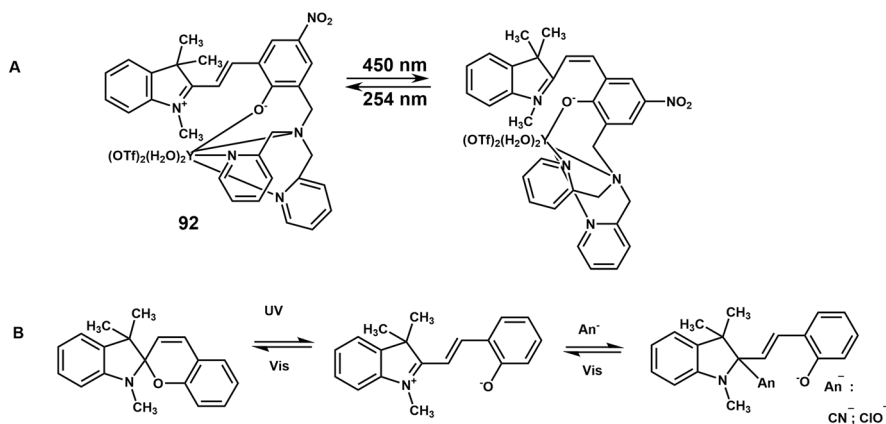


Fig. 20 Luminescence maps of spiropyran **90** complexes with lanthanides under different excitation irradiation wavelengths. Reprinted from [206]



Scheme 21 Spiropyran complexes with yttrium cation and CCC isomer formation (A) and nucleophilic addition of anions to MC (B)

Spiropyran attached to nanoparticles and fibers can be used as sensor systems for metal cations in living cells [281] or aqueous medium [267].

However, spirocyclic compounds can be used not only for the detection of metal cations, but due to the localization of a partial positive charge near the indoline ring, they can serve as effective sensors for some important anions. Thus, nucleophilic addition of cyanide [282, 283] and hypochlorite anions [284] to the C(2) atom leads to a decrease in MC absorption band intensity with the subsequent appearance of a new absorption and/or fluorescence band in the range of 421–435 nm (Scheme 21B). Zhou et al. reported the possibility of detecting cyanide anions in liquids over a wide range of concentrations and with relatively high accuracy using the bis-spiropyran molecule [285]. The optimized analysis conditions were irradiation at 320 nm for 4 min after mixing with CN^- and detection at 440 nm. Also, a bis-spiropyran probe-based fluorescence method was established for CN^- quantitation with a response range of 1.0–50.0 $\mu\text{mol}\cdot\text{L}^{-1}$ and detection limit of 0.21 $\mu\text{mol}\cdot\text{L}^{-1}$. This selective and rapid CN^- detection method has potential application in express tests of food safety. Sanjabi et al. showed the

possibility of detecting cyanide ion trace amounts via a ring-opening process without the use of UV irradiation in a 1:1 M ratio [286].

Spiropyrans can also be used for highly sensitive colorimetric detection of certain organic substances, such as amines [287] and thiophenols [288]. In the first case, sensing was realized due to the hydrolysis of spiropyrans with the subsequent formation of their Schiff bases, which were distinguished according to the shapes and trends of their UV–Vis absorption spectra. In the case of thiophenol sensing, on the contrary, it was caused by the removal of the protective group from the phenolate oxygen atom and the closure of the cycle, accompanied by decolorization of the solution. Xiao et al. proposed a very interesting and intricate “double-check” method for detecting serum albumin based on spiropyran [289].

3.4.4 Fluorescence Properties

Fluorescence is an interesting and important aspect of spiropyran derivatives. To investigate the fluorescence properties of spiropyrans, different fragments capable of serving as acceptors for FRET, such as tetraphenylethylene [290, 291], tetrathio-phenylene [158], anthracene [66], pyrene [84, 292, 293], and others [294, 295], were introduced into spiropyran molecules. Complex compounds of spiropyrans with some metals were also characterized by pronounced fluorescence due to the energy transfer phenomenon in the metal–ligand system [206, 296].

An important circumstance is the fact that the closed spirocyclic form, as a rule, does not exhibit photoluminescence behavior, while the open merocyanine form is capable of emitting fluorescent radiation with quite good quantum yield values. Thus, fluorescence properties can be easily controlled by external influences, such

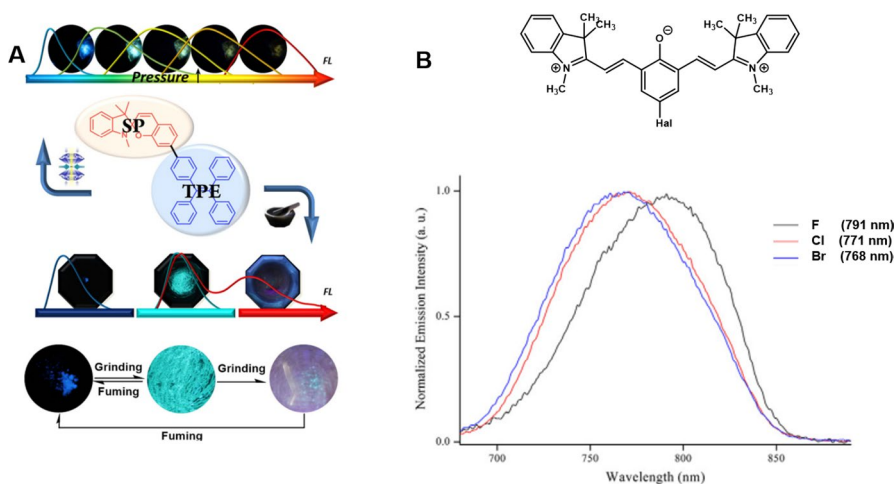


Fig. 21 Changes in fluorescence properties of spiropyran-tetraphenylethylene dyad induced by mechanical stress (A) and NIR photoluminescence of cationic spiropyran derivatives **47** (c–e) (B). Adapted from Ref. [297] by permission of John Wiley & Sons Ltd. and from Ref. [101] (Copyright 2020, with permission from Elsevier)

as UV/visible light and heating/cooling. As was shown earlier, mechanical stress can produce changes in the fluorescence spectra [297–299] (Fig. 21A). It is also possible to enhance the intensity of fluorescence by introducing some metal cations into the system [300, 301]. The presence of lithium or calcium cations in a double molar excess made it possible to increase the fluorescence intensity of indoline spiropyran with a pyrene fragment at the nitrogen atom and azacrown ether fragment in the 2*H*-chromene part three and seven times, correspondingly. The opposite effect was observed for cesium and manganese cations.

It is important to note that in some cases, both isomers can exhibit fluorescence. In this case, the fluorescence spectra of the SP and MC isomers differ significantly. Thus, for indoline bis-spiropyran based on acridone, the fluorescence spectra before UV irradiation of a dichloromethane solution were characterized by short-wave absorption maxima. When irradiated with ultraviolet light for 20 min, a bathochromic shift of the fluorescence peaks by about 200 nm was observed (\approx 540 and 600 nm) [60].

Controlled fluorescence of spiropyrans is widely used in bioimaging and chemosensing. Usually, the wavelength of the photoluminescence emission maximum lies in the range of 600–650 nm [302, 303]. However, application as a fluorescent probe in the field of bioimaging requires detectable fluorescence in the “biological window” range (650–1000 nm) [304]. Doddi et al. observed detectable fluorescence for a diketopyrrolopyrrole-spiropyran dyad in the region of 700 nm in acetonitrile solution [82]. Moreover, an increase in the emission intensity in the range of 700–800 nm was reached by introducing this dyad into a polyethylene glycol matrix. The prospects for bioimaging spiropyrans **47(c–e)** demonstrating photoswitchable NIR fluorescence properties were described by Lukyanov’s group [101, 106] (Fig. 21B). Their emission maxima were found in the range of 768–791 nm in acetonitrile solution due to the increase of the conjugation chain length in the 2*H*-chromene moiety of the molecules. Quantum yields of fluorescence varied in the range of 0.012–0.023.

Thus, a detailed study of the wide variety of spiropyran properties and the features of their response to various external stimuli helps to discover new applications for T-type photochromic compounds, which traditionally include spirocyclic systems. For the successful application of spiropyrans in the creation of functional materials, it is equally important to accumulate and systematize experimental data on the correlation between the structure of compounds and their properties.

4 Design of Smart Materials and Systems

Finally, all attempts of scientists to tune the characteristics of spiropyran are intended primarily to allow the creation of material with switchable properties. In this section, we briefly summarize the types of such materials and the possibilities they open up. In the case of each possible application, some of the properties discussed above are important. Since a detailed description of materials based on spiropyrans was reported several years ago by Klajn [3], in this section we will point out only those that are currently of the greatest interest to the scientific community. The

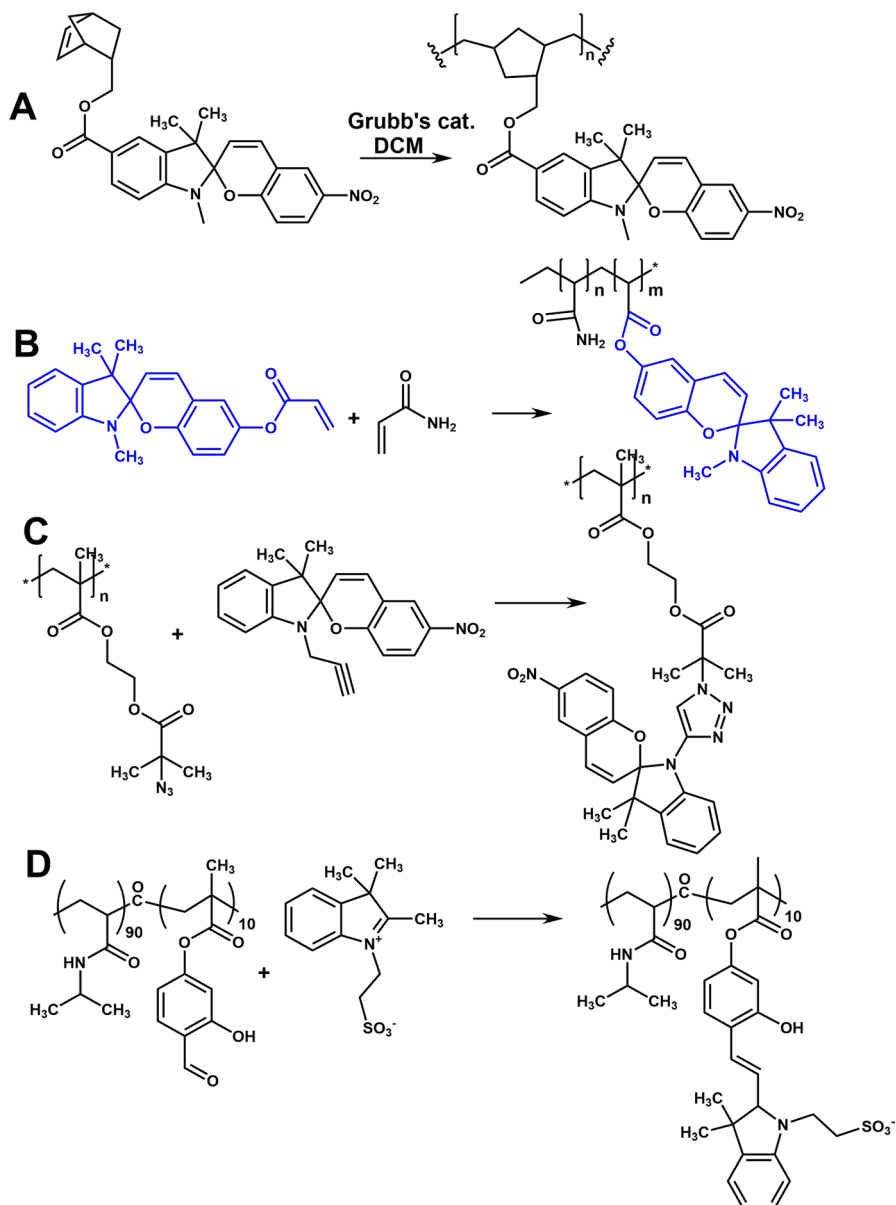
main purpose is to show what properties are needed in each of the cases and what compounds were used at the time.

4.1 Smart Polymers

The incorporation of spiropyrans into polymers is attracting particular attention. Sensor systems and traps [296, 305, 306], electronic devices [307, 308], and textiles [309–311] such as X-ray-sensitive fibers [124] can be created based on spiropyran derivatives. Owing to the polymer cavities, the transformation of spiropyran molecules can easily occur. To design spiropyran structures for subsequent implementation, specific groups capable of binding with polymer surfaces were added to their moieties. Spiropyran molecules can be directly involved in the polymerization reaction due to the presence of unsaturated fragments or functional substituents [312]. Moreover, spiropyrans can be attached to the polymer backbone using various linkers [313, 314], and introduced to the main [315] or the side chain [316] of the polymer (Scheme 22). Thermo- and photochromic polymer structures were created using the ring-opening polymerization method (Scheme 22A) [215, 315, 317]. Several samples of spiropyran-containing hydrogels and polymers were obtained by reacting the corresponding Fischer base with the main chain containing *o*-hydroxyaldehyde fragments (Scheme 22D) [246, 318]. Khalil et al. demonstrated that the presence of an acidic proton in the structure of spiropyran-based photoacids generally prevents the polymerization reaction, and triethylamine was used as a temporary protective group [319]. Polynorbornenes [215, 315], polyacrylates [320, 321], and polyanilines [322] can be noted as some of the most popular and promising copolymers and matrices for the creation of smart polymers containing spiropyrans.

To synthesize smart polymers based on spiropyrans, the thermal stability of spiropyrans and the polymer matrix should be identified. Thermochromic polymers can be used as filters, sensors, and materials with the ability to control overheating [215]. Furthermore, the functionality of polymer systems can be greatly expanded by modification of the polymer structure. The treatment of polymer surfaces with plasma or dielectric barrier discharge in air made it possible to fabricate non-porous materials used for the manufacture of membranes for reverse osmosis, nanofiltration, or molecular separation in the gas phase.

Mechanochromic polymeric materials have been widely used in the preparation of smart polymers [223, 324]. The change in polymer color indicates an excessive stretching that prevents mechanism parts damage [325]. Also, color changes can help to track tissue [326] and brain damage [327]. The latter becomes possible due to a passive strain sensor based on polydimethylsiloxane elastomer with covalently incorporated spiropyran mechanophore at 0.25 wt% level. Such a smart polymer can adequately measure impact strain via color change under a high strain rate of 1500 s^{-1} within a fraction of a millisecond. Moreover, it can be used repeatedly owing to the reversibility of the ring-opening reaction. Soft robotics [328], flexible electronics [307, 308, 329] and microcantilevers for stress sensing [330, 331] can be created based on mechanochromic polymeric materials.



Scheme 22 The main methods for the preparation of spiropyran-containing polymers: polymerization of spiropyran-containing monomer with a polymerizable substituent [215] (**A**); copolymerization of spiropyran and monomers [323] (**B**); attaching of spiropyran to the side chain of the polymer due to active functional groups [316] (**C**); in situ synthesis of spiropyran by the interaction of the Fischer base with the polymer chain containing sterically unimpeded salicylaldehyde fragments [246] (**D**)

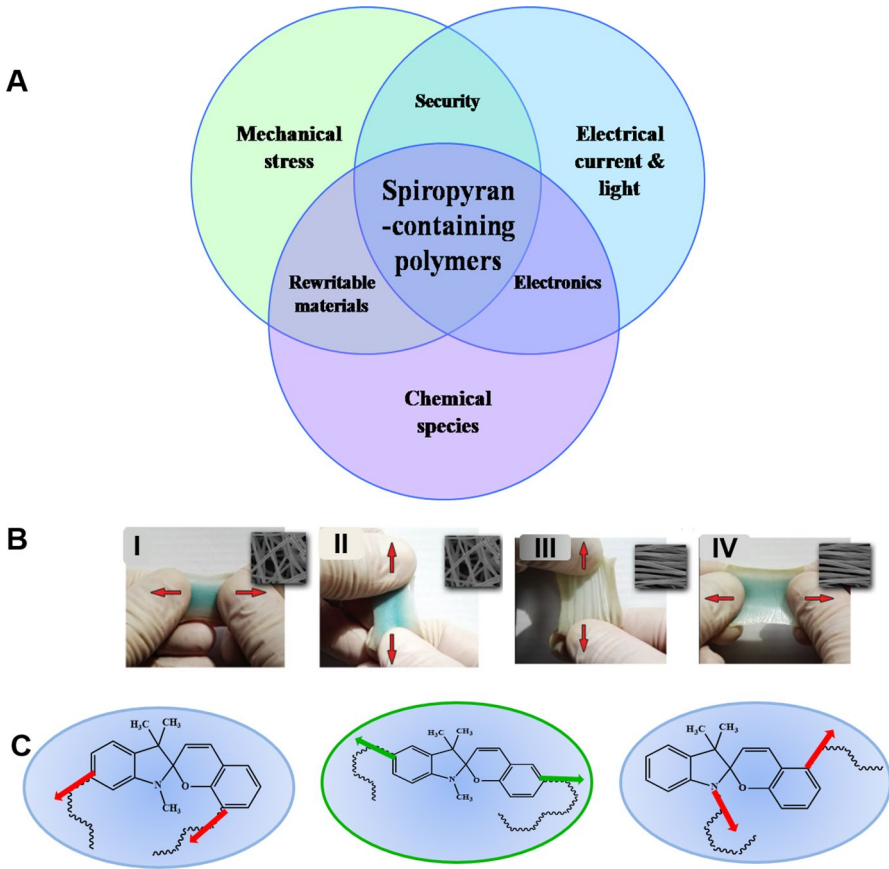


Fig. 22 The possible applications of spiropyran-containing polymers (A); mechanochromic tensile properties of a spiropyran-containing polymer in different directions with random fiber morphology (i and ii) and with aligned fibers (iii and iv) (B) and dependence between binding positions of spiropyran molecule and mechanical stress sensing effectiveness (C). Adopted from Ref. [334] with permission of John Wiley & Sons Ltd

The 3D-printing technique enabled numerous details with different forms and sizes to be obtained [332, 333].

The mechanical sensitivity of spiropyrans is directly dependent on two factors. Firstly, the level of ordering of the polymer material fibers plays a significant role. Raich et al. showed that in the case of randomly oriented fibers, mechanochromism was conferred to the composite in all stretching directions. For material with aligned fibers, there is only one "active" stretching direction (Fig. 22) [334]. On the other hand, the method of attachment into the polymer chain determines the direction of the tensile force application. Better results were shown by spiropyrans covalently linked to the polymer strands through positions 5 and 6' (Fig. 22B). More recently, two different research groups obtained and simultaneously investigated polymeric materials with shape memory and mechanochromic

properties [289, 335]. These studies can certainly open up new possibilities for the use of spiropyrans.

Impregnation of cellulose by spiropyran solutions allowed the creation of rewritable paper. Writing can be performed using pure water or simple acidic solutions [320, 336, 337]. Moreover, fluorescent spiropyran derivatives were proposed as analogues of document security watermarks [290, 337]. Mechanochromic, acidochromic, and photochromic properties with high contrast are also successfully used for counterfeit protection sign creation [291, 338–340]. Moreover, the combination of PRF, polyacrylonitrilic, luminescent, and photochromic fibers can be applied in UV detection and high-level encryption in the future [341].

Spiropyranes are also applied as active elements of molecular electronics. For instance, spiropyran-containing diketopyrrolopyrrole-based conjugated donor–acceptor polymer films can be used as photo-, thermo-, and acido-controlled semiconductive layers [342]. Their conductive properties may be improved by the addition of transition metal cations [343] or partial protonation with a subsequent increase in the contribution of hole conductivity [344]. However, it is worth considering the likelihood of side redox reactions [70, 75, 78]. Thin polymer films of trisoxalatochromate-spiropyran complexes with controllable magnetic properties were studied by Sanina et al. as prospective materials for high-density information-recording memory devices [345]. Triolo et al. investigated the possibility of fabrication of a photocontrolled structure over the substrate with a high degree of accuracy and produced patterns in micrometer scale [346]. This can be useful for creating light-sensitive molecular memory devices.

4.2 Crystalline and Amorphous Solid-State Hybrid Materials

New possibilities have been proposed for cationic spiropyranes to prepare crystalline and amorphous hybrid materials. Due to the presence of charged fragments, they can be combined with different inorganic counterparts to create hybrid materials exhibiting remarkable properties. Spiropyran-based single-molecule magnets (SMM) were first obtained by Bénard et al. [185]. The honeycomb structure of chromium-manganese oxalates with spiropyran interlayer molecules initiated the electron transfer, and it was described by Kida et al. for iron dithiooxalates [347] (Fig. 23A–C). Many related systems were obtained and comprehensively characterized by Aldoshin's group [348]. However, this direction remains a challenge, because it has not been possible to obtain SMM operating at sufficiently high temperatures. Nowadays, the prepared samples of SMM exhibit photomagnetic properties only in the range of 2 to 50 K. At the same time, various photoresponsive organic–inorganic hybrid magnets based on spiropyranes and inorganic nanomaterials are known [349, 350]. In this case, the creation of photomagnets operating at room temperature was possible. Thus, a hybrid magnet with a giant photomagnetic effect based on spiropyran and FePt nanoparticles was prepared and investigated [351].

Photomagnetism has also been revealed in solid state for cationic spiropyran iodides **93** (Fig. 23D). A thin coating layer made from them was positioned by Frolova et al. [159] as an active information storage medium (Fig. 23E). A

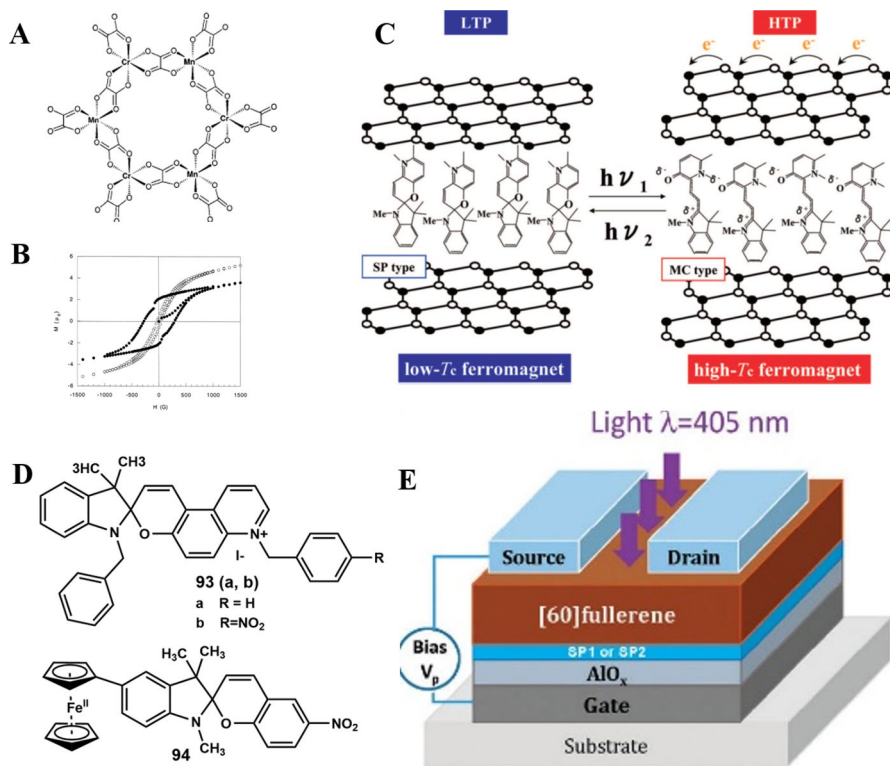


Fig. 23 The structure of the magnetically active complex with chromium-manganese oxalate anion (A) and the hysteresis loop before (white points) and after (black points) irradiation with UV light (B); schematic representation of the phenomenon of charge transfer in layer (C); structures of compounds **93** and **94** (D); model of data storage devices based on cationic spiroyrans **93** (E). Adopted from Refs. [159, 185] (Copyright 2001 American Chemical Society) and [347] (Copyright 2009 American Chemical Society) with permission

significant effect of the benzyl fragment of the *2H*-chromene moiety on the properties is very interesting. Flash memory devices can be created based on unsubstituted analogue **93a**, while the presence of a nitro group in **93b** leads to the irreversibility of the spirocycle opening reaction. Thus, spiropyran **93b** is a potential basis for ROM media. Spiropyran complexes with lanthanide cations can also act as SMMs with anisotropic magnetic properties [352]. One more promising example of the compound for designing molecular memory devices is ferrocene-containing spiropyran **94**. In this case, the ability to rewrite information can, if necessary, be regulated by the redox transitions in the ferrocene-ferrocenyl cycle [353]. In addition, a series of polyoxometallate photosensitive multi-photochromic structures with covalent or ionic binding type [40, 354–356] and MOFs [201, 357–359] have been developed based on cationic and covalently anchored neutral spiroyrans.

Recently, research articles on the use of spiropyrans as photosensitizers for dye-sensitized solar cells began to appear [360–362]. The photoswitching ability of spiropyrans when exposed to light of different wavelengths opens up new possibilities in photovoltaics. Due to the photoinduced structural transformation and sharp change in properties, it becomes possible to create smart dye-sensitized solar cells and smart windows with self-regulation of absorption.

4.3 Molecular Machines and Nanoarchitectures

The developments in the molecular electronics and nanomaterials field are a wonderful illustration of the current trend towards turning attention to the microcosm, not only in the field of physics but also in chemistry. This direction received special publicity after the Nobel Prize awarded in 2016 [363–365]. Due to changes in geometric characteristics and charge distribution, spiropyrans are also promising elements of molecular machines. Thus, bis-spiropyran **95** can serve as a molecular rotor when the polarity of the medium changes [64]. Spontaneous rotation around a single bond occurs due to steric hindrances caused by transitions between diastereomers (S–S, R–R, and R–S). In solution, the substance is in the form of an equilibrium mixture of atropisomers. Molecular machines such as pseudorotaxanes [275,

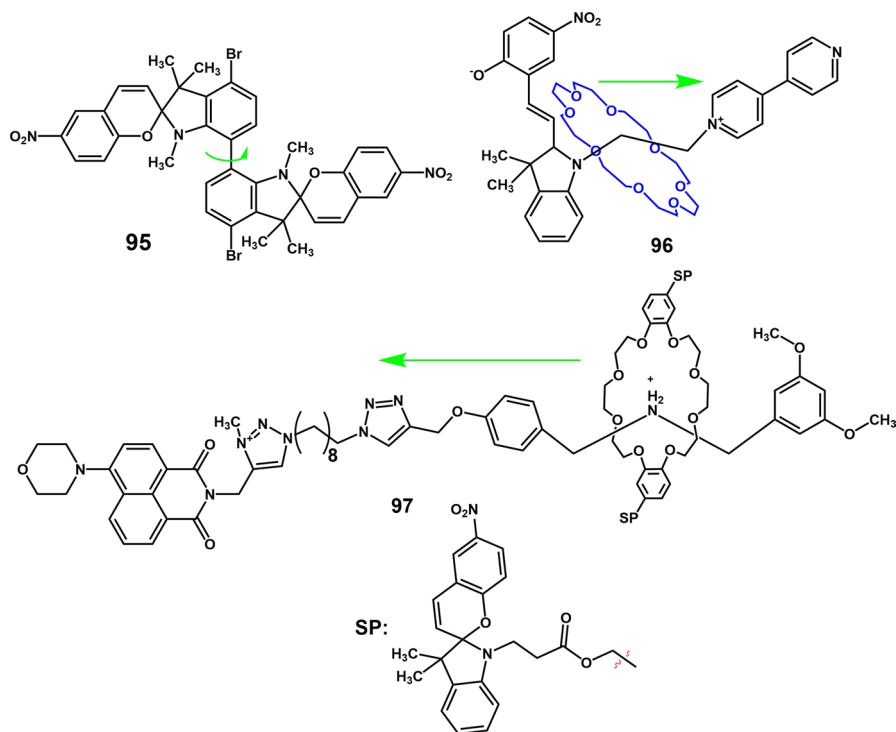


Fig. 24 Chemical structures of bis spiropyran **95**, pseudorotaxane **96**, and rotaxane **97**

366] and rotaxanes [367, 368] have also been described (Fig. 24). In this case, the movement along the guest molecule can be caused by planarization and the appearance of a positive charge on the indoline moiety of spiropyran during the transition to the merocyanine form, as in compound **96**, and as a result of the guest molecule protonation (the case of **97**). The complexation of spiropyran-containing ligands with platinum compounds allows the creation of photochromic macrocycles capable of contracting, expanding, and exhibiting high fatigue resistance [369].

In recent years, the design and creation of molecular mechanisms based on DNA and RNA chains have been actively developing. In the scope of these studies, the introduction of spiropyran molecules into polynucleotide sequences was repeatedly proposed; however, due to the high flexibility and tendency of the resulting structures to degrade in aqueous media, the idea did not gain popularity. These issues were later eliminated in the work of Brieke et al. [95] through the use of cationic spiropyran. Samples of polyphosphate derivatives **99** containing it in the backbone of the chain possessed high solubility and hydrolytic stability in aqueous media in contrast to previously obtained nucleoside sequence **98** as shown in Fig. 25.

The far-reaching prospects are opened by the tendency of spiropyrans for self-organization upon transformation between the SP and MC forms. It has been observed in liquid crystals [370–372] and hydrogels [373, 374], and during the formation of dendrimer micelles [375, 376]. This phenomenon made it possible to control the morphology of nanomaterials with light [377] and to create amazing nano-assemblies. Several polymeric [201, 378, 379], metallic [380, 381], and core–shell nanoparticles [382] with switchable properties have been also obtained based on spiropyrans. Such systems often demonstrate fluorescence properties unusual for individual spiropyrans [383].

The attachment of molecules to the surface of the nanostructured material can additionally stabilize the MC isomers [384]. The method of MC form stabilization

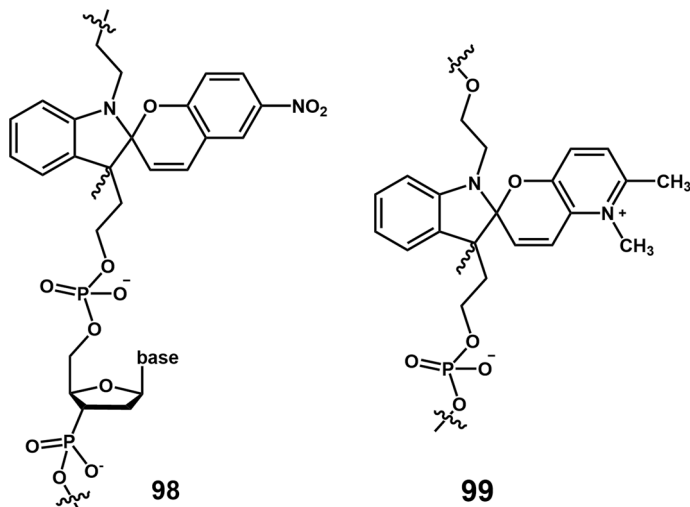


Fig. 25 The chemical structures of alkyl polyphosphate chains containing spiropyrans

through complexation was recently proposed by Seiler et al. [385]. In this case, the formation of brightly colored crystalline forms was achieved due to the formation of halogen bonds between spiropyran molecules and the range of substituted halobenzenes as halogen donors. This approach demonstrates the extraordinary trigger type that can be used to control the spiropyran properties and opens up new possibilities for the design of photochromic materials using the co-crystallization method. Samanta et al. established that the MC form can be stabilized by incorporation of spiropyrans into flexible Mukherjee coordination cages [386]. The obtained molecular assemblies were also characterized by good water solubility.

4.4 Prospects for Applications in Photobiology and Photopharmacology

Changing the properties of closed systems without the need to violate their integrity is certainly of interest and utility, especially in living organisms. Since light is one of the least penetrating types of exposure, spiropyrans are considered as highly promising molecular switches for this purpose. The introduction of spiropyran into living systems makes it possible to study and control bioprocesses *in vitro*. The main requirements for such systems are water solubility and stability in the aqueous medium. Good results were demonstrated by derivatives **100** containing ionic fragments [387] and grafted onto water-soluble polymeric materials [388, 389] or carbon nanostructures [390] spiropyran **101** (Fig. 26).

The ability for tunable aggregation with spiropyrans allows the enzymatic activity to be controlled (Fig. 27) [391]. In addition, they can be associated with cells to anchor them during biological tests [392]. The material developed for this purpose is a silicon-carbon surface modified with spiropyran-containing poly-2-hydroxyethylmethacrylate. The researchers reported the effective binding of cancer cells using pre-precipitated bovine serum albumin and streptavidin as a bridge. Moreover, several targeted drug delivery systems have been developed based on the controlled micelle formation of spiropyran-modified surfactants and polymers [321].

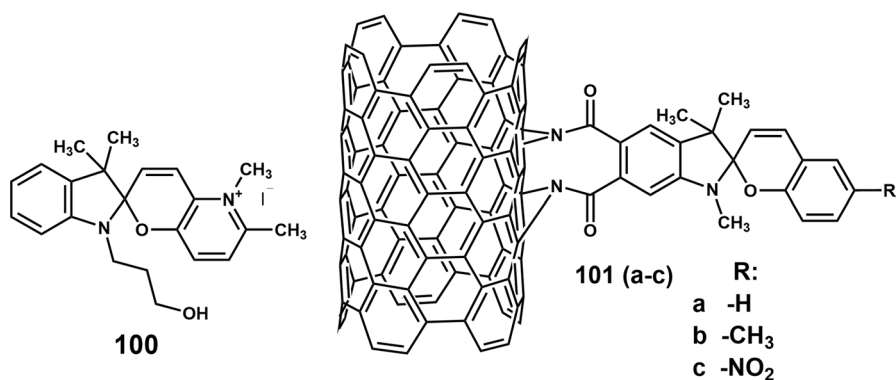


Fig. 26 The chemical structures of spiropyran systems with high solubility and stability in aqueous medium

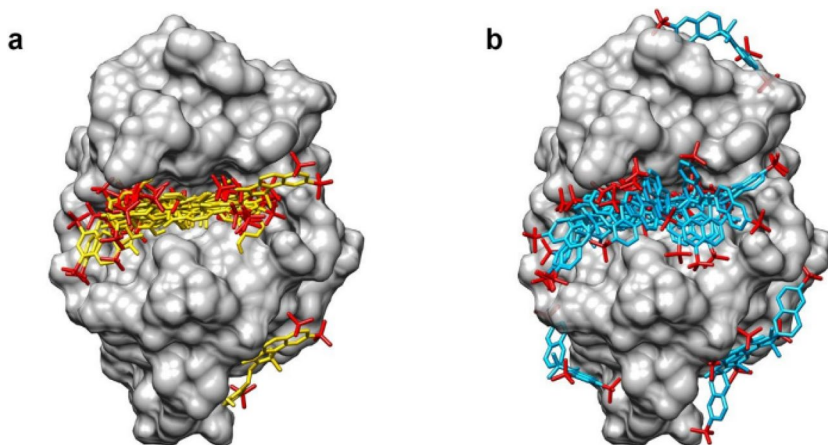
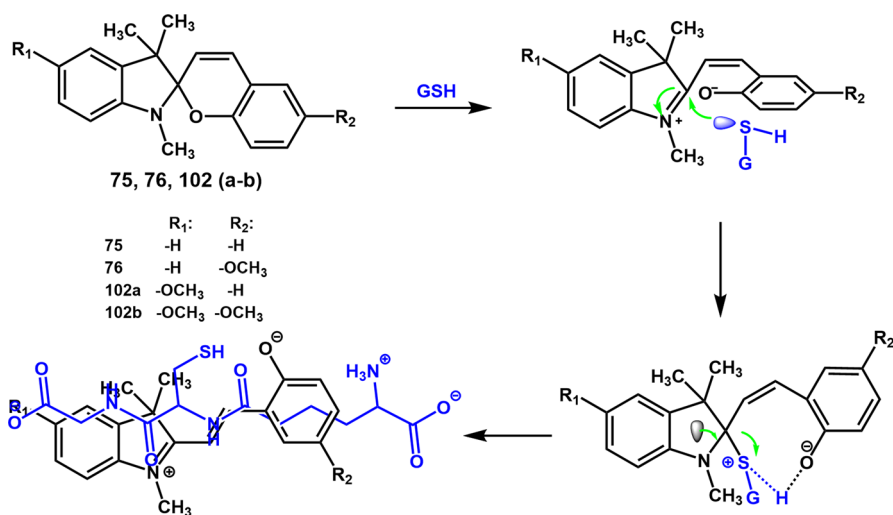


Fig. 27 Control of lysozyme enzymatic activity by spiropyran aggregation in MC (a) and SP (b) forms. Reprinted from Ref. [391] with permission (Copyright 2019 American Chemical Society)

A wide range of fluorescent biomarkers have been developed based on spiropyrans. In this case, the position of the MC emission maximum is the most important characteristic aside from the fluorescence intensity. Since living tissues have natural fluorescence in the green range of the spectrum, it is necessary to obtain the most contrasting fluorescence of the marker for effective detection. The wavelength range suitable for this is called the “biological window” and lies between 650 and 1300 nm. Such markers allow to observe the vital activity of individual cells and bacterial cultures [393] and even to track the activity of individual organelles: lysosomes and mitochondria [394, 395]. Due to the ability



Scheme 23 Proposed mechanism of interaction between spiropyran and glutathione molecules

to bind to certain molecules with high selectivity, spiropyrans are postulated as effective biosensors for the early diagnosis of Alzheimer's disease [396] or oxidative stress. In the latter case, molecules of glutathione (GSH), an effective natural antioxidant [162, 397, 398], are used as markers. Garcia et al. emphasized that the ability of spiropyrans to detect GSH is largely influenced by the electronic effects of substituents [162]. The systems **75**, **76**, **102(a, b)** (Scheme 23), which exist in solutions as a mixture of SP and MC forms, demonstrated a very good response. A mechanism for the interaction of glutathione with spiropyran molecules was proposed based on NMR spectroscopy data. The ring-opening was initiated by GSH nucleophilic attack and further MC stabilization due to the mutual orientation of GSH and MC charged moieties, as shown in Scheme 23. Researchers from Southern Federal University offered a spectrophotometric and fluorescent probe for glutathione and cysteine sensing using 5,6'-dichloro-1,3,3-trimethylspiro[indoline-2,2'-2*H*-pyrano[2,3]quinoline] [399]. The proposed methods are characterized by low limits of detection, which are quite sufficient to quantify analytes at the level of their physiological concentration. Using a solid-phase nanofiber mat containing spiropyran **26** in their composition provided a means for ratiometric fluorescence sensing and fine visual colorimetric detection of tetracycline based on a unique dynamic solid-phase sensing mode [400]. This is of great significance for food safety and human health. Kurihara et al. succeeded in photocontrol of cellular uptake using selective adsorption of indoline spiropyran with nitro and pyridinium groups on albumin [401]. This made it possible to track the cellular uptake of anti-cancer drugs.

The ability of spiropyran complexes with metals for pronounced fluorescence is also often used for early diagnosis of various diseases. The most widely explored metals are lithium [258, 402], zinc [269, 403, 404], aluminum [270], and calcium [405]. In addition, spiropyran complexes are utilized for smart delivery [277, 376], ion detection [281, 404], and ion channel operation control [200, 405].

Spiropyrans can be used as photoswitching molecules within the concept of photopharmacology [406, 407]. The addition of spiropyran units into the structure

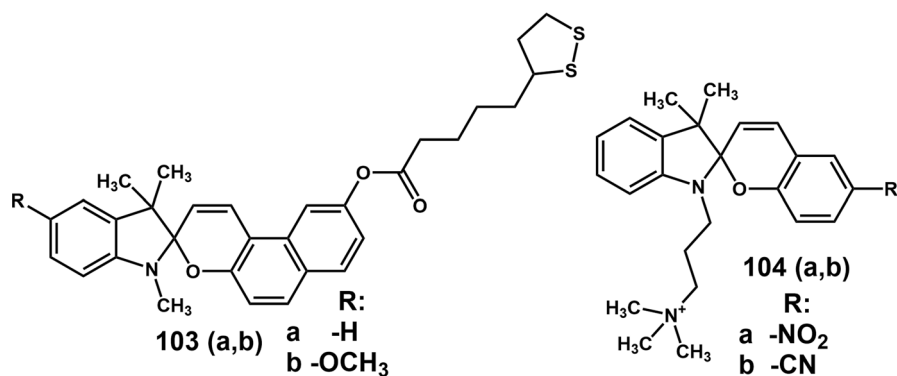
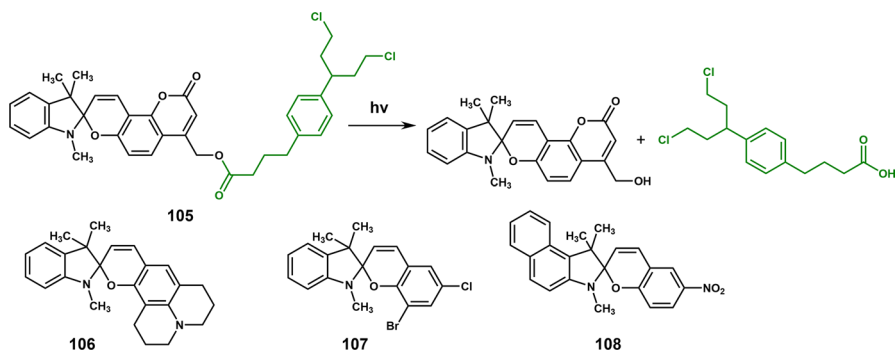


Fig. 28 Spiropyrans with potential bioactivity



Scheme 24 Structure and processes underlying target delivery of chlorambucil using spiropyran and structures of spiropyrans used for separation by dynamic enantioselective crystallization method

of biologically active substances allows their bioactivity to be controlled and may lead to an increase in selectivity, which in turn will reduce or completely avoid potentially serious side effects of proposed drugs.

Spiropyran **103** (a, b) (Fig. 28) containing the α -lipoic acid fragment were obtained and tested for their cytotoxicity and antioxidant activity [48, 408, 409]. The results of cytotoxicity studies showed unpredictable bio-safety of the hybrids in comparison with the parent hydroxyl-substituted spiropyran and α -lipoic acid. Thus, while the parent spiropyran differed in their toxicity from slightly to extremely toxic, their hybrids appeared surprisingly and similarly safe at both investigated concentrations. At the higher concentration of 2 mM, they were even less toxic than α -lipoic acid, which is well known for its bio-safety. It was also shown that both hybrids possess emergent biochemical and signaling antioxidant properties, exceeding those of α -lipoic acid. Kurihara et al. demonstrated the possibility for photocontrol of cytotoxicity toward HeLa cells for amphiphilic salt spiropyran with hydrophobic hexyl and hydrophilic pyridinium groups introduced in the structure as substituents in the indoline and 2*H*-chromene moieties, respectively [410]. This research could lead to the development of novel next-generation photochemotherapy and photoimmunotherapy drugs.

A significant challenge in the field of photopharmacology is the development of gentle anticancer agents. The key problem is the lack of selectivity in the therapeutics, which leads to healthy cell death. The main feature of tumor cells is imbalance in the acidity level of the medium in their localized areas [411]. Thus, the concentration of hydrogen ions is higher inside a cancer cell than outside. Firstly, this difference allows the use of spiropyran for fluorescent detection of the localized tumor formation [412]. Moreover, the drug can be administered or activated locally in the future. The cytotoxic effect of the MC forms of some spiropyran including **104** (a, b) on tumor cells was confirmed earlier [413–415]. Rad et al. [416] created a multifunctional smart nanoprobe based on spiropyran for targeted photodynamic and photothermal therapy, and the selective removal of brain cancer cells (C6 glioma).

In addition to their own toxic effects, spiropyran can be used as targeted drug delivery systems. For example, Barman et al. proposed a monomolecular chlorambucil

delivery system. Its mode of action is based on the photolytic cleavage of a drug molecule from coumarin-containing spiropyran **105** (Scheme 24) [412] or derivatives, which are incorporated into the bilipid layer of the cell membrane to facilitate drug penetration [417]. The controlled opening of micelles caused by a great difference in the dipole moment between the SP and photogenerated MC forms was developed for the same purpose [418]. A photoresponsive molecular-gated drug delivery system based on silicone-hydrogel interpenetrating polymer networks functionalized with carboxylated spiropyran was developed and investigated by Ghani et al. [419]. Light-induced drug release of a model substance (doxycycline) showed that the spiropyran (SP) molecules provide a hydrophobic layer around the drug carrier and have a good gate-closing efficiency for a system with 20–30% hydrogel content. However, drug delivery systems operating in the NIR range are more significant, since activating radiation is less destructive and has the greatest penetration depth in living tissues [420]. On the other hand, there are systems that do not require the use of activating radiation. Thus, a team of authors from the University of Nottingham proposed an alternative means of drug release using ultrasound at a frequency of 1 MHz. This was achieved by incorporating a mechanoresponsive 6-nitro-substituted indoline spiropyran or its *N*-alkylcarboxylated derivative into the liposomal lipid bilayer [421].

Non-toxic spiropyran **106** was proposed for using in early cancer diagnostics due to its ability to produce an intense fluorescence response when bound to guanine quadruplex structures [422].

The spiropyrans allow the biological activity of some compounds to be controlled by changing the molecular structure [48, 423] or acidity of the medium. For instance, spiropyran **82** can increase the antimicrobial effect of colistin against *Pseudomonas aeruginosa* upon irradiation [424], reducing the required dosage of this antibiotic and diminishing its effect on the body. Moreover, this spiropyran itself is non-toxic to mammalian cells. When photoacid without colistin was spiked to the bacterial medium, a sharp decrease in the number of colonies was also observed. However, the combined action was more effective.

Since the activity and effect of many pharmaceuticals and bioactive species strongly depend on their optical isomeric form, it should be kept in mind that racemization is observed quite often in them [64, 148, 194]. Achieving stereoselectivity in the synthesis of spiropyrans is extremely difficult due to the high rate of racemization. Ishikawa et al. showed the possibility of racemate separation by the dynamic enantioselective crystallization method [425]. Using compounds **107** and **108** as an example (Scheme 24), the authors demonstrated the effectiveness of Viedma ripening to obtain crystals of one of the enantiomers. In the case of compound **107**, the possibility of separation of the racemic mixture by introducing a seed crystal of a pure enantiomer was observed.

5 Summary and Outlook

In the current review, we have attempted to take a fresh look at the well-known family of organic “multi-chromic” compounds—indoline spiropyrans. Although the first representatives of these compounds were obtained more than 80 years ago, every

new year of studies brings something new to the variety of properties and possible applications of spirocyan systems. A variety of materials with controlled properties can be designed based on them, and the interest in this direction has increased continuously in recent decades. In each case, the future field of application determines the properties that the compounds should have. Studies of the structure and properties of even one family of spirocyan described in this work are still very far from completion. Even a small structural change can lead to a strong variation in the rate and mutual stability of the isomeric forms. This becomes possible due to an extremely strong dependence between the chemical hardness of the spirocycle and the electronic effects of substituents. In addition to a direct impact on the photo-, thermo-, and other -chromic characteristics, some substituents allow certain properties to be imparted to the system, such as water solubility, the ability to covalently bind with the surfaces, and so on. The structure–property relationships are the key point of material developers’ interest, which allows them to support and optimize their work. The general pattern of currently known structure–property relationships can be summarized as follows:

- The addition of electron-withdrawing groups into benzopyran moiety and electron-donating ones into the indoline cycle promotes the tendency of spirocyan opening and leads to a more stable MC.
- The introduction of heteroatoms to the benzopyran moiety also facilitates photoisomerization by increasing the contribution of low-lying MOs and following decreasing the highest occupied molecule orbital (HOMO)–lowest unoccupied molecule orbital (LUMO) gap.
- The photoinduced MC lifetime can be increased by the presence of bulky substituents prone to internal rotations near the C_{spiro} due to the steric hindrances.
- Formation of an extended conjugation chain or extreme electron deficit in benzopyran moiety caused by a strong $-I$ substituent effect stabilizes an MC and can sometimes lead to the appearance of such interesting phenomena as negative or bidirectional photochromism.
- Solid-state photochromism is typically observed for powders or crystalline structures with a high volume of cavities (for example, cationic derivatives or spirocyan containing bulky side groups).
- Regarding acidochromic properties, the pH value of the sudden color change point gradually increases passing from electron-withdrawing to donor substituents. The sensitivity of acid-induced isomerization depends mainly on the strength of the acid, and the coloration of all protonated forms is similar.
- For effective complex formation, the presence of only phenolate MC oxygen is not sufficient in most cases, and the addition of other chelating centers is necessary.

Throughout the history of spirocyan research, a huge number of potential applications have been proposed in various fields of science and technology. The most common areas of research during this time have been the creation of devices for recording and storing information, elements of molecular electronics and photonics, and various types of sensors. Many years of fundamental research on new properties

of spirocyclic compounds and the application of their useful features, together with other organic and inorganic substances, have led to the creation of a huge number of hybrid and smart materials. Thanks to these materials, the range of applications of spiropyrans has increased significantly, and this has happened uninterruptedly. Nowadays, the use of this class of compounds in photopharmacology, creating drug delivery systems, applying them as fluorescent probes and markers for bioimaging studies, and creating mechanosensitive materials and photocontrolled molecular photomagnets is rapidly gaining popularity. Research is also underway on the utilization of spiropyrans as elements of anti-counterfeiting signs and high-level encryption, dye-sensitized solar cells, and photocontrolled conductive polymers. It is important that in recent years, increasing numbers of unique opportunities have been reported for the potential practical use of spiropyrans at the junction of these areas. The clearest example of this is the design of a system for detecting mechanical damage to the brain. The constantly expanding range of applications of spirocyclic compounds, both by themselves and as part of hybrid and functional materials, suggests that research on this topic is highly relevant and will remain so in the future.

Acknowledgements This work was financially supported by the Ministry of Science and Higher Education of the Russian Federation; project 0852-2020-00-19.

Data availability This work is a review article, readers will need to contact referenced authors to obtain additional information regarding the data presented.

Declarations

Conflict of interest There are no conflicts of interest.

References

1. Bouas-Laurent H, Dürr H (2001) Organic photochromism (IUPAC Technical Report). *Pure Appl Chem* 73:639–665. <https://doi.org/10.1351/pac200173040639>
2. Crano JC, Guglielmetti RJ (2002) Organic photochromic and thermochromic compounds, vol 1. Kluwer Academic Publishers, New York
3. Klajn R (2014) Spiropyran-based dynamic materials. *Chem Soc Rev* 43:148–184. <https://doi.org/10.1039/c3cs60181a>
4. Lukyanov BS, Lukyanova MB (2005) Spiropyrans: synthesis, properties, and application (review). *Chem Heterocycl Compd* 4:281–311. <https://doi.org/10.1007/s10593-005-0148-x>
5. Burri P (1982) Indolospiropyrane compounds, US4339385A/en
6. Wizinger R, Wenning H (1940) Über intramolekulare Ionisation. *Helv Chim Acta* 43:247–271. <https://doi.org/10.1002/hlca.19400230133>
7. Luk'yanov BS, Nivorozhkin LE, Minkin VI (1993) Photo- and thermochromic spirans. *Chem Heterocycl Compd* 29:52–154. <https://doi.org/10.1007/BF00531656>
8. Kagawa N, Takabatake H, Masuda Y (2014) Synthesis of 3'-allylindoline spirobenzopyrans derived from 3-allyl-3H-indoles. *Tetrahedron Lett* 55:6427–6431. <https://doi.org/10.1016/j.tetlet.2014.09.121>
9. Kleizienė N, Amankavičienė V, Berg U, Schicktzan C, Schlothauer K, Šačkus A (2006) Cyclization of nitrospirobenzopyrans to bridged benzoxazepino[3,2-a]indoles. *Monatsh Chem* 137:1109–1117. <https://doi.org/10.1007/s00706-005-0504-7>
10. Abdollahi A, Roghani-Mamaqani H, Salami-Kalajahi M, Razavi B, Sahandi-Zangabad K (2020) Encryption and optical authentication of confidential cellulosic papers by ecofriendly

- multi-color photoluminescent inks. *Carbohydr Polym* 245:116507. <https://doi.org/10.1016/j.carbpol.2020.116507>
11. Ryabukhin YI, Mezheritskii VV, Dorofeenko GN (1975) Synthesis of 4H-1,3-benzoxazin-4-onium salts and 4-H-1,3-benzoxazin-4-ones. *Chem Heterocycl Comp* 11:404–407. <https://doi.org/10.1007/BF00502422>
 12. Luk'yanov BS, Ryabukhin YuI, Dorofeenko GN, Nivorozhkin LE, Minkin VI (1978) Photochromic and thermochromic spirans. *Chem Heterocycl Compd* 14:122–127. <https://doi.org/10.1007/BF00945321>
 13. Voloshin NA, Chernyshev AV, Metelitsa AV, Raskita IM, Voloshina EN, Minkin VI (2005) Spiropyran and spirooxazines. 3. Synthesis of photochromic 5'-(4,5-diphenyl-1,3-oxazol-2-yl)-spiro[indoline-2,3'-naphtho[2,3-b]pyran]. *Russ Chem Bull* 54:705–710. <https://doi.org/10.1007/s11172-005-0308-2>
 14. Chernyshev AV, Voloshin NA, Raskita IM, Metelitsa AV, Minkin VI (2006) Photo- and ionochromism of 5'-(4,5-diphenyl-1,3-oxazol-2-yl) substituted spiro[indoline-naphthopyrans]. *J Photochem Photobiol A* 184:289–297. <https://doi.org/10.1016/j.jphotochem.2006.04.042>
 15. Pargaonkar JG, Patil SK, Vajekar SN (2017) Greener route for the synthesis of photo- and thermochromic spiropyran using a highly efficient, reusable, and biocompatible choline hydroxide in an aqueous medium. *Synth Commun* 48:208–215. <https://doi.org/10.1080/00397911.2017.1395053>
 16. Swinson H, Perry A (2020) Three-component spiropyran synthesis via tandem alkylation-condensation. *Tetrahedron* 76:131219. <https://doi.org/10.1016/j.tet.2020.131219>
 17. Pugachev AD, Kozlenko AS, Lukyanova MB, Lukyanov BS, Tkachev VV, Shilov GV, Demidov OP, Minkin VI, Aldoshin SM (2019) One-pot synthesis and structure study of a new indoline spiropyran with cationic substituent. *Dokl Chem* 488:252–256. <https://doi.org/10.1134/S0012500819100021>
 18. Laptev AV, Lukin AYu, Belikov NE, Zvezdin KV, Demina OV, Barachevsky VA, Varfolomeev SD, Khodonov AA, Shvets VI (2014) Synthesis and studies of photochromic properties of spirobenzopyran carboxy derivatives and their model compounds as potential markers. *Russ Chem Bull* 63:2026–2035. <https://doi.org/10.1007/s11172-014-0695-3>
 19. Laptev AV, Belikov NE, Lukin AYu, Strokach YuP, Barachevsky VA, Alfimov MV, Demina OV, Shvets VI, Skladnev DA, Khodonov AA (2008) Synthesis of spiropyran analogues of retinal and study of their interaction with bacterioopsin from *Halobacterium salinarum*. *Russ J Bioorg Chem* 34:276–284. <https://doi.org/10.1134/S1068162008020179>
 20. Nikolaeva OG, Metelitsa AV, Cheprasov AS, Karlutova OYu, Starikov AG, Dubonosov AD, Bren VA, Minkin VI (2016) Synthesis and studies of new photochromic spiropyran containing a formylcoumarin fragment. *Russ Chem Bull Int Ed* 65:944–951. <https://doi.org/10.1007/s11172-016-1396-x>
 21. Luk'yanov BS, Nivorozhkin LE, Minkin VI (1993) Photo- and thermochromic spirans. *Chem Heterocycl Compd* 29:152–154. <https://doi.org/10.1007/BF00531656>
 22. Laptev AV, Lukin AY, Belikov NE, Shvets VI, Demina OV, Barachevskii VA, Khodonov AA (2009) RF Patent No. 2358977
 23. Demina OV, Levin PP, Belikov NE, Laptev AV, Lukin AYu, Barachevsky VA, Shvets VI, Varfolomeev SD, Khodonov AA (2013) Synthesis and photochromic reaction kinetics of unsaturated spiropyran derivatives. *J Photochem Photobiol A* 270:60–66. <https://doi.org/10.1016/j.jphotochem.2013.06.023>
 24. Zvezdin KV, Belikov NE, Laptev AV, Lukin AYu, Demina OV, Levin PP, Brichtkin SB, Spirin MG, Razumov VF, Shvets VI, Khodonov AA (2012) New hybrid photochromic materials with switchable fluorescence. *Nanotechnol Russia* 7:308–317. <https://doi.org/10.1134/S1995078012030172>
 25. Galimov DI, Tuktarov AR, Sabirov DSh, Khuzin AA, Dzhemilev UM (2019) Reversible luminescence switching of a photochromic fullerene[60]-containing spiropyran. *J Photochem Photobiol A* 375:64–70. <https://doi.org/10.1016/j.jphotochem.2019.02.017>
 26. Solov'eva EV, Rostovtseva IA, Shepelenko KE, Voloshin NA, Chernyshev AV, Borodkin GS, Trofimova NS, Metelitsa AV, Minkin VI (2018) Synthesis and complex formation of rhodamine-substituted spirobenzopyranindolines. *Russ J Gen Chem* 88:968–972. <https://doi.org/10.1134/S1070363218050225>
 27. Solovyova EV, Rostovtseva IA, Shepelenko KE, Voloshin NA, Chernyshev AV, Borodkin GS, Metelitsa AV, Minkin VI (2017) Synthesis and complex formation of spirobenzopyranindolines containing rhodamine fragment. *Russ J Gen Chem* 87:1007–1014. <https://doi.org/10.1134/S107036321705019X>

28. Laptev AV, Lukin AYu, Belikov NE, Barachevskii VA, Demina OV, Khodonov AA, Varfolomeev SD, Shvets VI (2013) Ethynyl-equipped spirobenzopyrans as promising photochromic markers for nucleic acid fragments. *Mendeleev Commun* 23:145–146. <https://doi.org/10.1016/j.mencom.2013.05.008>
29. Lukyanov B, Vasilyuk G, Mukhanov E, Ageev L, Lukyanova M, Alexeenko Y, Besugliy S, Tkachev V (2009) Multifunctional spirocyclic systems. *Int J Photoenergy* 2009:689450. <https://doi.org/10.1155/2009/689450>
30. Lukyanova MB, Tkachev VV, Lukyanov BS, Aldoshin SM, Utenyshev AN, Bezuglyi SO, Minkin VI, Kogan VA (2008) Photo- and thermochromic spiranes 31.* Structure and photochromic properties of functionalized benzoxazine spiroopyrans. *Chem Heterocycl Comp* 44:1384–1390. <https://doi.org/10.1007/s10593-009-0189-7>
31. Shiraiishi Y, Tanaka K, Hirai T (2013) Colorimetric sensing of Cu(II) in aqueous media with a spiroopyran derivative via an oxidative dehydrogenation mechanism. *ACS Appl Mater Interfaces* 5:3456–3463. <https://doi.org/10.1021/am4005804>
32. Komissarova OA, Lukyanov BS, Lukyanova MB, Ozhogin IV, Mukhanov EL, Korobov MS, Rostovtseva IA, Minkin VI (2017) New indoline spiroopyrans containing azomethine fragment. *Russ Chem Bull* 66:2122–2125. <https://doi.org/10.1007/s11172-017-1990-6>
33. Komissarova OA, Luk'yanov BS, Luk'yanova MB, Makarova NI, Rostovtseva IA, Ozhogin IV, Korobov MS (2018) New photochromic spiroopyrans with ortho-hydroxyaldimine substituent. *Dokl Chem* 482:229–232. <https://doi.org/10.1134/S001250081810004X>
34. Liubimov AV, Venidiktova OV, Valova TM, Shienok AI, Koltsova LS, Liubimova GV, Popov LD, Zaichenko NL, Barachevsky VA (2018) Photochromic and luminescence properties of a hybrid compound based on indoline spiroopyran of the coumarin type and azomethinocoumarin. *Photochem Photobiol Sci* 17:1365–1375. <https://doi.org/10.1039/C8PP00172C>
35. Zhao W, Carreira EM (2005) Solid-phase synthesis of photochromic spiroopyrans. *Org Lett* 7:1609–1612. <https://doi.org/10.1021/ol050302b>
36. Keum SR, Roh HJ, Choi YK, Lim SS, Kim SH, Koh K (2005) Complete ^1H and ^{13}C NMR spectral assignment of symmetric and asymmetric bis-spiroopyran derivatives. *Magn Reson Chem* 43:873–876. <https://doi.org/10.1002/mrc.1640>
37. Ozhogin IV, Chernyavina VV, Lukyanov BS, Malay VI, Rostovtseva IA, Makarova NI, Tkachev VV, Lukyanova MB, Metelitsa AV, Aldoshin SM (2019) Synthesis and study of new photochromic spiroopyrans modified with carboxylic and aldehyde substituents. *J Mol Struct* 1196:409–416. <https://doi.org/10.1016/j.molstruc.2019.06.094>
38. Satoh T, Sumaru K, Takagi T, Takai K, Kanamori T (2011) Isomerization of spirobenzopyrans bearing electron-donating and electron-withdrawing groups in acidic aqueous solutions. *Phys Chem Chem Phys* 13:7322–7329. <https://doi.org/10.1039/c0cp01989e>
39. Boulmier A, Vacher A, Zang D, Yang S, Saad A, Marrot J, Oms O, Mialane P, Ledoux I, Ruhlmann L, Lorcy D, Dolbecq A (2018) Anderson-type polyoxometalates functionalized by tetrathiafulvalene groups: synthesis, electrochemical studies, and NLO properties. *Inorg Chem* 57:3742–3752. <https://doi.org/10.1021/acs.inorgchem.7b02976>
40. Dridi H, Boulmier A, Bolle P, Dolbecq A, Rebilly J-N, Banse F, Ruhlmann L, Serier-Brault H, Dessapt R, Mialane P, Oms O (2020) Directing the solid-state photochromic and luminescent behaviors of spiro molecules with Dawson and Anderson polyoxometalate units. *J Mater Chem C* 8:637–649. <https://doi.org/10.1039/c9tc05906g>
41. Laptev AV, Lukin AYu, Belikov NE, Demina OV, Khodonov AA, Shvets VI (2014) New maleimide spirobenzopyran derivatives as photochromic labels for macromolecules with sulfhydryl groups. *Mendeleev Commun* 24:245–246. <https://doi.org/10.1016/j.mencom.2014.06.020>
42. Sugahara A, Tanaka N, Okazawa A, Matsushita N, Kojima N (2014) Photochromic property of anionic spiroopyran with sulfonate-substituted indoline moiety. *Chem Lett* 43:281–283. <https://doi.org/10.1246/cl.130904>
43. Johns VK, Wang Z, Li X, Liao Y (2013) Physicochemical study of a metastable-state photoacid. *J Phys Chem A* 117:13101–13104. <https://doi.org/10.1021/jp409111m>
44. Florea L, Wagner K, Wagner P, Wallace GG, Benito-Lopez F, Officer DL, Diamond D (2014) Photo-chemopropulsion—light-stimulated movement of microdroplets. *Adv Mater* 26:7339–7345. <https://doi.org/10.1002/adma.201403007>

45. Seiler VK, Callebaut K, Robeyns K, Tumanov N, Wouters J, Champagne B, Leyssens T (2018) Acidochromic spiropyran–merocyanine stabilisation in the solid state. *CrystEngComm* 20:3318–3327. <https://doi.org/10.1039/c8ce00291f>
46. May F, Peter M, Hütten A, Prodi L, Mattay J (2011) Synthesis and characterization of photoswitchable fluorescent SiO₂ nanoparticles. *Chem Eur J* 18:814–821. <https://doi.org/10.1002/chem.201102961>
47. Shi Z, Peng P, Strohecker D, Liao Y (2011) Long-lived photoacid based upon a photochromic reaction. *J Am Chem Soc* 133:14699–14703. <https://doi.org/10.1021/ja203851c>
48. Ozhogin IV, Zolotukhin PV, Mukhanov EL, Rostovtseva IA, Makarova NI, Tkachev VV, Beseda DK, Metelitsa AV, Lukyanov BS (2021) Novel molecular hybrids of indoline spiropyran and α -lipoic acid as potential photopharmacological agents: synthesis, structure, photochromic and biological properties. *Bioorg Med Chem Lett* 31:127709. <https://doi.org/10.1016/j.bmcl.2020.127709>
49. Malai VI, Ozhogin IV, Lukyanov BS, Mukhanov EL, Lukyanova MB, Makarova NI, Rostovtseva IA (2018) Novel spirocyclic condensation products of Gossypol and Fischer's bases. *Chem Nat Compd* 54:1081–1084. <https://doi.org/10.1007/s10600-018-2560-3>
50. Ozhogin IV, Tkachev VV, Mukhanov EL, Lukyanov BS, Chernyshev AV, Lukyanova MB, Aldoshin SM (2015) Studies of structure and photochromic properties of spiropyran based on 4,6-diformyl-2-methylresorcinol. *Russ Chem Bull* 64:672–676. <https://doi.org/10.1007/s11172-015-0917-3>
51. Lukyanov BS, Alekseenko YuS, Mukhanov EL, Lukyanova MB, Metelitsa AV, Khalanskij KN, Tkachev VV, Ryashin ON (2007) Spiropyran containing the reactive substituents in the 2H-chromene moiety. *Int J Photoenergy* 2007:010583. <https://doi.org/10.1155/2007/10583>
52. Ozhogin IV, Chernyshev AV, Butova VV, Lukyanov BS, Radchenko EA, Mukhanov EL, Soldatov AV (2020) Structure and photochromic properties of new spiropyran of indoline series containing free carboxylic groups. *J Synth Investig* 14:534–539. <https://doi.org/10.1134/S1027451020030362>
53. Perry A, Davis K, West L (2018) Synthesis of stereochemically-biased spiropyran by microwave-promoted, one-pot alkylation–condensation. *Org Biomol Chem* 16:7245–7254. <https://doi.org/10.1039/C8OB01996G>
54. Schulz-Senft M, Gates PJ, Sönnichsen FD, Staubitz A (2017) Diversely halogenated spiropyran—useful synthetic building blocks for a versatile class of molecular switches. *Dyes Pigment* 136:292–301. <https://doi.org/10.1016/j.dyepig.2016.08.039>
55. Ozhogin IV, Tkachev VV, Lukyanov BS, Mukhanov EL, Chernyshev AV, Komissarova OA, Minkin VI, Aldoshin SM (2016) Synthesis and study of photochromic asymmetric bis-spiropyran. *Dokl Chem* 471:378–383. <https://doi.org/10.1134/S0012500816120090>
56. Mukhanov EL, Alekseenko YS, Lukyanov BS, Dorogan IV, Bezuglyi SO (2010) New photochromic nonsymmetric bis-spiropyran of the 2,3-dihydro-4-oxonaphtho[2,1-e][1,3]oxazine series. *High Energy Chem* 44:220–223. <https://doi.org/10.1134/S0018143910030112>
57. Alekseenko YuS, Lukyanov BS, Utenyshev AN, Mukhanov EL, Kletskii ME, Tkachev VV, Kravchenko NN, Minkin VI, Aldoshin SM (2006) Photo- and thermo-chromic spiranes. 24. Novel photochromic spiropyran from 2,4-dihydroxyisophthalaldehyde. *Chem Heterocycl Compd* 42:803–812. <https://doi.org/10.1007/s10593-006-0165-4>
58. Ozhogin IV, Mukhanov EL, Chernyshev AV, Pugachev AD, Lukyanov BS, Metelitsa AV (2020) Synthesis and study of new photochromic unsymmetrical bis-spiropyran with nonequivalent heteroarene fragments conjugated through the common 2*H*,8*H*-pyranof[2,3-*f*]chromene moiety. *J Mol Str* 1221:128808. <https://doi.org/10.1016/j.molstruc.2020.128808>
59. Nikolaeva OG, Karlutova OY, Cheprasov AS, Metelitsa AV, Dorogan IV, Dubonosov AD, Bren'VA (2015) Synthesis of bis-spiropyran based on 6,8-diformyl-5,7-dihydroxy-4-methylcoumarin and photochromic properties thereof. *Chem Heterocycl Comp* 51:229–233. <https://doi.org/10.1007/s10593-015-1689-2>
60. Chen P, Wang Y, Zhang Y-M, Zhang SX-A (2016) Design, synthesis and property study of bispiropyran switchable molecule based on acridone. *Acta Chim Sin* 74:669–675. <https://doi.org/10.6023/A16040162>
61. Samsoniya ShA, Trapaidze MV, Nikoleishvili NN, Japaridze KG, Maisuradze JP, Kazmaier U (2011) New condensed indoline bis-spiropyran. *Chem Heterocycl Comp* 47:1098–1104. <https://doi.org/10.1007/s10593-011-0880-3>
62. Mardaleishvili IR, Lyubimova GV, Lyubimov AV, Koltsova LS, Shienok AI, Levin PP, Tatikolov AS, Zaichenko NL (2019) Reverse photochromism of nitrosubstituted bispiropyran based on benzopyrroloindole. *High Energy Chem* 53:13–21. <https://doi.org/10.1134/S0018143919010089>

63. Lee S, Ji S, Kang Y (2012) Synthesis and characterizations of bis-spiropyran derivatives. *Bull Korean Chem Soc* 33:3740–3744. <https://doi.org/10.5012/bkcs.2012.33.11.3740>
64. Kundu PK, Lerner A, Kučanda K, Leitus G, Klajn R (2014) Cyclic kinetics during thermal equilibration of an axially chiral bis-spiropyran. *J Am Chem Soc* 136:11276–11279. <https://doi.org/10.1021/ja505948q>
65. Nourmohammadian F, Abdi AA (2016) Development of molecular photoswitch with very fast photoresponse based on asymmetrical bis-azospiropyran. *Spectrochim Acta A Mol Biomol Spectrosc* 153:53–62. <https://doi.org/10.1016/j.saa.2015.07.110>
66. Qi Q, Li C, Liu X, Jiang S, Xu Z, Lee R, Zhu M, Xu B, Tian W (2017) Solid-state photoinduced luminescence switch for advanced anticounterfeiting and super-resolution imaging applications. *J Am Chem Soc* 139:16036–16039. <https://doi.org/10.1021/jacs.7b07738>
67. Wang L, Xiong W, Tang H, Cao D (2019) A multistimuli-responsive fluorescent switch in the solution and solid states based on spiro[fluorene-9,9'-xanthene]-spiropyran. *J Mater Chem C* 7:9102–9111. <https://doi.org/10.1039/C9TC02129A>
68. Ma G, Zhou Q, Zhang X, Xu Y, Liu H (2014) Crown ethers with spiropyran units incorporated in the ring frameworks for pH-triggered ion recognition at the air–water interface. *New J Chem* 38:552–560. <https://doi.org/10.1039/C3NJ01238G>
69. Khalanskiy KN, Alekseenko YuS, Lukyanov BS, Borodkin GS, Bezuglyi SO (2012) Photo- and thermochromic spirans 36.* Synthesis, structure and photochromic properties of 7',7''-{1,4-phenylenedi(methylene)-bis(5-chloro-1,3,3-trimethyl-1,3-dihydrospiro-[indole-2,3'-pyranol[3,2-f]quinolinium])} diiodide. *Chem Heterocycl Comp* 48:1090–1097. <https://doi.org/10.1007/s10593-012-1114-z>
70. Li H, Ding J, Chen S, Beyer C, Liu S-X, Wagenknecht H-A, Hauser A, Decurtins S (2013) Synthesis and redox and photophysical properties of benzodifuran-spiropyran ensembles. *Chem Eur J* 19:6459–6466. <https://doi.org/10.1002/chem.201204043>
71. Dissanayake DS, McCandless GT, Stefan MC, Biewer MC (2017) Systematic variation of thiophene substituents in photochromic spiropyran. *Photochem Photobiol Sci* 16:1057–1062. <https://doi.org/10.1039/C7PP00057J>
72. Parrot A, Izzet G, Chamoreau L-M, Proust A, Oms O, Dolbecq A, Hakouk K, El Bekkachi H, Deniard P, Dessapt R, Mialane P (2013) Photochromic properties of polyoxotungstates with grafted spiropyran molecules. *Inorg Chem* 52:11156–11163. <https://doi.org/10.1021/ic401380a>
73. Burns CT, Choi SY, Dietz ML, Firestone MA (2008) Acidichromic spiropyran-functionalized mesoporous silica: towards stimuli-responsive metal ion separations media. *Sep Sci Technol* 43:2503–2519. <https://doi.org/10.1080/01496390802122311>
74. Lee J, Choi EJ, Kim I, Lee M, Satheshkumar C, Song C (2017) Tuning sensory properties of triazole-conjugated spiropyran: metal-ion selectivity and paper-based colorimetric detection of cyanide. *Sensors* 17:1816. <https://doi.org/10.3390/s17081816>
75. Ivashenko O, van Herpt JT, Rudolf P, Feringa BL, Browne WR (2013) Oxidative electrochemical aryl C-C coupling of spiropyran. *Chem Commun* 49:6737–6739. <https://doi.org/10.1039/C3CC42396D>
76. Ivashenko O, van Herpt JT, Feringa BL, Rudolf P, Browne WR (2013) Electrochemical write and read functionality through oxidative dimerization of spiropyran self-assembled monolayers on gold. *J Phys Chem C* 117:18567–18577. <https://doi.org/10.1021/jp406458a>
77. Kortekaas L, Ivashenko O, van Herpt JT, Browne WR (2016) A remarkable multitasking double spiropyran: bidirectional visible-light switching of polymer-coated surfaces with dual redox and proton gating. *J Am Chem Soc* 138:1301–1312. <https://doi.org/10.1021/jacs.5b11604>
78. Natali M, Giordani S (2012) Interaction studies between photochromic spiropyran and transition metal cations: the curious case of copper. *Org Biomol Chem* 10:1162–1171. <https://doi.org/10.1039/C1OB06375H>
79. Yu Q, Su X, Zhang T, Zhang Y-M, Li M, Liu Y, Zhang SX-A (2018) Non-invasive fluorescence switch in polymer films based on spiropyran-photoacid modified TPE. *J Mater Chem C* 6:2113–2122. <https://doi.org/10.1039/C7TC05142E>
80. Xiong Y, Rivera-Fuentes P, Sezgin E, Jentsch AV, Eggeling C, Anderson HL (2016) Photoswitchable spiropyran dyads for biological imaging. *Org Lett* 18:3666–3669. <https://doi.org/10.1021/acs.orglett.6b01717>
81. Zhu J-F, Yuan H, Chan W-H, Lee AWM (2010) A FRET fluorescent chemosensor SPAQ for Zn²⁺ based on a dyad bearing spiropyran and 8-aminoquinoline unit. *Tetrahedron Lett* 51(27):3550–3554. <https://doi.org/10.1016/j.tetlet.2010.04.127>

82. Doddi S, Narayanaswamy K, Ramakrishna B, Singh SP, Bangal PR (2016) Synthesis and spectroscopic investigation of diketopyrrolopyrrole—spiropyran dyad for fluorescent switch application. *J Fluoresc* 26:1939–1949. <https://doi.org/10.1007/s10895-016-1886-0>
83. Park IS, Jung Y-S, Lee K-J, Kim J-M (2010) Photoswitching and sensor applications of a spiropyran–polythiophene conjugate. *Chem Commun* 46:2859–2861. <https://doi.org/10.1039/B926211C>
84. Perry A, Green SJ, Horsell DW, Hornett SM, Wood ME (2015) A pyrene-appended spiropyran for selective photo-switchable binding of Zn(II): UV–visible and fluorescence spectroscopy studies of binding and non-covalent attachment to graphene, graphene oxide and carbon nanotubes. *Tetrahedron* 71:6776–6783. <https://doi.org/10.1016/j.tet.2015.07.035>
85. Kawanishi Y, Seki K, Tamaki T, Sakuragi M, Suzuki Y (1997) Tuning reverse ring closure in the photochromic and thermochromic transformation of 1',3',3'-trimethyl-6-nitrospiro[2H-1-benzopyran-2,2'-indoline] analogues by ionic moieties. *J Photochem Photobiol A* 109:237–242. [https://doi.org/10.1016/S1010-6030\(97\)00141-X](https://doi.org/10.1016/S1010-6030(97)00141-X)
86. Yagi S, Maeda K, Nakazumi H (1999) Photochromic properties of cationic merocyanine dyes. Thermal stability of the spiropyran form produced by irradiation with visible light. *J Mater Chem* 9:2991–2997. <https://doi.org/10.1039/A905098A>
87. Hammarson M, Nilsson JR, Li S, Lincoln P, Andréasson J (2014) DNA-binding properties of amidine-substituted spiropyran photoswitches. *Chemistry* 20:15855–15862. <https://doi.org/10.1002/chem.201405113>
88. Sanina NA, Aldoshin SM, Shilov GV, Kurganova EV, Yurieva EA, Voloshin NA, Minkin VI, Nadochenko VA, Morgunov RB (2008) Synthesis and photochemical and magnetic properties of Cr, Mn, Fe, and Co complexes based on the 1-[(1',3',3'-trimethyl-spiro[2H-1-benzopyran-2,2'-indolin]-8-yl)methyl]pyridinium cation. *Russ Chem Bull* 57:1451–1460. <https://doi.org/10.1007/s11172-008-0188-3>
89. Voloshin NA, Bezugliy SO, Solov'eva EV, Metelitsa AV, Minkin VI (2008) Photo- and thermochromic spiranes. 31.* Photochromic cationic spiropyranes with a pyridinium fragment in the aliphatic side chain*. *Chem Heterocycl Comp* 44:1229–1237. <https://doi.org/10.1007/s10593-009-0175-0>
90. Zimmermann T, Brede O (2003) Ring transformations of heterocyclic compounds. XXIII. The UV irradiation product of photochromic 2,4,6-triaryl-1-(spiro[2H-1-benzopyran-2,2'-indoline]-6-yl)pyridinium salts - A phenolate betaine or a pyridinium substituted merocyanine dye? *J Heterocycl Chem* 40:611–616. <https://doi.org/10.1002/jhet.5570400409>
91. Bénard S, Yu P (2000) New spiropyranes showing crystalline-state photochromism. *Adv Mater* 12:48–50. [https://doi.org/10.1002/\(SICI\)1521-4095\(200001\)12:1%3c48::AID-ADMA48%3e3.0.CO;2-G](https://doi.org/10.1002/(SICI)1521-4095(200001)12:1%3c48::AID-ADMA48%3e3.0.CO;2-G)
92. Aldoshin SM, Nikonova LA, Shilov GV, Bikanina EA, Artemova NK, Smirnov VA (2006) The influence of an N-substituent in the indoline fragment of pyrano-pyridine spiropyran salts on their crystalline structure and photochromic properties. *J Mol Str* 794:103–109. <https://doi.org/10.1016/j.molstruc.2006.01.041>
93. Yurieva EA, Aldoshin SM, Nikonova LA, Shilov GV, Nadochenko VA (2011) 1-Benzyl-3,3,5',6'-tetramethylspiro[indoline-2,2'-[2H]pyrano[3,2-b]-pyridinium] iodide, its hydrate, and a neutral precursor of the salts: synthesis, crystal structure, photochromic transformations in solutions and in crystals. *Russ Chem Bull* 60:1401–1408. <https://doi.org/10.1007/s11172-011-0210-z>
94. Tkachev VV, Aldoshin SM, Sanina NA, Lukyanov BS, Minkin VI, Utenyshev AN, Khalanskiy KN, Alekseenko YuS (2007) Photo- and thermochromic spiranes. 29. New photochromic indolinospiryranes containing a quinoline fragment. *Chem Heterocycl Compd* 43:576–586. <https://doi.org/10.1007/s10593-007-0092-z>
95. Brieke C, Heckel A (2013) Spiropyran photoswitches in the context of DNA: synthesis and photochromic properties. *Chem Eur J* 19:15726–15734. <https://doi.org/10.1002/chem.201302640>
96. Stafforst T, Hilvert D (2009) Kinetic characterization of spiropyran in aqueous media. *Chem Commun* 3:287–288. <https://doi.org/10.1039/B818050D>
97. Tkachev VV, Lukyanova MB, Lukyanov BS, Pugachev AD, Aldoshi SM, Minkin VI (2016) Investigation of a new product of a condensation reaction between 1,2,3,3-tetramethylindolenilium perchlorate and 2,6-diformyl-4-methyl-phenol. *J Struct Chem* 57:1270–1271. <https://doi.org/10.1134/S0022476616060299>

98. Luk'yanova MB, Tkachev VV, Pugachev AD, Luk'yanov BS, Shilov GV, Minkin VI, Aldoshin SM (2018) New salt spiropyran of indoline series with fluorine substituent. *Dokl Chem* 480:81–84. <https://doi.org/10.1134/S0012500818050014>
99. Pugachev AD, Lukyanova MB, Tkachev VV, Lukyanov BS, Makarova NI, Shilov GV, Rostovtseva IA, Lapshina LS, Minkin VI, Aldoshin SM (2019) New photochromic salt spiropyrans of indoline series. *Dokl Chem* 484:58–63. <https://doi.org/10.1134/S0012500819020113>
100. Pugachev AD, Lukyanova MB, Lukyanov BS, Ozhogin IV, Kozlenko AS, Rostovtseva IA, Makarova NI, Tkachev VV, Aksenov NA (2019) New photochromic indoline spiropyrans containing cationic substituent in the 2H-chromene moiety. *J Mol Str* 1178:590–598. <https://doi.org/10.1016/j.molstruc.2018.10.062>
101. Pugachev AD, Ozhogin IV, Lukyanova MB, Lukyanov BS, Rostovtseva IA, Dorogan IV, Makarova NI, Tkachev VV, Metelitsa AV, Aldoshin SM (2020) Visible to near-IR molecular switches based on photochromic indoline spiropyrans with a conjugated cationic fragment. *Spectrochim Acta A* 230:118041. <https://doi.org/10.1016/j.saa.2020.118041>
102. Kozlenko AS, Makarova NI, Ozhogin IV, Pugachev AD, Lukyanova MB, Rostovtseva IA, Borodkin GS, Stankevich NV, Metelitsa AV, Lukyanov BS (2021) New indoline spiropyrans with highly stable merocyanine forms. *Mendeleev Commun* 31:403–406. <https://doi.org/10.1016/j.mencom.2021.04.040>
103. Pugachev AD, Lukyanova MB, Lukyanov BS, Ozhogin IV, Kozlenko AS, Tkachev VV, Chepurnoi PB, Shilov GV, Minkin VI, Aldoshin SM (2020) Replacement of the hetarene moiety of molecule in the synthesis of indoline spiropyran with cationic fragment. *Dokl Chem* 492:76–83. <https://doi.org/10.1134/S0012500820350013>
104. Yue Y, Huo F, Lee S, Yin C, Yoon J, Chao J, Zhang Y, Cheng F (2016) A dual colorimetric/fluorescence system for determining pH based on the nucleophilic addition reaction of an O-hydroxymercocyanine dye. *Chemistry* 22:1239–1243. <https://doi.org/10.1002/chem.201504395>
105. Karton-Lifshin N, Segal E, Omer L, Portnoy M, Satchi-Fainaro R, Shabat D (2011) A unique paradigm for a turn-ON near-infrared cyanine-based probe: noninvasive intravital optical imaging of hydrogen peroxide. *J Am Chem Soc* 133:10960–10965. <https://doi.org/10.1021/ja203145v>
106. Pugachev AD, Ozhogin IV, Makarova NI, Rostovtseva IA, Lukyanova MB, Kozlenko AS, Borodkin GS, Tkachev VV, El-Sewify IM, Dorogan IV, Metelitsa AV, Aldoshin SM, Lukyanov BS (2022) Novel polychromogenic fluorine-substituted spiropyrans demonstrating either uni- or bidirectional photochromism as multipurpose molecular switches. *Dyes Pigm* 199:110043. <https://doi.org/10.1016/j.dyepig.2021.110043>
107. Gao H, Guo T, Chen Y, Kong Y, Peng Z (2016) Reversible negative photochromic sulfo-substituted spiropyrans. *J Mol Str* 1123:426–432. <https://doi.org/10.1016/j.molstruc.2016.07.050>
108. Schnurbus M, Kabat M, Jarek E, Krzan M, Warszynski P, Braunschweig B (2020) Spiropyran sulfonates for photo- and pH-responsive air-water interfaces and aqueous foam. *Langmuir* 36:6871–6879. <https://doi.org/10.1021/acs.langmuir.9b03387>
109. Takagi K (1996) Ionic spiropyran compound and photochromic material conjugated it with clay, Patent EP0738728A2
110. Moldenhauer D, Gröhn F (2017) Water-soluble spiropyrans with inverse photochromism and their photoresponsive electrostatic self-assembly. *Chem Eur J* 23:3966–3978. <https://doi.org/10.1002/chem.201605621>
111. Kortekaas L, Browne WR (2019) The evolution of spiropyran: fundamentals and progress of an extraordinarily versatile photochrome. *Chem Soc Rev* 48:3406–3424. <https://doi.org/10.1039/C9CS00203K>
112. Fischer E, Hirschberg Y (1952) Formation of coloured forms of spirans by low-temperature irradiation. *J Chem Soc (Res)*. <https://doi.org/10.1039/jr9520004518>
113. Heiligman-Rim R, Hirschberg Y, Fischer E (1962) Photochromism in spiropyrans. Part V. 1 On the mechanism of phototransformation. *J Phys Chem* 66:2470–2477. <https://doi.org/10.1021/j100818a036>
114. Sklar AL (1937) Theory of color of organic compounds. *J Chem Phys* 5:669–681. <https://doi.org/10.1063/1.1750099>
115. Lewis GN, Calvin M (1939) The color of organic substances. *Chem Rev* 25:273–328. <https://doi.org/10.1021/cr60081a004>
116. Rogers RA, Rodier AR, Stanley JA, Douglas NA, Li X, Brittain WJ (2014) A study of the spiropyran–merocyanine system using ion mobility-mass spectrometry: experimental support for the cisoid conformation. *Chem Commun* 50:3424–3426. <https://doi.org/10.1039/C3CC47697A>

117. Naumov P, Yu P, Sakurai K (2008) Electronic tera-order stabilization of photoinduced metastable species: structure of the photochromic product of spiropyran determined with in situ single crystal X-ray photodiffraction. *J Phys Chem A* 112:5810–5814. <https://doi.org/10.1021/jp711922k>
118. Fleming C, Li S, Grøtli M, Andréasson J (2018) Shining new light on the spiropyran photoswitch: a photocage decides between cis–trans or spiro-merocyanine isomerization. *J Am Chem Soc* 140:14069–14072. <https://doi.org/10.1021/jacs.8b09523>
119. Hobley J, Malatesta V, Millini R, Montanari L, Neil Parker OW (1999) Proton exchange and isomerisation reactions of photochromic and reverse photochromic spiro-pyrans and their merocyanine forms. *Phys Chem Chem Phys* 1:3259–3267. <https://doi.org/10.1039/A902379H>
120. Nuernberger P, Ruetzel S, Brixner T (2015) Multidimensional electronic spectroscopy of photochemical reactions. *Angew Chem Int Ed* 54:11368–11386. <https://doi.org/10.1002/anie.201502974>
121. Toppet S, Quintens W, Smets G (1975) NMR study of the inversion at carbon 2 of some 1'3'3'-trimethylindolino disubstituted spirobenzopyranes. *Tetrahedron* 31:1957–1958. [https://doi.org/10.1016/0040-4020\(75\)87058-X](https://doi.org/10.1016/0040-4020(75)87058-X)
122. Metelitsa A, Chernyshev A, Voloshin N, Solov'eva E, Rostovtseva I, Dorogan I, Gaeva E, Guseva A (2021) Semipermanent merocyanines of spirocyclic compounds: photochromic “balance.” *Dyes Pigm* 186:109070. <https://doi.org/10.1016/j.dyepig.2020.109070>
123. Metelitsa A, Chernyshev A, Voloshin N, Demidov O, Solov'eva E, Rostovtseva I, Gaeva E (2021) Photo-controlled bipolar absorption switches based on 5-dimethylamino substituted indoline spiropyrans with semipermanent merocyanines. *New J Chem* 45:13529–13538. <https://doi.org/10.1039/d1nj02371c>
124. Kinashi K, Miyamae Y, Nakamura R, Sakai W, Tsutsumi N, Yamane H, Hatsukano G, Ozaki M, Jimbo K, Okabe T (2015) A spiropyran-based X-ray sensitive fiber. *Chem Commun* 51:11170–11173. <https://doi.org/10.1039/C5CC03977K>
125. Hirshberg Y (1957) Formation of reversible colored modifications at low temperatures by bombardment with electrons. *J Chem Phys* 27:758–763. <https://doi.org/10.1063/1.1743827>
126. Joubert-Doriol L, Lasorne B, Lauvergnat D, Meyer H-D, Gatti F (2014) A generalised vibronic-coupling Hamiltonian model for benzopyran. *J Chem Phys* 140:044301. <https://doi.org/10.1063/1.4861226>
127. Gonon B, Lasorne B, Karras G, Joubert-Doriol L, Lauvergnat D, Billard F, Lavorel B, Faucher O, Guérin S, Hertz E, Gatti F (2019) A generalized vibronic-coupling Hamiltonian for molecules without symmetry: application to the photoisomerization of benzopyran. *J Chem Phys* 150:124109. <https://doi.org/10.1063/1.5085059>
128. Saab M, Joubert-Doriol L, Lasorne B, Guérin S, Gatti F (2014) A quantum dynamics study of the benzopyran ring opening guided by laser pulses. *Chem Phys* 442:93–102. <https://doi.org/10.1016/j.chemphys.2014.01.016>
129. Chibisov AK, Görner H (1997) Singlet versus triplet photoprocesses in indodicarbocyanine dyes and spiropyran-derived merocyanines. *J Photochem Photobiol A* 105:261–267. [https://doi.org/10.1016/S1010-6030\(96\)04604-7](https://doi.org/10.1016/S1010-6030(96)04604-7)
130. Sheng Y, Leszczynski J, Garcia AA, Rosario R, Gust D, Springer J (2004) Comprehensive theoretical study of the conversion reactions of spiropyrans: substituent and solvent effects. *J Phys Chem B* 108:16233–16243. <https://doi.org/10.1021/jp0488867>
131. Breslin VM, Barbour NA, Dang D-K, Lopez SA, Garcia-Garibay MA (2018) Nanosecond laser flash photolysis of a 6-nitroindolinospirocyanine in solution and in nanocrystalline suspension under single excitation conditions. *Photochem Photobiol Sci* 17:741–749. <https://doi.org/10.1039/C8PP00095F>
132. Dorogan IV, Minkin VI (2016) Theoretical modeling of electrocyclic 2H-pyran and 2H-1,4-oxazine ring opening reactions in photo- and thermochromic spiropyrans and spirooxazines. *Chem Heterocycl Compd* 52:730–735. <https://doi.org/10.1007/s100593-016-1956-x>
133. Roohi H, Rostami T (2020) Mechanism of the photo triggered ring-opening reaction of spiropyran derivatives (SP-X₁₋₇; X₁₋₇ = H, NO₂, CF₃, CN, OH, OMe and NMe₂) in the gas phase and various solvent media: a GD3-TD-DFT approach. *Chemistry* 392:112410. <https://doi.org/10.1016/j.jphotochem.2020.112410>
134. Sanchez-Lozano M, Estévez CM, Hermida-Ramón J, Serrano-Andres L (2011) Ultrafast ring-opening/closing and deactivation channels for a model spiropyran-merocyanine system. *J Phys Chem A* 115:9128–9138. <https://doi.org/10.1021/jp2062095>

135. Prager S, Burghardt I, Dreuw A (2014) Ultrafast $C_{\text{spiro}}-O$ dissociation via a conical intersection drives spiropyran to merocyanine photoswitching. *J Phys Chem A* 118:1339–1349. <https://doi.org/10.1021/jp4088942>
136. Futami Y, Chin MLS, Kudoh S, Takayanagi M, Nakata M (2003) Conformations of nitro-substituted spiropyran and merocyanine studied by low-temperature matrix-isolation infrared spectroscopy and density functional theory calculation. *Chem Phys Lett* 370:460–468. [https://doi.org/10.1016/S0009-2614\(03\)00136-2](https://doi.org/10.1016/S0009-2614(03)00136-2)
137. Aldoshin SM, Bozhenko KV, Utenyshev AN (2013) Quantum chemical study of the $C_{\text{spiro}}-O$ bond dissociation in spiropyran molecules. *Russ Chem Bull* 62:1740–1743. <https://doi.org/10.1007/s11172-013-0250-7>
138. Wang PX, Bai FQ, Zhang ZX, Wang YP, Wang J, Zhang HX (2017) The theoretical study of substituent and charge effects in the conformational transformation process of molecular machine unit spiropyran. *Org Electron Phys Mater Appl* 45:33–41. <https://doi.org/10.1016/j.orgel.2017.02.031>
139. Abdel-Mottaleb SA, Ali SN (2016) A new approach for studying bond rupture/closure of a spiro benzopyran photochromic material: reactivity descriptors derived from frontier orbitals and DFT computed electrostatic potential energy surface maps. *Int J Photoenergy* 2016:6765805. <https://doi.org/10.1155/2016/6765805>
140. Liu F, Morokuma K (2013) Multiple pathways for the primary step of the spiropyran photochromic reaction: a CASPT2/CASSCF study. *J Am Chem Soc* 135:10693–10702. <https://doi.org/10.1021/ja402868b>
141. Liu F, Kurashige Y, Yanai T, Morokuma K (2013) Multireference ab initio density matrix renormalization group (DMRG)-CASSCF and DMRG-CASPT2 study on the photochromic ring opening of spiropyran. *J Chem Theory Comput* 9:4462–4469. <https://doi.org/10.1021/ct400707k>
142. Savarese M, Raucci U, Netti PA, Adamo C, Rega N, Ciofini I (2016) A qualitative model to identify non-radiative decay channels: the spiropyran as case study. *Theor Chem Acc* 135:1–7. <https://doi.org/10.1007/s00214-016-1966-x>
143. Zhai G, Shao S, Wu S, Lei Y, Dou Y (2014) Detailed molecular dynamics of the photochromic reaction of spiropyran: a semiclassical dynamics study. *Int J Photoenergy* 2014:541791. <https://doi.org/10.1155/2014/541791>
144. Bittmann SF, Dsouza R, Siddiqui KM, Hayes SA, Rossos A, Corthey G, Kochman M, Prokhorenko VI, Murphy RS, Schwoerer H, Miller RJD (2019) Ultrafast ring-opening and solvent-dependent product relaxation of photochromic spironaphthopyran. *Phys Chem Chem Phys* 21:18119–18127. <https://doi.org/10.1039/C9CP02950H>
145. Kim D, Zhang Z, Xu K (2017) Spectrally resolved super-resolution microscopy unveils multipath reaction pathways of single spiropyran molecules. *J Am Chem Soc* 139:9447–9450. <https://doi.org/10.1021/jacs.7b04602>
146. Aldoshin SM (1990) Spiropyran: structural features and photochemical properties. *Russ Chem Rev* 59:663–684. <https://doi.org/10.1070/RC1990v059n07ABEH003549>
147. Nunes CM, Pereira NA, Fausto R (2022) Photochromism of a spiropyran in low-temperature matrices: unprecedented bidirectional switching between a merocyanine and an allene intermediate. *J Phys Chem A* 126:2222–2233. <https://doi.org/10.1021/acs.jpca.2c01105>
148. Sheng Y, Leszczynski J (2014) Thermal racemization of spiropyran: implication of substituent and solvent effects revealed by computational study. *Struct Chem* 25:667–677. <https://doi.org/10.1007/s11224-013-0374-2>
149. Buback J, Nuernberger P, Kullmann M, Langhojer F, Schmidt R, Würthner F, Brixner T (2011) Ring-closure and isomerization capabilities of spiropyran-derived merocyanine isomers. *J Phys Chem A* 115:3924–3935. <https://doi.org/10.1021/jp108322u>
150. Mendive-Tapia D, Kortekaas L, Steen JD, Perrier A, Lasorne B, Browne WR, Jacquemin D (2016) Accidental degeneracy in the spiropyran radical cation: charge transfer between two orthogonal rings inducing ultra-efficient reactivity. *Phys Chem Chem Phys* 18:31244–31253. <https://doi.org/10.1039/C6CP06907J>
151. Minkin VI, Metelitsa AV, Dorogan IV, Lukyanov BS, Besugliy SO, Micheau J (2005) Spectroscopic and theoretical evidence for the elusive intermediate of the photoinitiated and thermal rearrangements of photochromic spiropyran. *J Phys Chem A* 109:9605–9616. <https://doi.org/10.1021/jp050552+>
152. Menzonatto TG, Lopes JF (2022) The role of intramolecular interactions on the stability of the conformers of a spiropyran derivative. *Chem Phys* 562:111654. <https://doi.org/10.1016/j.chemphys.2022.111654>

153. Matczyszyn K, Olesiak-Banska J, Nakatani K, Yu P, Murugan NA, Zalesny R, Roztoczyńska A, Bednarska J, Bartkowiak W, Kongsted J, Ågren H, Samoć M (2015) One- and two-photon absorption of a spiropyran-merocyanine system: experimental and theoretical studies. *J Phys Chem B* 119:1515–1522. <https://doi.org/10.1021/jp5071715>
154. Ivashenko O, van Herpt JT, Feringa BL, Rudolf P, Browne WR (2013) UV/Vis and NIR light-responsive spiropyran self-assembled monolayers. *Langmuir* 29:4290–4297. <https://doi.org/10.1021/la400192c>
155. Ruetzel S, Diekmann M, Nuernberger P, Walter C, Engels B, Brixner T (2014) Photoisomerization among ring-open merocyanines. I. Reaction dynamics and wave-packet oscillations induced by tunable femtosecond pulses. *J Chem Phys* 140:22. <https://doi.org/10.1063/1.4881258>
156. Song X, Zhou J, Li Y, Tang Y (1995) Correlations between solvatochromism, Lewis acid-base equilibrium and photochromism of an indoline spiropyran. *J Photochem Photobiol A* 92:99–103. [https://doi.org/10.1016/1010-6030\(95\)04164-5](https://doi.org/10.1016/1010-6030(95)04164-5)
157. Cottone G, Noto R, La Manna G (2008) Density functional theory study of the trans-trans-cis (TTC)→trans-trans-trans (TTT) isomerization of a photochromic spiropyran merocyanine. *Molecules* 13:1246–1252. <https://doi.org/10.3390/molecules13061246>
158. Zanoni M, Coleman S, Fraser KJ, Byrne R, Wagner K, Gambhir S, Officer DL, Wallace GG, Diamond D (2012) Physicochemical study of spiropyran–terthiophene derivatives: photochemistry and thermodynamics. *Phys Chem Chem Phys* 14:9112–9120. <https://doi.org/10.1039/C2CP41137G>
159. Frolova LA, Rezvanov AA, Lukyanov BS, Sanina NA, Troshin PA, Aldoshin SM (2015) Design of rewritable and read-only non-volatile optical memory elements using photochromic spiropyran-based salts as light-sensitive materials. *J Mater Chem C* 3:11675–11680. <https://doi.org/10.1039/C5TC02100F>
160. Voloshin NA, Chernyshev AV, Solov'eva EV, Rostovtseva IA, Metelitsa AV, Borodkin GS, Kogan VA, Minkin VI (2014) Spiroyrans and spirooxazines 10. Synthesis of photochromic 5'-(1,3-benzoxazol-2-yl)-substituted spiro[indoline-naphthopyrans]. *Russ Chem Bull* 63:1373–1377. <https://doi.org/10.1007/s11172-014-0605-8>
161. Balmont EI, Tautges BK, Faulkner AL, Or VW, Hodur BM, Shaw JT, Louie AY (2016) Comparative evaluation of substituent effect on the photochromic properties of spiropyrans and spirooxazines. *J Org Chem* 81:8744–8758. <https://doi.org/10.1021/acs.joc.6b01193>
162. Garcia J, Addison JB, Liu SZ, Lu S, Faulkner AL, Hodur BM, Balmont EI, Or VW, Yun JH, Trevino K, Shen B, Shaw JT, Frank NL, Louie AY (2019) Antioxidant sensing by spiropyrans: substituent effects and NMR spectroscopic studies. *J Phys Chem B* 123:6799–6809. <https://doi.org/10.1021/acs.jpcc.9b03424>
163. Brügger O, Reichenbach T, Sommer M, Walter M (2017) Substituent correlations characterized by hammett constants in the spiropyran-merocyanine transition. *J Phys Chem A* 121:2683–2687. <https://doi.org/10.1021/acs.jpca.7b01248>
164. Görner H (2001) Photochromism of nitrospiropyrans: effects of structure, solvent and temperature. *Phys Chem Chem Phys* 3:416–423. <https://doi.org/10.1039/B007708I>
165. Chernyshev AV, Guda AA, Cannizzo A, Soloveva EV, Voloshin NA, Rusalev Y, Shapovalov VV, Smolentsev G, Soldatov AV, Metelitsa AV (2019) Operando XAS and UV–vis characterization of the photodynamic spiropyran-zinc complexes. *J Phys Chem B* 123:1324–1331. <https://doi.org/10.1021/acs.jpcc.8b11010>
166. Barbee MH, Kouznetsova T, Barrett SL, Gossweiler GR, Lin Y, Rastogi SK, Brittain WJ, Craig SL (2018) Substituent effects and mechanism in a mechanochemical reaction. *J Am Chem Soc* 140:12746–12750. <https://doi.org/10.1021/jacs.8b09263>
167. Solov'eva EV, Chernyshev AV, Voloshin NA, Metelitsa AV, Minkin VI (2013) Photo- and thermo-chromic spirans. 38*. New (1-alkyl-4,5-diphenyl)imidazolyl-substituted spirobenzopyrans. *Chem Heterocycl Comp* 48:1533–1538. <https://doi.org/10.1007/s10593-013-1169-5>
168. Levin PP, Tatikolov AS, Laptev AV, Lukin AY, Belikov NE, Demina OV, Khodonov AA, Shvets VI, Varfolomeev SD (2012) The investigation of the intermediates of spiropyran retinal analogs by laser flash photolysis techniques with different excitation wavelengths. *J Photochem Photobiol A* 231:41–44. <https://doi.org/10.1016/j.jphotochem.2011.12.024>
169. Dagilienė M, Martynaitis V, Vengris M, Redeckas K, Voiciuk V, Holzer W, Šačkus A (2013) Synthesis of 1',3,3',4-tetrahydrospiro[chromene-2,2'-indoles] as a new class of ultrafast light-driven molecular switch. *Tetrahedron* 69:9309–9315. <https://doi.org/10.1016/j.tet.2013.08.020>
170. Chernyshev AV, Voloshin NA, Rostovtseva IA, Demidov OP, Shepelenko KE, Solov'eva EV, Gaeva EB, Metelitsa AV (2020) Benzothiazolyl substituted spiropyrans with ion-driven

- photochromic transformation. *Dyes Pigm* 178:108337. <https://doi.org/10.1016/j.dyepig.2020.108337>
171. Voloshin NA, Bezuglyi SO, Metelitsa AV, Solov'evaShepelenkoMinkin EVKEVI (2012) Photo- and thermochromic spirans. 35.* Synthesis and photochromic properties of spiro[indoline-2,3'-pyrano[3,2-f]quinolines] and their cationic derivatives. *Chem Heterocycl Comp* 48:525–531. <https://doi.org/10.1007/s10593-012-1025-z>
 172. Tyurin RV, Lukyanov BS, Chernyshev AV, Malay VI, Kozlenko AS, Tkacheva NS, Burov ON, Lukyanova MB (2016) Effect of bulky substituents on the photochromic properties of indoline spiroopyrans containing an annelated aromatic or heteroaromatic fragment. *Dokl Chem* 470:268–273. <https://doi.org/10.1134/S0012500816090081>
 173. Zhou T, Lia Z, Wang J (2019) Spiropyran-based photoswitchable dimethylaminopyridine. *New J Chem* 43:8869–8872. <https://doi.org/10.1039/C9NJ01727E>
 174. Aakeröy CB, Hurley EP, Desper J, Natali M, Douglawi A, Giordani S (2010) The balance between closed and open forms of spiroopyrans in the solid state. *CrystEngComm* 12:1027–1033. <https://doi.org/10.1039/B914566D>
 175. Lukyanova MB, Tkachev VV, Lukyanov BS, Pugachev AD, Ozhogin IV, Komissarova OA, Aldoshin SM, Minkin VI (2018) Structure investigation of new condensation products of 1,2,3,3-tetramethylindolenium with metoxysubstituted diformylphenols. *J Struct Chem* 59:565–570. <https://doi.org/10.1134/S0022476618030095>
 176. Groom CR, Bruno IJ, Lightfoot MP, Ward SC (2016) The Cambridge structural database. *Acta Crystallogr Sect B* 72:171–179. <https://doi.org/10.1107/S2052520616003954>
 177. Chernyshev AV, Dorogan IV, Voloshin NA, Metelitsa AV, Minkin VI (2014) Spectroscopic, photochromic and kinetic properties of 5'-benzothiazolyl derivatives of spiroindolinenaphthopyrans: an experimental and theoretical study. *Dyes Pigm* 111:108–115. <https://doi.org/10.1016/j.dyepig.2014.05.032>
 178. Mukhanov EL, Alekseenko YuS, Dorogan IV, Tkachev VV, Lukyanov BS, Aldoshin SM, Bezuglyi SO, Minkin VI, Utenyshev AN, Ryashchin ON (2010) Photochromic and thermochromic spiranes 33. Synthesis of a new indolinonaphthoxazino- bis Spiropyran and investigation of its photochromic characteristics. *Chem Heterocycl Comp* 46:279–290. <https://doi.org/10.1007/s10593-010-0503-4>
 179. Kortekaas L, Steen JD, Duijnste DR, Jacquemin D, Browne WR (2020) Noncommutative switching of double spiroopyrans. *J Phys Chem A* 124:6458–6467. <https://doi.org/10.1021/acs.jpca.0c02286>
 180. Mukhanov EL, Dorogan IV, Chernyshev AV, Bezuglyi SO, Ozhogin IV, Lukyanova MB, Lukyanov BS (2013) Theoretical and experimental study of new photochromic bis-spiropyrans with hydroxyethyl and carboxyethyl substituents. *Int J Photoenergy* 2013:752949. <https://doi.org/10.1155/2013/752949>
 181. Liu D, Yu B, Su X, Wang X, Zhang Y-M, Li M, Zhang SX-A (2019) Photo-/baso-chromisms and the application of a dual-addressable molecular switch. *Asian J Chem* 14:2838–2845. <https://doi.org/10.1002/asia.201900600>
 182. Funasako Y, Miyazaki H, Sasaki T, Goshima K, Inokuchi M (2020) Synthesis, photochromic properties, and crystal structures of salts containing a pyridinium-fused spiroopyran: positive and negative photochromism in the solution and solid state. *J Phys Chem B* 124:7251–7257. <https://doi.org/10.1021/acs.jpcc.0c04994>
 183. Funasako Y, Okada H, Inokuchi M (2019) Photochromic ionic liquids containing cationic spiroopyran derivatives. *ChemPhotoChem* 3:28–30. <https://doi.org/10.1002/cptc.201800197>
 184. Menet C, Serier-Brault H, Oms O, Dolbecq A, Marrot J, Saad A, Mialane P, Jobic S, Deniarda P, Dessapt R (2015) Influence of electronic vs. steric factors on the solid-state photochromic performances of new polyoxometalate/spirooxazine and spiroopyran hybrid materials. *RSC Adv* 5:79635–79643. <https://doi.org/10.1039/C5RA15860E>
 185. Bénard S, Rivière E, Yu P, Nakatani K, Delouis JF (2001) A photochromic molecule-based magnet. *Chem Mater* 13:159–162. <https://doi.org/10.1021/cm001163p>
 186. Pugachev AD, Ozhogin IV, Lukyanova MB, Lukyanov BS, Kozlenko AS, Rostovtseva IA, Makarova NI, Tkachev VV, Aldoshin SM, Metelitsa AV (2021) Synthesis, structure and photochromic properties of indoline spiroopyrans with electron-withdrawing substituents. *J Mol Str* 1229:129615. <https://doi.org/10.1016/j.molstruc.2020.129615>
 187. Aldoshin SM, Nikonova LA, Smirnov VA, Shilov GV, Nagaeva NK (2005) Structure and photochromic properties of single crystals of spiroopyran salts. *J Mol Str* 750:158–165. <https://doi.org/10.1016/j.molstruc.2005.04.030>

188. Lukyanov BS, Metelitsa AV, Voloshin NA, Alexeenko YuS, Lukyanova MB, Vasilyuk GT, Maskovich SA, Mukhanov EL (2005) Solid state photochromism of spiropyrans. *Int J Photoenergy* 7:404697. <https://doi.org/10.1155/S1110662X05000036>
189. Lukyanov BS, Metelitsa AV, Lukyanova MB, Mukhanov EL, Borisenko NI, Alekseenko YS, Bezugliy SO (2005) Photochromism of the spiropyran thin solid films. *Mol Cryst Liq Cryst* 431:351–356. <https://doi.org/10.1080/15421400590946730>
190. Nickel F, Bernien M, Kraffert K, Krüger D, Arruda LM, Kippen L, Kuch W (2017) Reversible switching of spiropyran molecules in direct contact with a Bi(111) single crystal surface. *Adv Funct Mater* 27:1702280. <https://doi.org/10.1002/adfm.201702280>
191. Harada J, Kawazo Y, Ogawa K (2010) Photochromism of spiropyrans and spirooxazines in the solid state: low temperature enhances photocoloration. *Chem Commun* 46:2593–2595. <https://doi.org/10.1039/B925514A>
192. Suzuki M, Asahi T, Masuhara H (2002) Photochromic reactions of crystalline spiropyrans and spirooxazines induced by intense femtosecond laser excitation. *Phys Chem Chem Phys* 4:185–192. <https://doi.org/10.1039/B108108J>
193. Asahi T, Suzuki M, Masuhara H (2002) Cooperative photochemical reaction in molecular crystal induced by intense femtosecond laser excitation: photochromism of spironaphthooxazine. *J Phys Chem A* 106:2335–2340. <https://doi.org/10.1021/jp0129838>
194. Funasako Y, Ason M, Takebayashi J, Inokuchi M (2019) Solid-state photochromism of salts of cationic spiropyran with various anions: a correlation between reaction cavity volumes and reactivity. *Cryst Growth Des* 19:7308–7314. <https://doi.org/10.1021/acs.cgd.9b01185>
195. Yang Y, He J, He Z, Jiang G (2021) Enhancement of solid-state reversible photochromism by incorporation of rigid steric hindrance groups. *Adv Optical Mater* 9:2001584. <https://doi.org/10.1002/adom.202001584>
196. Sekine A, Tanaka M, Uekusa H, Yasuda N (2018) In situ control of photochromic behavior through dual photo-isomerization using cobaloxime complexes with a spiropyran derivative and 2-cyanoethyl ligands. *CrystEngComm* 20:6061–6069. <https://doi.org/10.1039/C8CE00982A>
197. Zhang L, Deng Y, Tang Y, Xie C, Wu Z (2021) Solid-state spiropyran exhibiting photochromic properties based on molecular flexibility. *Mater Chem Front* 5:3119–3124. <https://doi.org/10.1039/DOQM01086C>
198. Wu Z, Wang Q, Li P, Fanga B, Yin M (2021) Photochromism of neutral spiropyran in the crystalline state at room temperature. *J Mater Chem C* 9:6290–6296. <https://doi.org/10.1039/D1TC00974E>
199. Seiler VK, Tumanov N, Robeyns K, Wouters J, Champagne B, Leyssens T (2017) A structural analysis of spiropyran and spirooxazine compounds and their polymorphs. *Crystals* 7:84. <https://doi.org/10.3390/cryst7030084>
200. Dunne A, Delaney C, McKeon A, Nesterenko P, Paull B, Benito-Lopez F, Diamond D, Florea L (2018) Micro-capillary coatings based on spiropyran polymeric brushes for metal ion binding, detection, and release in continuous flow. *Sensors* 18:1083. <https://doi.org/10.3390/s18041083>
201. Schwartz HA, Olthof S, Schaniel D, Meerholz K, Ruschewitz U (2017) Solution-like behavior of photoswitchable spiropyran embedded in metal-organic frameworks. *Inorg Chem* 56:13100–13110. <https://doi.org/10.1021/acs.inorgchem.7b01908>
202. Martin CR, Park KC, Leith GA, Yu J, Mathur A, Wilson GR, Gange GB, Barth EL, Ly RT, Manley OM, Forrester KL, Karakalos SG (2022) Stimuli-modulated metal oxidation states in photochromic MOFs. *J Am Chem Soc* 144:4457–4468. <https://doi.org/10.1021/jacs.1c11984>
203. Truong VX, Ehrmann K, Seifermann M, Levkin PA, Barner-Kowollik C (2022) Wavelength orthogonal photodynamic networks. *Chem Eur J* 28:e202104466. <https://doi.org/10.1002/chem.202104466>
204. Grady ME, Birrenkott CM, May PA, White SR, Moore JS, Sottos NR (2020) Localization of spiropyran activation. *Langmuir* 36:5847–5854. <https://doi.org/10.1021/acs.langmuir.0c00568>
205. Bazzan I, Bolle P, Oms O, Salmi H, Aubry-Barroca N, Dolbecq A, Serier-Brault H, Dessapt R, Roger P, Mialane P (2017) The design of new photochromic polymers incorporating covalently or ionically linked spiropyran/polyoxometalate hybrids. *J Mater Chem C* 5:6343–6351. <https://doi.org/10.1039/C7TC01296A>
206. Attia MS, Khalil MH, Abdel-Mottaleb MSA, Lukyanova MB, Alekseenko YuA, Lukyanov B (2006) Effect of complexation with lanthanide metal ions on the photochromism of (1,3,3-trimethyl-5'-hydroxy-6'-formyl)-indoline-spiro,2',2'-[2H]chromene) in different media. *Int J Photoenergy* 2006:042846. <https://doi.org/10.1155/IJP/2006/42846>

207. Balasubramanian G, Schulte J, Müller-Plathe F, Böhm MC (2012) Structural and thermochemical properties of a photoresponsive spiropyran and merocyanine pair: basis set and solvent dependence in density functional predictions. *Chem Phys Lett* 554:60–66. <https://doi.org/10.1016/j.cplett.2012.10.014>
208. Eilmles A (2013) Spiropyran to merocyanine conversion: explicit versus implicit solvent modeling. *J Phys Chem A* 117:2629–2635. <https://doi.org/10.1021/jp3117209>
209. Tian W, Tian J (2014) An insight into the solvent effect on photo-, solvato-chromism of spiropyran through the perspective of intermolecular interactions. *Dyes Pigm* 105:66–74. <https://doi.org/10.1016/j.dyepig.2014.01.020>
210. Liu G, Li Y, Cui C, Wang M, Gao H, Gao J, Wang J (2022) Solvatochromic spiropyran—a facile method for visualized, sensitive and selective response of lead (Pb²⁺) ions in aqueous solution. *J Photochem Photobiol A* 424:113658. <https://doi.org/10.1016/j.jphotochem.2021.113658>
211. Florea L, McKeon A, Diamond D, Benito-Lopez F (2013) Spiropyran polymeric microcapillary coatings for photodetection of solvent polarity. *Langmuir* 29:2790–2797. <https://doi.org/10.1021/la304985p>
212. Gagliardi M, Pignatelli F, Mattoli V (2017) Time- and solvent-dependent self-assembly of photochromic crystallites. *J Phys Chem C* 121:24245–24251. <https://doi.org/10.1021/acs.jpcc.7b06388>
213. Gao M, Lian C, Xing R, Wang J, Wang X, Tian Z (2020) The photo-/thermo-chromism of spiropyran in alkanes as a temperature abuse indicator in the cold chain of vaccines. *New J Chem* 44:15350–15353. <https://doi.org/10.1039/D0NJ02975K>
214. Gerkman MA, Yuan S, Duan P, Taufan J, Schmidt-Rohra K, Han GGD (2019) Phase transition of spiropyran: impact of isomerization dynamics at high temperatures. *Chem Commun* 55:5813–5816. <https://doi.org/10.1039/C9CC02141H>
215. Ahmed SA, Okasha RM, Khairou KS, Afifi TH, Mohamed A-AH, Abd-El-Aziz AS (2017) Design of thermochromic polynorbornene bearing spiropyran chromophore moieties: synthesis, thermal behavior and dielectric barrier discharge plasma treatment. *Polymers* 9:630. <https://doi.org/10.3390/polym9110630>
216. Shiraishi Y, Itoh M, Hirai T (2010) Thermal isomerization of spiropyran to merocyanine in aqueous media and its application to colorimetric temperature indication. *Phys Chem Chem Phys* 12:13737–13745. <https://doi.org/10.1039/C0CP00140F>
217. Iqbal A, Iqbal G, Umar MN, Rashid H, Khan SW (2022) Synthesis of novel silica encapsulated spiropyran-based thermochromic materials. *R Soc Open Sci* 9:211385. <https://doi.org/10.1098/rsos.211385>
218. Julià-López A, Hernando J, Ruiz-Molina D, González-Monje P, Sedó J, Roscini C (2016) Temperature-controlled switchable photochromism in solid materials. *Angew Chem Int Ed* 128:15268–15272. <https://doi.org/10.1002/ange.201608408>
219. Metelitsa AV, Chernyshev AV, Voloshin NA, Solov'eva EV, Dorogan IV (2022) Chromogenic properties of heterocyclic compounds: barochromic effect of indoline spiropyran in the gas phase. *J Photochem Photobiol A* 430:113982. <https://doi.org/10.1016/j.jphotochem.2022.113982>
220. Renge I (2000) Pressure shift mechanisms of spectral holes in the optical spectra of dyes in polymer host matrices. *J Phys Chem A* 104:3869–3877. <https://doi.org/10.1021/jp9931206>
221. Poisson L, Raffael KD, Soep B, Mestdagh J-M, Buntinx G (2006) Gas-phase dynamics of spiropyran and spirooxazine molecules. *J Am Chem Soc* 128:3169–3178. <https://doi.org/10.1021/ja055079s>
222. Markworth PB, Adamson BD, Coughlan NJA, Goerigk L, Bieske EJ (2015) Photoisomerization action spectroscopy: flicking the protonated merocyanine–spiropyran switch in the gas phase. *Phys Chem Chem Phys* 17:25676–25688. <https://doi.org/10.1039/C5CP01567G>
223. Pugachev AD, Mukhanov EL, Ozhogin IV, Kozlenko AS, Metelitsa AV, Lukyanov BS (2021) Isomerization and changes of the properties of spiropyran by mechanical stress: advances and outlook. *Chem Heterocycl Comp* 57:122–130. <https://doi.org/10.1007/s10593-021-02881-y>
224. Funasako Y, Takaki A, Inokuchi M, Mochida T (2016) Photo-, thermo-, and piezochromic nafion film incorporating cationic spiropyran. *Chem Lett* 45:1397–1399. <https://doi.org/10.1246/cl.160757>
225. Rencheck ML, Mackey BT, Hu Y-Y, Chang C-C, Sangid MD, Davis CS (2022) Identifying internal stresses during mechanophore activation. *Adv Eng Mater* 24:2101080. <https://doi.org/10.1002/adem.202101080>

226. Ramirez ALB, Kean ZS, Orlicki JA, Champhekar M, Elsagr SM, Krause WE, Craig SL (2013) Mechanochemical strengthening of a synthetic polymer in response to typically destructive shear forces. *Nat Chem* 5:757–761. <https://doi.org/10.1038/nchem.1720>
227. Yoon S, Choi JH, Sung BJ, Bang J, Kim TA (2022) Mechanochromic and thermally reprocessable thermosets for autonomic damage reporting and self-healing coatings. *NPG Asia Mater* 14:61. <https://doi.org/10.1038/s41427-022-00406-3>
228. Wojtyk JTC, Wasey A, Xiao N-N, Kazmaier PM, Hoz S, Yu C, Lemieux RP, Buncel E (2007) Elucidating the mechanisms of acidochromic spiropyran-merocyanine interconversion. *J Phys Chem A* 111:2511–2516. <https://doi.org/10.1021/jp068575r>
229. Kortekaas L, Chen J, Jacquemin D, Browne WR (2018) Proton-stabilized photochemically reversible E/Z isomerization of spiropyrans. *J Phys Chem B* 122:6423–6430. <https://doi.org/10.1021/acs.jpcc.8b03528>
230. Kovalenko O, Reguero M (2020) Why thermal isomerization of the chromic switch spiropyran-merocyanine is enhanced in polar protic solvents? A computational study of the reaction mechanism. *Phys Scr* 95:055402. <https://doi.org/10.1088/1402-4896/ab5ff2>
231. Hammarson M, Nilsson JR, Li S, Beke-Somfai T, Andréasson J (2013) Characterization of the thermal and photoinduced reactions of photochromic spiropyrans in aqueous solution. *J Phys Chem B* 117:13561–13571. <https://doi.org/10.1021/jp408781p>
232. Cui L, Zhang H, Zhang G, Zhou Y, Fan L, Shi L, Zhang C, Shuang S, Dong C (2018) Substituent effect on the acid-induced isomerization of spiropyran compounds. *Spectrochim Acta A Mol Biomol Spectrosc* 202:13–17. <https://doi.org/10.1016/j.saa.2018.04.076>
233. Nam Y-S, Yoo I, Yarimaga O, Park IS, Park D-H, Song S, Kim J-M, Lee CW (2014) Photochromic spiropyran-embedded PDMS for highly sensitive and tunable optochemical gas sensing. *Chem Commun* 50:4251–4254. <https://doi.org/10.1039/C4CC00567H>
234. Rad JK, Ghomi AR, Karimipour K, Mahdavian AR (2020) Progressive readout platform based on photoswitchable polyacrylic nanofibers containing spiropyran in photopatterning with instant responsivity to acid-base vapors. *Macromolecules* 53:1613–1622. <https://doi.org/10.1021/acs.macromol.9b02603>
235. Wan S, Zheng Y, Shen J, Yang W, Yin M (2014) “On–off–on” switchable sensor: a fluorescent spiropyran responds to extreme pH conditions and its bioimaging applications. *ACS Appl Mater Interfaces* 6:19515–19519. <https://doi.org/10.1021/am506641t>
236. Liao Y (2017) Design and applications of metastable-state photoacids. *Acc Chem Res* 50:1956–1964. <https://doi.org/10.1021/acs.accounts.7b00190>
237. Halbritter T, Kaiser C, Wachtveitl J, Heckel A (2017) Pyridine-spiropyran derivative as a persistent, reversible photoacid in water. *J Org Chem* 82:8040–8047. <https://doi.org/10.1021/acs.joc.7b01268>
238. Abeyrathna N, Liao Y (2017) Photoactivity, reversibility, and stability of a merocyanine-type photoacid in polymer films. *J Photochem Photobiol A* 332:196–199. <https://doi.org/10.1016/j.jphotochem.2016.08.025>
239. Kaiser C, Halbritter T, Heckel A, Wachtveitl J (2021) Proton-transfer dynamics of photoacidic merocyanines in aqueous solution. *Chem Eur J* 27:9160–9173. <https://doi.org/10.1002/chem.202101168>
240. Kagel H, Bier FF, Frohme M, Glöckler JF (2019) A novel optical method to reversibly control enzymatic activity based on photoacids. *Sci Rep* 9:14372. <https://doi.org/10.1038/s41598-019-50867-w>
241. Gajst O, Pinto da Silva L, Esteves da Silva JCG, Huppert D (2019) Enhanced excited-state proton transfer via a mixed methanol-water molecular bridge of 1-naphthol-3,6-disulfonate in methanol-water mixtures. *J Phys Chem A* 123:48–58. <https://doi.org/10.1021/acs.jpca.8b10374>
242. Abeyrathna N, Liao Y (2017) Stability of merocyanine-type photoacids in aqueous solutions. *J Phys Org Chem* 30:e3664. <https://doi.org/10.1002/poc.3664>
243. Berton C, Busiello DM, Zamuner S, Scopelliti R, Fadaei-Tirani F, Severin K, Pezzato C (2021) Light-switchable buffers. *Angew Chem Int Ed* 60:21737–21740. <https://doi.org/10.1002/anie.202109250>
244. Shi Q, Chen C-F (2017) Switchable complexation between (O-Methyl)6–2,6-helic[6]arene and protonated pyridinium salts controlled by acid/base and photoacid. *Org Lett* 19:3175–3178. <https://doi.org/10.1021/acs.orglett.7b01296>
245. Liu J, Tang W, Sheng L, Du Z, Zhang T, Su X, Zhang SX-A (2019) Effects of substituents on metastable-state photoacids: design, synthesis, and evaluation of their photochemical properties. *Asian J Chem* 14:438–445. <https://doi.org/10.1002/asia.201801687>

246. Yang L, Caire da Silva L, Thérien-Aubin H, Bannwarth MB, Landfester K (2019) A reversible proton generator with on/off thermostitch. *Macromol Rapid Commun* 40:1800713. <https://doi.org/10.1002/marc.201800713>
247. Tatum LA, Foy JT, Aprahamian I (2014) Waste management of chemically activated switches: using a photoacid to eliminate accumulation of side products. *J Am Chem Soc* 136:17438–17441. <https://doi.org/10.1021/ja511135k>
248. Patel PK, Arias JE, Gongora RS, Hernandez FE, Moncomble A, Aloïsec S, Chumbimuni-Torres KY (2018) Visible light-triggered fluorescence and pH modulation using metastable-state photoacids and BODIPY. *Phys Chem Chem Phys* 20:26804–26808. <https://doi.org/10.1039/C8CP03977A>
249. Vallet J, Micheau J-C, Coudret C (2016) Switching a pH indicator by a reversible photoacid: a quantitative analysis of a new two-component photochromic system. *Dyes Pigm* 125:179–184. <https://doi.org/10.1016/j.dyepig.2015.10.025>
250. Kusumoto S, Nakagawa T, Yokoyama Y (2016) All-optical fine-tuning of absorption band of diarylethene with photochromic acid-generating spiropyran. *Adv Opt Mater* 4:1350–1353. <https://doi.org/10.1002/adom.201600228>
251. Alghazwat O, Elgattar A, Khalil T, Wang Z, Liao Y (2019) Red-light responsive metastable-state photoacid. *Dyes Pigm* 171:107719. <https://doi.org/10.1016/j.dyepig.2019.107719>
252. Xuan J, Tian J (2019) Heating promoted fluorescent recognition of Cu^{2+} with high selectivity and sensitivity based on spiropyran derivative. *Anal Chim Acta* 1061:161–168. <https://doi.org/10.1016/j.aca.2019.02.028>
253. Seiler VK, Robeyns K, Tumanov N, Cinčić D, Wouters J, Champagne B, Leyssens T (2019) A coloring tool for spiropyrans: solid state metal–organic complexation versus salification. *CrystEngComm* 21:4925–4933. <https://doi.org/10.1039/C9CE00805E>
254. Machitani K, Nakamura M, Sakamoto H, Ohata N, Masudab H, Kimura K (2008) Structural characterization for metal-ion complexation and isomerization of crowned bis(spirobenzopyran)s. *J Photochem Photobiol A* 200:96–100. <https://doi.org/10.1016/j.jphotochem.2008.02.019>
255. Stubing DB, Henga S, Abell AD (2016) Crowned spiropyran fluoroionophores with a carboxyl moiety for the selective detection of lithium ions. *Org Biomol Chem* 14:3752–3757. <https://doi.org/10.1039/C6OB00468G>
256. Abdullah A, Roxburgh CJ, Sammes PG (2008) Photochromic crowned spirobenzopyrans: quantitative metal-ion chelation by UV, competitive selective ion-extraction and metal-ion transportation demonstration studies. *Dyes Pigm* 76:319–326. <https://doi.org/10.1016/j.dyepig.2006.09.002>
257. Lukyanova MB, Kogan VA, Lukyanov BS (2007) A new spiropyran with a cation receptor. *Chem Heterocycl Comp* 43:1477–1478. <https://doi.org/10.1007/s10593-007-0227-2>
258. Kang J, Li E, Cui L, Shao Q, Yin C, Cheng F (2021) Lithium ion specific fluorescent reversible extraction-release based on spiropyran isomerization combining crown ether coordination and its bioimaging. *Sens Actuators B Chem* 327:128941. <https://doi.org/10.1016/j.snb.2020.128941>
259. Chernyshev AV, Metelitsa AV, Rostovtseva IA, Voloshin NA, Soloveva EV, Gaeva EB, Minkin VI (2018) Chromogenic systems based on 8-(1,3-benzoxazol-2-yl) substituted spirobenzopyrans undergoing ion modulated photochromic rearrangements. *J Photochem Photobiol A* 360:174–180. <https://doi.org/10.1016/j.jphotochem.2018.04.031>
260. Rostovtseva IA, Chernyshev AV, Tkachev VV, Dorogan IV, Voloshin NA, Solov'eva EV, Metelitsa AV, Gaeva EB, Aldoshin SM, Minkin VI (2017) Experimental and theoretical insight into the complexation behavior of spironaphthopyrans bearing o-positioning benzazole moiety. *J Mol Str* 1145:55–64. <https://doi.org/10.1016/j.molstruc.2017.05.089>
261. Chernyshev AV, Voloshin NA, Metelitsa AV, Tkachev VV, Aldoshin SM, Solov'eva E, Rostovtseva IA, Minkin VI (2013) Metal complexes of new photochromic chelator: structure, stability and photodissociation. *J Photochem Photobiol A* 265:1–9. <https://doi.org/10.1016/j.jphotochem.2013.05.001>
262. Abdel-Mottaleb MSA, Saif M, Attia MS, Abo-Alya MM, Mobarez SN (2018) Lanthanide complexes of spiropyran photoswitch and sensor: spectroscopic investigations and computational modeling. *Photochem Photobiol Sci* 17:221–230. <https://doi.org/10.1039/C7PP00226B>
263. Baldrighi M, Locatelli G, Desper J, Aakeröy CB, Giordani S (2016) Probing metal ion complexation of ligands with multiple metal binding sites: the case of spiropyrans. *Chem Eur J* 22:13976–13984. <https://doi.org/10.1002/chem.201602608>
264. Wang L, Yao Y, Wang J, Dong C, Han H (2019) Selective sensing Ca^{2+} with a spiropyran-based fluorometric probe. *Luminiscence* 34:707–714. <https://doi.org/10.1002/bio.3656>

265. Miguez FB, Menzonatto TG, Netto JFZ, Silva IMS, Verano-Braga T, Fedoce J, Lopes DS, F.B. (2020) Photo-dynamic and fluorescent zinc complex based on spiropyran ligand. *J Mol Str* 1211:128105. <https://doi.org/10.1016/j.molstruc.2020.128105>
266. Sylvia GM, Mak AM, Heng S, Bachhuka A, Ebendorff-Heidepriem H, Abell AD (2018) A rationally designed spiropyran-based chemosensor for magnesium. *Chemosensors* 6:17. <https://doi.org/10.3390/chemosensors6020017>
267. Machado RCL, Alexis F, De Sousa FB (2019) Nanostructured and photochromic material for environmental detection of metal ions. *Molecules* 24:4243. <https://doi.org/10.3390/molecules24234243>
268. Zhang R, Hu L, Xu Z, Song Y, Li H, Zhang X, Gao X, Wang M, Xian C (2020) A highly selective probe for fluorescence turn-on detection of Fe³⁺ ion based on a novel spiropyran derivative. *J Mol Str* 1204:127481. <https://doi.org/10.1016/j.molstruc.2019.127481>
269. Rivera-Fuentes P, Wrobel AT, Zastrow ML, Khan M, Georgiou J, Luyben TT, Roder JC, Okamoto K, Lippard SJ (2015) A far-red emitting probe for unambiguous detection of mobile zinc in acidic vesicles and deep tissue. *Chem Sci* 6:1944–1948. <https://doi.org/10.1039/C4SC03388D>
270. Goswami S, Aich K, Das S, Das AK, Sarkar D, Panja S, Mondal TK, Mukhopadhyay S (2013) A red fluorescence ‘off–on’ molecular switch for selective detection of Al³⁺, Fe³⁺ and Cr³⁺: experimental and theoretical studies along with living cell imaging. *Chem Commun* 49:10739–10741. <https://doi.org/10.1039/C3CC46860G>
271. Nourmohammadian F, Ghahari M, Gholami MD (2015) Spectral properties of a bis-azospiropyran complexed with europium. *J Appl Spectrosc* 82:561–566. <https://doi.org/10.1007/s10812-015-0145-5>
272. Yagi S, Nakamura S, Watanabe D, Nakazumi H (2009) Colorimetric sensing of metal ions by bis(spiropyran) podands: towards naked-eye detection of alkaline earth metal ions. *Dyes Pigm* 80:98–105. <https://doi.org/10.1016/j.dyepig.2008.05.012>
273. Natali M, Aakeröy C, Desperb J, Giordani S (2010) The role of metal ions and counterions in the switching behavior of a carboxylic acid functionalized spiropyran. *Dalton Trans* 39:8269–8277. <https://doi.org/10.1039/C0DT00242A>
274. Wojtyk JTC, Kazmaier PM, Buncel E (2001) Modulation of the spiropyran–merocyanine reversion via metal-ion selective complexation: trapping of the “transient” cis-merocyanine. *Chem Mater* 13:2547–2551. <https://doi.org/10.1021/cm010038q>
275. Ho F-C, Huang Y-J, Weng C-C, Wu C-H, Li Y-K, Wu JI, Lin H-C (2020) Efficient FRET approaches toward copper(II) and cyanide detections via host-guest interactions of photo-switchable [2]pseudo-rotaxane polymers containing naphthalimide and merocyanine moieties. *ACS Appl Mater Interfaces* 12:53257–53273. <https://doi.org/10.1021/acsami.0c15049>
276. Gao M, Shen B, Zhou J, Kapre R, Louie AY, Shaw JT (2020) Synthesis and comparative evaluation of photoswitchable magnetic resonance imaging contrast agents. *ACS Omega* 5:14759–14766. <https://doi.org/10.1021/acsomega.0c01534>
277. Cardano F, Del Canto E, Giordani S (2019) Spiroyrans for light-controlled drug delivery. *Dalton Trans* 48:15537–15544. <https://doi.org/10.1039/C9DT02092F>
278. Selvanathan P, Dorcet V, Roisnel T, Bernot K, Huang G, Le Guennic B, Norel L, Rigaut S (2018) trans to cis photo-isomerization in merocyanine dysprosium and yttrium complexes. *Dalton Trans* 47:4139–4148. <https://doi.org/10.1039/C8DT00299A>
279. Zhao H, Huai J, Weng C, Han H (2022) A new spiropyran compound for selective naked-eye detection of copper ions in aqueous media and on test paper strips. *J Mol Str* 1263:133146. <https://doi.org/10.1016/j.molstruc.2022.133146>
280. Arjmanda F, Mohamadnia Z (2022) Fabrication of a light-responsive polymer nanocomposite containing spiropyran as a sensor for reversible recognition of metal ions. *Polym Chem* 13:937–945. <https://doi.org/10.1039/D1PY01620B>
281. Heng S, Mak AM, Kostecki R, Zhang X, Pei J, Stubing DB, Ebendorff-Heidepriem H, Abell AD (2017) Photoswitchable calcium sensor: ‘On’–‘Off’ sensing in cells or with microstructured optical fibers. *Sensor Actuat B-Chem* 252:965–972. <https://doi.org/10.1016/j.snb.2017.06.051>
282. Shiraishi Y, Adachi K, Itoh M, Hirai T (2009) Spiropyran as a selective, sensitive, and reproducible cyanide anion receptor. *Org Lett* 11:3482–3485. <https://doi.org/10.1021/o1901399a>
283. Prakash K, Sahoo PR, Kumar S (2016) A substituted spiropyran for highly sensitive and selective colorimetric detection of cyanide ions. *Sensor Actuat B-Chem* 237:856–864. <https://doi.org/10.1016/j.snb.2016.06.170>
284. Samanta S, Halder S, Manna U, Das G (2019) Specific detection of hypochlorite: a cyanide based turn-on fluorescent sensor. *J Chem Sci* 131:36. <https://doi.org/10.1007/s12039-019-1612-y>

285. Zhou Z, Hu H, Xia L, Li G, Xiao X (2022) A bisspiropyran fluorescent probe for the selective and rapid detection of cyanide anion in liqueurs. *New J Chem* 46:7992–7998. <https://doi.org/10.1039/D1NJ05773A>
286. Sanjabi S, Rad JK, Mahdavian AR (2022) Spiropyran and spironaphthoxazine based opto-chemical probes for instant ion detection with high selectivity and sensitivity to trace amounts of cyanide. *J Photochem Photobiol A* 424:113626. <https://doi.org/10.1016/j.jphotochem.2021.113626>
287. Xue Y, Tian J, Tian W, Zhang K, Xuan J, Zhang X (2021) Spiropyran based recognitions of amines: UV–Vis spectra and mechanisms. *Spectrochim Acta A Mol Biomol Spectrosc* 250:119385. <https://doi.org/10.1016/j.saa.2020.119385>
288. Yang L, Li Y, Song H, Zhang H, Yang N, Peng Q, He G (2020) A highly sensitive probe based on spiropyran for colorimetric and fluorescent detection of thiophenol in aqueous media. *Dyes Pigm* 175:108154. <https://doi.org/10.1016/j.dyepig.2019.108154>
289. Xiao X, Yang G, Chen A, Zheng Z, Zhang C, Zhang Y, Liao L (2022) Multi-responsive chromatic hydrogel exhibiting reversible shape deformations. *Dyes Pigm* 204:110364. <https://doi.org/10.1016/j.dyepig.2022.110364>
290. Qi Q, Qian J, Ma S, Xu B, Zhang SX-A, Tian W (2015) Reversible multistimuli-response fluorescent switch based on tetraphenylethene-spiropyran molecules. *Chem Eur J* 21:1149–1155. <https://doi.org/10.1002/chem.201405426>
291. Wu L, Chen R, Luo Z, Wang P (2020) Solid-state photochromism and acidochromism multifunctional materials constructed by tetraphenylethene and spiropyran. *J Mater Sci* 55:12826–12835. <https://doi.org/10.1007/s10853-020-04930-x>
292. Su X, Ji Y, Pan W, Chen S, Zhang Y-M, Lin T, Liu L, Li M, Liu Y, Zhang SX-A (2018) Pyrene spiropyran dyad: solvato-, acido- and mechanofluorochromic properties and its application in acid sensing and reversible fluorescent display. *J Mater Chem C* 6:6940–6948. <https://doi.org/10.1039/C8TC02208A>
293. Benniston AC, Harriman A, Howell SL, Li P, Lydon DP (2007) Opening a spiropyran ring by way of an exciplex intermediate. *J Org Chem* 72:888–897. <https://doi.org/10.1021/jo062124l>
294. Remón P, Hammarson M, Li S, Kahnt A, Pischel U, Andréasson J (2011) Molecular implementation of sequential and reversible logic through photochromic energy transfer switching. *Chem Eur J* 17:6492–6500. <https://doi.org/10.1002/chem.201100027>
295. Chai X, Han H-H, Sedgwick AC, Li N, Zang Y, James TD, Zhang J, Hu X-L, Yu Y, Li Y, Wang Y, Li J, He X-P, Tian H (2020) Photochromic fluorescent probe strategy for the super-resolution imaging of biologically important biomarkers. *J Am Chem Soc* 142:18005–18013. <https://doi.org/10.1021/jacs.0c05379>
296. Florea L, Diamond D, Benito-Lopez F (2012) Photo-responsive polymeric structures based on spiropyran. *Macromol Mater Eng* 297:1148–1159. <https://doi.org/10.1002/mame.201200306>
297. Meng X, Chen C, Qi G, Li X, Wang K, Zou B, Ma Y (2017) From two, to three, to multi-color switches: developing AIEgen-based mechanochromic materials. *ChemNanoMat* 3:569–574. <https://doi.org/10.1002/cnma.201700120>
298. Wan S, Ma Z, Chen C, Li F, Wang F, Jia X, Yang W, Yin M (2015) A supramolecule-triggered mechanochromic switch of cyclodextrin-jacketed rhodamine and spiropyran derivatives. *Adv Funct Mater* 26:353–364. <https://doi.org/10.1002/adfm.201504048>
299. Meng X, Qi G, Li X, Wang Z, Wang K, Zou B, Ma Y (2016) Spiropyran-based multi-colored switching tuned by pressure and mechanical grinding. *J Mater Chem C* 4:7584–7588. <https://doi.org/10.1039/c6tc02578a>
300. Sylvia G, Heng S, Abell AD (2016) Fluorescence enhancement of photoswitchable metal ion sensors. *SPIE BioPhoton Austral* 10013:100131X. <https://doi.org/10.1117/12.2244656>
301. Sylvia GM, Heng S, Bachhuka A, Ebendorff-Heidepriem H, Abell AD (2018) A spiropyran with enhanced fluorescence: a bright, photostable and red-emitting calcium sensor. *Tetrahedron* 74:1240–1244. <https://doi.org/10.1016/j.tet.2017.11.020>
302. Kubinyi M, Varga O, Baranyai P, Kállay M, Mizsei R, Tárkányi G, Vidóczy T (2011) Metal complexes of the merocyanine form of nitrobenzopyran: structure, optical spectra, stability. *J Mol Struct* 1000:77–84. <https://doi.org/10.1016/j.molstruc.2011.05.055>
303. Wu Y, Yin C, Zhang W, Chao J, Huo F (2021) A red-emitting fluorescent probe imaging release of calcium ions from lysosome induced by chloroquine based on a photochromic crowned spirobenzopyran. *Dyes Pigm* 193:109467. <https://doi.org/10.1016/j.dyepig.2021.109467>

304. Zhao M, Dong L, Liu Z, Yang S, Wu W, Lin J (2018) In vivo fluorescence imaging of hepatocellular carcinoma using a novel GPC3-specific aptamer probe. *Quant Imaging Med Surg* 8:151–160. <https://doi.org/10.21037/qims.2018.01.09>
305. Fries KH, Driskell JD, Sheppard GR, Locklin J (2011) Fabrication of spiropyran-containing thin film sensors used for the simultaneous identification of multiple metal ions. *Langmuir* 27:12253–12260. <https://doi.org/10.1021/la202344w>
306. Fries KH, Sheppard GR, Bilbrey JA, Locklin J (2014) Tuning chelating groups and comonomers in spiropyran-containing copolymer thin films for color-specific metal ion binding. *Polym Chem* 5:2094–2102. <https://doi.org/10.1039/C3PY01296D>
307. Barbee MH, Mondal K, Deng JZ, Bharambe V, Neumann TV, Adams JJ, Boechler N, Dickey MD, Craig SL (2018) Mechanochromic stretchable electronics. *ACS Appl Mater Interfaces* 10:29918–29924. <https://doi.org/10.1021/acsami.8b09130>
308. Zhu M-Q, Chen T, Zhang G-F, Li C, Gong W-L, Chena Z-Q, Aldred MP (2014) Spiropyran-based biodegradable polymer all-optical transistors integrate the switching and modulation of visible light frequency. *Chem Commun* 50:2664–2666. <https://doi.org/10.1039/C3CC49016E>
309. Fan J, Bao B, Wang Z, Xu R, Wang W, Yu D (2020) High tri-stimulus response photochromic cotton fabrics based on spiropyran dye by thiol-ene click chemistry. *Cellulose* 27:493–510. <https://doi.org/10.1007/s10570-019-02786-2>
310. Bao B, Bai S, Fan J, Su J, Wang W, Yu D (2019) A novel and durable photochromic cotton-based fabric prepared via thiol-ene click chemistry. *Dyes Pigm* 171:171778. <https://doi.org/10.1016/j.dyepig.2019.107778>
311. He Z, Bao B, Fan J, Wang W, Yu D (2020) Photochromic cotton fabric based on microcapsule technology with anti-fouling properties. *Colloids Surf A Physicochem Eng Asp* 594:124661. <https://doi.org/10.1016/j.colsurfa.2020.124661>
312. Schmidt SB, Kempe F, Brünger O, Walter M, Sommer M (2017) Alkyl-substituted spiropyran: electronic effects, model compounds and synthesis of aliphatic main-chain copolymers. *Polym Chem* 8:5407–5414. <https://doi.org/10.1039/C7PY00987A>
313. Jiang F, Chen S, Cao Z, Wang G (2016) A photo, temperature, and pH responsive spiropyran-functionalized polymer: synthesis, self-assembly and controlled release. *Polymer* 83:85–91. <https://doi.org/10.1016/j.polymer.2015.12.027>
314. Seok WC, Son SH, An TK, Kim SH, Lee SW (2016) Photo-enhanced polymer memory device based on polyimide containing spiropyran. *Electron Mater Lett* 12:537–544. <https://doi.org/10.1007/s13391-016-4019-7>
315. Hauser L, Knall A-C, Roth M, Trimmel G, Edler M, Griesser T, Kern W (2012) Reversible photochromism of polynorbornenes bearing spiropyran side groups. *Monatsh Chem* 143:1551–1558. <https://doi.org/10.1007/s00706-012-0827-0>
316. Ventura C, Thornton P, Giordanic S, Heise A (2014) Synthesis and photochemical properties of spiropyran graft and star polymers obtained by ‘click’ chemistry. *Polym Chem* 5:6318–6324. <https://doi.org/10.1039/C4PY00778F>
317. Keum S, Ahn S, Roh S, Ma S (2010) The synthesis and spectroscopic properties of novel, photochromic indolinobenzospiropyran-based homopolymers prepared via ring-opening metathesis polymerization. *Dyes Pigm* 86:74–80. <https://doi.org/10.1016/j.dyepig.2009.12.002>
318. Ziółkowski B, Florea L, Theobald J, Benito-Lopez F, Diamond D (2013) Self-protonating spiropyran-co-NIPAM-co-acrylic acid hydrogel photoactuators. *Soft Matter* 9:8754–8760. <https://doi.org/10.1039/c3sm51386f>
319. Khalil T, Alharbi A, Baum C, Liao Y (2018) Facile synthesis and photoactivity of merocyanine-photoacid polymers. *Macromol Rapid Commun* 39:1800319. <https://doi.org/10.1002/marc.201800319>
320. Karimipour K, Rad JK, Ghomi AR, Salehi H, Mahdavian AR (2020) Hydrochromic and photoswitchable polyacrylic nanofibers containing spiropyran in eco-friendly ink-free rewritable sheets with responsivity to humidity. *Dyes Pigm* 175:108185. <https://doi.org/10.1016/j.dyepig.2020.108185>
321. Razavi B, Abdollahi A, Roghani-Mamaqani H, Salami-Kalajahi M (2020) Light-, temperature-, and pH-responsive micellar assemblies of spiropyran-initiated amphiphilic block copolymers: kinetics of photochromism, responsiveness, and smart drug delivery. *Mater Sci Eng C* 109:110524. <https://doi.org/10.1016/j.msec.2019.110524>

322. Bardavid Y, Goykhman I, Nozaki D, Cuniberti G, Yitzchaik S (2011) Dipole assisted photogated switch in spiropyran grafted polyaniline nanowires. *J Phys Chem C* 115:3123–3128. <https://doi.org/10.1021/jp110665j>
323. Ahmadi S, Nasiri M, Miandoab AP (2020) Synthesis and characterization of a pH and photoreponsive copolymer of acrylamide and spiropyran. *Polym Adv Technol* 31:2545–2551. <https://doi.org/10.1002/pat.4981>
324. Abdollahi A, Roghani-Mamaqani H, Razavi B (2019) Stimuli-chromism of photoswitches in smart polymers: recent advances and applications as chemosensors. *Prog Polym Sci* 98:101149. <https://doi.org/10.1016/j.progpolymsci.2019.101149>
325. Cao Z (2020) Highly stretchable tough elastomers crosslinked by spiropyran mechanophores for strain-induced colorimetric sensing. *Macromol Chem Phys* 221:2000190. <https://doi.org/10.1002/macp.202000190>
326. Giordano G, Gagliardi M, Huan Y, Carlotti M, Mariani A, Menciasci A, Sinibaldi E, Mazzolai B (2021) Toward mechanochromic soft material-based visual feedback for electronics-free surgical effectors. *Adv Sci* 8:2100418. <https://doi.org/10.1002/advs.202100418>
327. Xia Z, Alphonse VD, Trigg DB, Harrigan TP, Paulson JM, Luong QT, Lloyd EP, Barbee MH, Craig SL (2019) “Seeing” strain in soft materials. *Molecules* 24:542. <https://doi.org/10.3390/molecules24030542>
328. Gossweiler GR, Brown CL, Hewage GB, Sapiro-Gheiler E, Trautman WJ, Welshofer GW, Craig SL (2015) Mechanochemically active soft robots. *ACS Appl Mater Interfaces* 7:22431–22435. <https://doi.org/10.1021/acsami.5b06440>
329. Jeong YJ, Yoo EJ, Kim LH, Park S, Jang J, Kim SH, Lee SW, Park CE (2016) Light-responsive spiropyran based polymer thin films for use in organic field-effect transistor memories. *J Mater Chem C* 4:5398–5406. <https://doi.org/10.1039/C6TC00798H>
330. Grogan C, Florea L, Koprivica S, Scarmagnani S, O’Neill L, Lyng F, Pedreschi F, Benito-Lopez F, Raiteri R (2016) Microcantilever arrays functionalised with spiropyran photoactive moieties as systems to measure photo-induced surface stress changes. *Sens Actuators B Chem* 237:479–486. <https://doi.org/10.1016/j.snb.2016.06.108>
331. Grogan C, Amarandei G, Lawless S, Pedreschi F, Lyng F, Benito-Lopez F, Raiteri R, Florea L (2020) Silicon microcantilever sensors to detect the reversible conformational change of a molecular switch. *Spiropyran Sens* 20:854. <https://doi.org/10.3390/s20030854>
332. Peterson GI, Larsen MB, Ganter MA, Storti DW, Boydston AJ (2015) 3D-printed mechanochromic materials. *ACS Appl Mater Interfaces* 7:577–583. <https://doi.org/10.1021/am506745m>
333. Reghely M, Garmshausen Y, Reuter M, König NF, Israel E, Kelly DP, Chou C-Y, Koch K, Asfari B, Hecht S (2020) Xolography for linear volumetric 3D printing. *Nature* 588:620–624. <https://doi.org/10.1038/s41586-020-3029-7>
334. Raich M, Genovese D, Zaccheroni N, Schmidt SB, Focarete ML, Sommer M, Gualandi C (2018) Highly sensitive, anisotropic, and reversible stress/strain-sensors from mechanochromic nanofiber composites. *Adv Mater* 30:1802813. <https://doi.org/10.1002/adma.201802813>
335. Wang X, He Y, Leng J (2022) Smart shape memory polyurethane with photochromism and mechanochromism properties. *Macromol Mater Eng* 307:2100778. <https://doi.org/10.1002/mame.20210778>
336. Yang Y, Chen Y, Li Y, Wang Z, Zhao H (2022) Acid-, mechano- and photochromic molecular switches based on a spiropyran derivative for rewritable papers. *Mater Chem Front* 6:916–923. <https://doi.org/10.1039/D1QM01637G>
337. Abdollahi A, Herizchi A, Roghani-Mamaqani H, Alidaei-Sharif H (2020) Interaction of photoswitchable nanoparticles with cellulosic materials for anticounterfeiting and authentication security documents. *Carbohydr Polym* 230:115603. <https://doi.org/10.1016/j.carbpol.2019.115603>
338. Lin Z, Pan H, Tian Y, Tang J, Zhang C, Zhang P, Yang H, Chen J (2022) Photo-pH dual stimuli-responsive multicolor fluorescent polymeric nanoparticles for multicolor security ink, optical data encryption and zebrafish imaging. *Dyes Pigm* 205:110588. <https://doi.org/10.1016/j.dyepig.2022.110588>
339. Yang Y, Wang Z, Wu H, Li Y, Chen Y, Hu L, Wu W (2022) Dual-stimuli response of spiropyran derivative modified by long-chains: high-contrast photochromism and mechanochromism. *Mater Chem Front* 6:1948–1955. <https://doi.org/10.1039/D2QM00304J>
340. Azimi R, Abdollahi A, Roghani-Mamaqani H, Salami-Kalajahi M (2021) Dual-mode security anticounterfeiting and encoding by electrospinning of highly photoluminescent spiropyran nanofibers. *J Mater Chem C* 9:9571–9583. <https://doi.org/10.1039/d1tc01931g>

341. Shen X, Akbarzadeh A, Hu Q, Shi C, Jin Y, Ge M (2022) Novel photo-responsive composite fibers fabricated by facile wet-spinning process for UV detection and high-level encryption. *J Lumin* 251:119179. <https://doi.org/10.1016/j.jlumin.2022.119179>
342. Ma J, Tian J, Liu Z, Shi D, Zhang X, Zhang G, Zhang D (2019) Multi-stimuli-responsive field-effect transistor with conjugated polymer entailing spiropyran in the side chains. *CCS Chem* 1:632–641. <https://doi.org/10.31635/ccschem.019.20190056>
343. Tuktarov AR, Salikhov RB, Khuzin AA, Popod'ko NR, Safargalin IN, Mullagaliev IN, Dzhemilev UM (2019) Photocontrolled organic field effect transistors based on the fullerene C60 and spiropyran hybrid molecule. *RSC Adv* 9:7505–7508. <https://doi.org/10.1039/C9RA00939F>
344. Brohmann M, Wieland S, Angstenberger S, Herrmann NJ, Lüttgens J, Fazzi D, Zaumseil J (2020) Guiding charge transport in semiconducting carbon nanotube networks by local optical switching. *ACS Appl Mater Interfaces* 12:28392–28403. <https://doi.org/10.1021/acsami.0c05640>
345. Sanina NA, Grachev VP, Dmitriev AI, Morgunov RB, Koplak OV, Yur'eva EA, Anokhin DV, Ivanov DA, Aldoshin SM (2013) Synthesis and properties of polyvinylpyrrolidone films containing the photomagnetic chromium (tris)oxalate complex. *Russ Chem Bull* 62:554–559. <https://doi.org/10.1007/s11172-013-0077-2>
346. Triolo C, Patanè S, Mazzeo M, Gambino S, Gigli G, Allegrini M (2014) Pure optical nano-writing on light-switchable spiropyrans/merocyanine thin film. *Opt Express* 22:283–288. <https://doi.org/10.1364/OE.22.000283>
347. Kida N, Hikita M, Kashima I, Okubo M, Itoi M, Enomoto M, Kato K, Takata M, Kojima N (2009) Control of charge transfer phase transition and ferromagnetism by photoisomerization of spiropyran for an organic–inorganic hybrid system, (SP)[Fe^{II}Fe^{III}(dto)₃] (SP = spiropyran, dto = C₂O₂S₂). *J Am Chem Soc* 131:212–220. <https://doi.org/10.1021/ja806879a>
348. Aldoshin SM, Sanina NA (2016) Photochromic magnetic materials based on transition metal oxalate complexes. *Russ Chem Rev* 85:1185–1197. <https://doi.org/10.1070/RCR4652>
349. Tanaka N, Okazawa A, Sugahara A, Kojima N (2015) Development of a photoresponsive organic-inorganic hybrid magnet: layered cobalt hydroxides intercalated with spiropyran anions. *Bull Chem Soc Jpn* 88:1150–1155. <https://doi.org/10.1246/bcsj.20150129>
350. Li Z, Zhou Y, Peng L, Yan D, Wei M (2017) A switchable electrochromism and electrochemiluminescence bifunctional sensor based on the electro-triggered isomerization of spiropyran/layered double hydroxides. *Chem Commun* 53:8862–8865. <https://doi.org/10.1039/C7CC04421F>
351. Yamamoto T, Yurieva EA, Tsuda K, Hosomi T, Aldoshin SM, Einaga Y (2017) Gigantic photomagnetic effect at room temperature in spiropyran-protected FePt nanoparticles. *Phys Status Solidi RRL* 11:1700161. <https://doi.org/10.1002/pssr.201700161>
352. Selvanathan P, Huang G, Guizouarn T, Roisnel T, Fernandez-Garcia G, Totti F, Le Guennic B, Calvez G, Bernot K, Norel L, Rigaut S (2016) Highly axial magnetic anisotropy in a N₃O₅ Dysprosium(III) coordination environment generated by a merocyanine ligand. *Chem Eur J* 22:15222–15226. <https://doi.org/10.1002/chem.201603439>
353. Nagashima S, Murata M, Nishihara H (2006) A ferrocenylspiropyran that functions as a molecular photomemory with controllable depth. *Angew Chem* 45:4298–4301. <https://doi.org/10.1002/anie.200600535>
354. Hakouk K, Oms O, Dolbecq A, Marrot J, Saad A, Mialane P, El Bekkachi H, Jobic S, Deniard P, Dessapt R (2014) New photoresponsive charge-transfer spiropyran/polyoxometalate assemblies with highly tunable optical properties. *J Mater Chem C* 2:1628–1641. <https://doi.org/10.1039/C3TC31992J>
355. Compain J-D, Deniard P, Dessapt R, Dolbecq A, Oms O, Sécheresse F, Marrot J, Mialane P (2010) Functionalized polyoxometalates with intrinsic photochromic properties and their association with spiropyran cations. *Chem Commun* 46:7733–7735. <https://doi.org/10.1039/C0CC02533J>
356. Saad A, Oms O, Dolbecq A, Menet C, Dessapt R, Serier-Brault H, Allard E, Baczko K, Mialane P (2015) A high fatigue resistant, photoswitchable fluorescent spiropyran–polyoxometalate–BODIPY single-molecule. *Chem Commun* 51:16088–16091. <https://doi.org/10.1039/C5CC06217A>
357. Liang H-Q, Guo Y, Shi Y, Peng X, Liang B, Chen B (2020) A light-responsive metal-organic framework hybrid membrane with high On/Off photoswitchable proton conductivity. *Angew Chem Int Ed* 59:7732–7737. <https://doi.org/10.1002/anie.202002389>
358. Kanj AB, Chandresh A, Gerwien A, Grosjean S, Bräse S, Wang Y, Dube H, Heinke L (2020) Proton-conduction photomodulation in spiropyran-functionalized MOFs with large on–off ratio. *Chem Sci* 11:1404–1410. <https://doi.org/10.1039/C9SC04926F>

359. Williams DE, Martin CR, Dolgoplova EA, Swifton A, Godfrey DC, Ejegbavwo OA, Pellechia PJ, Smith MD, Shustova NB (2018) Flipping the switch: fast photoisomerization in a confined environment. *J Am Chem Soc* 140:7611–7622. <https://doi.org/10.1021/jacs.8b02994>
360. Ma S, Ting H, Ma Y, Zheng L, Zhang M, Xiao L, Chen Z (2015) Smart photovoltaics based on dye-sensitized solar cells using photochromic spiropyran derivatives as photosensitizers. *AIP Adv* 5:057154. <https://doi.org/10.1063/1.4921880>
361. Castán J-MA, Mwalukuku VM, Riquelme AJ, Liotier J, Hualumé Q, Anta JA, Maldivi P, Demadrille R (2022) Photochromic spiro-indoline naphthoxazines and naphthopyrans in dye-sensitized solar cells. *Mater Chem Front Adv* 20:20. <https://doi.org/10.1039/D2QM00375A>
362. Takeshita T, Umeda T, Hara M (2017) Fabrication of a dye-sensitized solar cell containing a non-carboxylated spiropyran-derived photomercyanine with cyclodextrin. *J Photochem Photobiol A* 33:87–91. <https://doi.org/10.1016/j.jphotochem.2016.10.017>
363. Feringa BL (2017) The art of building small: from molecular switches to motors (nobel lecture). *Angew Chem Int Ed* 56:11060–11078. <https://doi.org/10.1002/anie.201702979>
364. Sauvage J-P (2017) From chemical topology to molecular machines (nobel lecture). *Angew Chem Int Ed* 56:11080–11093. <https://doi.org/10.1002/anie.201702992>
365. Stoddart JF (2017) Mechanically interlocked molecules (MIMs)—molecular shuttles, switches, and machines (nobel lecture). *Angew Chem Int Ed* 56:11094–11125. <https://doi.org/10.1002/anie.201703216>
366. Hernández-Melo D, Tiburcio J (2015) Coupled molecular motions driven by light or chemical inputs: spiropyran to merocyanine isomerisation followed by pseudorotaxane formation. *Chem Commun* 25:17564–17567. <https://doi.org/10.1039/C5CC07056B>
367. Zhou W, Zhang H, Li H, Zhang Y, Wang Q-C, Qu D-H (2013) A bis-spiropyran-containing multi-state [2]rotaxane with fluorescence output. *Tetrahedron* 69:5319–5325. <https://doi.org/10.1016/j.tet.2013.04.119>
368. Nhien PQ, Cuc TTK, Khang TM, Wu C-H, Hue BTB, Wu JI, Mansel BW, Chen H-L, Lin H-C (2020) Highly efficient Förster resonance energy transfer modulations of dual-aiegens between a tetraphenylethylene donor and a merocyanine acceptor in photo-switchable [2]rotaxanes and reversible photo-patterning applications. *ACS Appl Mater Interfaces* 12:47921–47938. <https://doi.org/10.1021/acsami.0c12726>
369. Bhattacharyya S, Maity M, Chowdhury A, Saha ML, Panja SK, Stang PJ, Mukherjee PS (2020) Coordination-assisted reversible photoswitching of spiropyran-based platinum macrocycles. *Inorg Chem* 59:2083–2091. <https://doi.org/10.1021/acs.inorgchem.9b03572>
370. Malinčík J, Kohout M, Svoboda J, Stulov S, Pocięcha D, Böhmová Z, Novotná V (2022) Photochromic spiropyran-based liquid crystals. *J Mol Liq* 346:117842. <https://doi.org/10.1016/j.molliq.2021.117842>
371. Tangso KJ, Fong W-K, Darwish T, Kirby N, Boyd BJ, Hanley TL (2013) Novel spiropyran amphiphiles and their application as light-responsive liquid crystalline components. *J Phys Chem B* 117:10203–10210. <https://doi.org/10.1021/jp403840m>
372. Tan B-H, Yoshio M, Kato T (2008) Induction of columnar and smectic phases for spiropyran derivatives: effects of acidochromism and photochromism. *Asian J Chem* 3:534–541. <https://doi.org/10.1002/asia.200700225>
373. Liu M, Creemer CN, Reardona TJ, Parquette JR (2021) Light-driven dissipative self-assembly of a peptide hydrogel. *Chem Commun* 57:13776–13779. <https://doi.org/10.1039/D1CC04971B>
374. Li C, Iscen A, Palmer LC, Schatz GC, Stupp SI (2020) Light-driven expansion of spiropyran hydrogels. *J Am Chem Soc* 142:8447–8453. <https://doi.org/10.1021/jacs.0c02201>
375. Sakai H, Ebana H, Sakai K, Tsuchiya K, Ohkubo T, Abe M (2007) Photo-isomerization of spiropyran-modified cationic surfactants. *J Colloid Interface Sci* 316:1027–1030. <https://doi.org/10.1016/j.jcis.2007.08.042>
376. Zhang J, Zhang Y, Chen F, Zhang W, Zhao H (2015) Self-assembly of photoswitchable diblock copolymers: salt-induced micellization and the influence of UV irradiation. *Phys Chem Chem Phys* 20:12215–12221. <https://doi.org/10.1039/C5CP01560J>
377. Wu Z, Pan K, Lü B, Ma L, Yang W, Yin M (2016) Tunable morphology of spiropyran assemblies: from nanospheres to nanorods. *Asian J Chem* 11:3102–3106. <https://doi.org/10.1002/asia.201601114>
378. Zhu M-Q, Zhang G-F, Hu Z, Aldred MP, Li C, Gong W-L, Chen T, Huang Z-L, Liu S (2014) Reversible fluorescence switching of spiropyran-conjugated biodegradable nanoparticles for

- super-resolution fluorescence imaging. *Macromolecules* 47:1543–1552. <https://doi.org/10.1021/ma5001157>
379. Rad JK, Mahdavian AR, Khoei S, Janati A (2016) FRET-based acrylic nanoparticles with dual-color photoswitchable properties in DU145 human prostate cancer cell line labeling. *Polymer* 2:263–269. <https://doi.org/10.1016/j.polymer.2016.06.042>
380. Maskevich SA, Vasilyuk GT, Askirka VF, Strekal' ND, Luk'yanov BS, Starikov AG, Starikova AA, Luk'yanova MB, Pugachev AD, Minkin VI (2018) Photochromic properties and surface enhanced raman scattering spectra of indoline spiropyran in silver-based nanocomposite films. *Opt Spectrosc* 124:814–820. <https://doi.org/10.1134/S0030400X18060164>
381. Shiraishi Y, Shirakawa E, Tanaka K, Sakamoto H, Ichikawa S, Hirai T (2014) Spiropyran-modified gold nanoparticles: reversible size control of aggregates by UV and visible light irradiations. *ACS Appl Mater Interfaces* 6:7554–7562. <https://doi.org/10.1021/am5009002>
382. Lai J, Zhang Y, Pasquale N, Lee KB (2014) An upconversion nanoparticle with orthogonal emissions using dual NIR excitations for controlled two-way photoswitching. *Angew Chem Int Ed* 53:14419–14423. <https://doi.org/10.1002/anie.201408219>
383. Zhang H, Chen Z, He Y, Yang S, Wei J (2021) Spiropyran-modified upconversion nanoparticles for tunable fluorescent printing. *ACS Appl Nano Mater* 4:4340–4345. <https://doi.org/10.1021/acsnam.1c00601>
384. Elsässer C, Vüllings A, Karcher M, Fumagalli P (2009) Photochromism of spiropyran–cyclodextrin inclusion complexes on Au(111). *J Phys Chem C* 113:19193–19198. <https://doi.org/10.1021/jp810474v>
385. Seiler VK, Tumanov N, Robeyns K, Champagne B, Wouters J, Leyssens T (2020) Merocyanines in a halogen-bonded network involving inorganic building blocks. *Cryst Growth Des* 20:608–616. <https://doi.org/10.1021/acs.cgd.9b00903>
386. Samanta D, Galaktionova D, Gemen J, Shimon LJW, Diskin-Posner Y, Avram L, Král P, Klajn R (2018) Reversible chromism of spiropyran in the cavity of a flexible coordination cage. *Nat Commun* 9:641. <https://doi.org/10.1038/s41467-017-02715-6>
387. Kohl-Landgraf J, Braun M, Özçoban C, Gonçalves DPN, Heckel A, Wachtveitl J (2012) Ultrafast dynamics of a spiropyran in water. *J Am Chem Soc* 134:14070–14077. <https://doi.org/10.1021/ja304395k>
388. Xue R, Zhang X, Tian J (2018) Synthesis of water-soluble spiropyran-modified poly(acrylic acid) micelles and their optical behaviors. *J Photopolym Sci Technol* 31:739–746. <https://doi.org/10.2494/photopolymer.31.739>
389. Zou X, Xiao X, Zhang S, Zhong J, Hou Y, Liao L (2018) A photo-switchable and thermal-enhanced fluorescent hydrogel prepared from N-isopropylacrylamide with water-soluble spiropyran derivative. *J Biomater Sci Polym Ed* 29:1579–1594. <https://doi.org/10.1080/09205063.2018.1475942>
390. Guo T, Wu J, Gao H, Chen Y (2017) Covalent functionalization of multi-walled carbon nanotubes with spiropyran for high solubility both in water and in non-aqueous solvents. *Inorg Chem Commun* 83:31–35. <https://doi.org/10.1016/j.inoche.2017.06.002>
391. Moldenhauer D, Werner JPF, Strassert CA, Gröhn F (2019) Light-responsive size of self-assembled spiropyran-lysozyme nanoparticles with enzymatic function. *Biomacromol* 20:979–991. <https://doi.org/10.1021/acs.biomac.8b01605>
392. Li G, Wang H, Zhu Z, Fan J-B, Tian Y, Meng J, Wang S (2019) Photo-irresponsive molecule-amplified cell release on photoresponsive nanostructured surfaces. *ACS Appl Mater Interfaces* 11:29681–29688. <https://doi.org/10.1021/acsami.9b11957>
393. Putri RM, Fredy JW, Cornelissen JJ, Koay MS, Katsonis N (2016) Labelling bacterial nanocages with photo-switchable fluorophores. *ChemPhysChem* 17:1815–1818. <https://doi.org/10.1002/cphc.201600013>
394. Chen L, Wu J, Schmuck C, Tian H (2014) A switchable peptide sensor for real-time lysosomal tracking. *Chem Commun* 50:6443–6446. <https://doi.org/10.1039/C4CC00670D>
395. Li J, Li X, Jia J, Chen X, Lv Y, Guo Y, Li J (2019) A ratiometric near-infrared fluorescence strategy based on spiropyran in situ switching for tracking dynamic changes of live-cell lysosomal pH. *Dyes Pigm* 116:433–442. <https://doi.org/10.1016/j.dyepig.2019.03.060>
396. Lv G, Sun A, Wei P, Zhang N, Lana H, Yi T (2016) A spiropyran-based fluorescent probe for the specific detection of β -amyloid peptide oligomers in Alzheimer's disease. *Chem Commun* 52:8865–8868. <https://doi.org/10.1039/C6CC02741E>


397. Shao N, Jin J, Wang H, Zheng J, Yang R, Chan W, Abliz Z (2010) Design of bis-spiropyran ligands as dipolar molecule receptors and application to in vivo glutathione fluorescent probes. *J Am Chem Soc* 132:725–736. <https://doi.org/10.1021/ja908215t>
398. Heng S, Zhang X, Pei J, Abell AD (2017) A rationally designed reversible ‘turn-off’ sensor for glutathione. *Biosensors* 7:36. <https://doi.org/10.3390/bios7030036>
399. Shcherbatykh AA, Chernov’yants Voloshin Chernyshev MSNAAV (2022) Spiropyran 5,6'-dichloro-1,3,3-trimethylspiro[indoline-2,2'-2*H*-pyrano[3,2-*h*]quinoline] application as a spectrophotometric and fluorescent probe for glutathione and cysteine sensing. *Chem Pap* 76:5541–5550. <https://doi.org/10.1007/s11696-022-02259-0>
400. Zhang H, Nian Q, Dai H, Wan X, Xu Q (2022) A nanofiber-mat-based solid-phase sensor for sensitive ratiometric fluorescent sensing and fine visual colorimetric detection of tetracycline. *Food Chem* 395:133597. <https://doi.org/10.1016/j.foodchem.2022.133597>
401. Shinohara M, Xu W, Kim S, Fukaminato T, Niidome T, Kurihara S (2022) Photo-control of cellular uptake by the selective adsorption of spiropyran derivatives on albumin. *Chem Lett* 51:594–597. <https://doi.org/10.1246/cl.220082>
402. Pei JV, Heng S, De Leso ML, Sylvia G, Kourghi M, Nourmohammadi S, Abell AD, Yool AJ (2019) Development of a photoswitchable lithium-sensitive probe to analyze nonselective cation channel activity in migrating cancer cells. *Mol Pharmacol* 95:573–583. <https://doi.org/10.1124/mol.118.115428>
403. Heng S, McDevitt CA, Kostecki R, Morey JR, Eijkelkamp BA, Ebendorff-Heidepriem H, Monro TM, Abell AD (2016) Microstructured optical fiber-based biosensors: reversible and nanoliter-scale measurement of zinc ions. *ACS Appl Mater Interfaces* 8:12727–12732. <https://doi.org/10.1021/acsami.6b03565>
404. Heng S, Reineck P, Vidanapathirana AK, Pullen BJ, Drumm DW, Ritter LJ, Schwarz N, Bonder CS, Psaltis PJ, Thompson JG, Gibson BC, Nicholls SJ, Abell AD (2017) Rationally designed probe for reversible sensing of zinc and application in cells. *ACS Omega* 2:6201–6210. <https://doi.org/10.1021/acsomega.7b00923>
405. Li T, He X, Yu P, Mao L (2015) A bioinspired light-controlled ionic switch based on nanopipettes. *Electroanalysis* 27:879–883. <https://doi.org/10.1002/elan.201400661>
406. Lerch MM, Hansen MJ, van Dam GM, Szymanski W, Feringa BL (2016) Emerging targets in photopharmacology. *Angew Chem Int Ed* 55:10978–10999. <https://doi.org/10.1002/anie.201601931>
407. Zeng S, Zhang H, Shen Z, Huang W (2021) Photopharmacology of proteolysis-targeting chimeras: a new frontier for drug discovery. *Front Chem* 9:639176. <https://doi.org/10.3389/fchem.2021.639176>
408. Ozhogin IV, Zolotukhin PV, Tkachev VV, Pugachev AD, Kozlenko AS, Belanova AA, Aldoshin SM, Lukyanov BS (2021) Synthesis and study of new indoline spiropyran and its derivative with α -lipoic acid exhibiting low cytotoxicity. *Russ Chem Bull* 70:1388–1393. <https://doi.org/10.1007/s11172-021-3228-x>
409. Ozhogin IV, Tkachev VV, Kozlenko AS, Pugachev AD, Lukyanova MB, Aldoshin SM, Minkin VI, Lukyanov BS (2021) Comparative structural study and molecular docking of indoline spiropyran containing α -lipoic acid fragment. *Dokl Chem* 498:104–111. <https://doi.org/10.1134/S0012500821060021>
410. Shinohara M, Ashikaga Y, Xu W, Kim S, Fukaminato T, Niidome T, Kurihara S (2022) Photochemical OFF/ON cytotoxicity switching by using a photochromic surfactant with visible light irradiation. *ACS Omega* 7:6093–6098. <https://doi.org/10.1021/acsomega.1c06473>
411. Webb B, Chimenti M, Jacobson M, Barber DJ (2011) Dysregulated pH: a perfect storm for cancer progression. *Nat Rev Cancer* 11:671–677. <https://doi.org/10.1038/nrc3110>
412. Barman S, Das J, Biswas S, Maitib TK, Pradeep SND (2017) A spiropyran–coumarin platform: an environment sensitive photoresponsive drug delivery system for efficient cancer therapy. *J Mater Chem B* 5:3940–3944. <https://doi.org/10.1039/C7TB00379J>
413. Hammarsen M, Andersson J, Li S, Lincoln P, Andréasson J (2010) Molecular AND-logic for dually controlled activation of a DNA-binding spiropyran. *Chem Commun* 46:7130–7132. <https://doi.org/10.1039/C0CC01682A>
414. Andersson J, Li S, Lincoln P, Andréasson J (2008) Photoswitched DNA-binding of a photochromic spiropyran. *J Am Chem Soc* 130:11836–11837. <https://doi.org/10.1021/ja801968f>
415. Rastogi SK, Zhao Z, Gildner MB, Shoulders BA, Velasquez TL, Blumenthal MO, Wang L, Li X, Hudnall TW, Betancourt T, Du L, Brittain WJ (2021) Synthesis, optical properties and in vitro cell

- viability of novel spiropyran and their photostationary states. *Tetrahedron* 80:131854. <https://doi.org/10.1016/j.tet.2020.131854>
416. Rad JK, Mahdavian AR, Khoei S, Shirvalilou S (2018) Enhanced photogeneration of reactive oxygen species and targeted photothermal therapy of C6 glioma brain cancer cells by folate-conjugated gold-photoactive polymer nanoparticles. *ACS Appl Mater Interfaces* 10:19483–19493. <https://doi.org/10.1021/acsami.8b05252>
417. Jonsson F, Beke-Somfai T, Andréasson J, Nordén B (2013) Interactions of a photochromic spiropyran with liposome model membranes. *Langmuir* 29:2099–2103. <https://doi.org/10.1021/la304867d>
418. Son S, Shin E, Kim B-S (2014) Light-responsive micelles of spiropyran initiated hyperbranched polyglycerol for smart drug delivery. *Biomacromol* 15:628–634. <https://doi.org/10.1021/bm401670t>
419. Ghani M, Heiskanen A, Thomsen P, Alm M, Emnéus J (2021) Molecular-gated drug delivery systems using light-triggered hydrophobic-to-hydrophilic switches. *ACS Appl Bio Mater* 4:1624–1631. <https://doi.org/10.1021/acsabm.0c01458>
420. Sana B, Finne-Wistrand A, Pappalardo D (2022) Recent development in near infrared light-responsive polymeric materials for smart drug-delivery systems. *Mater Today Chem* 25:100963. <https://doi.org/10.1016/j.mtchem.2022.100963>
421. Catania R, Onion D, Russo E, Zelzer M, Mantovani G, Huett A, Stolnik S (2022) A mechanoreponsive nano-sized carrier achieves intracellular release of drug on external ultrasound stimulus. *RSC Adv* 12:16561–16569. <https://doi.org/10.1039/D2RA02307E>
422. Avagliano D, Sánchez-Murcia PA, González L (2020) Spiropyran meets guanine quadruplexes: isomerization mechanism and DNA binding modes of quinolizidine-substituted spiropyran probes. *Chemistry* 26:13039–13045. <https://doi.org/10.1002/chem.202001586>
423. Velema WA, Hansen MJ, Lerch MM, Driessen AJM, Szymanski W, Feringa BL (2015) Ciprofloxacin-photoswitch conjugates: a facile strategy for photopharmacology. *Bioconjug Chem* 26:2592–2597. <https://doi.org/10.1021/acs.bioconjchem.5b00591>
424. Luo Y, Wang C, Peng P, Hossain M, Jiang T, Fu W, Liao Y, Su M (2013) Visible light mediated killing of multidrug-resistant bacteria using photoacids. *J Mater Chem B* 1:997–1001. <https://doi.org/10.1039/C2TB00317A>
425. Ishikawa H, Uemura N, Saito R, Yoshida Y, Mino T, Kasashima Y, Sakamoto M (2019) Chiral symmetry breaking of spiropyrans and spirooxazines by dynamic enantioselective crystallization. *Chem Eur J* 25:9758–9763. <https://doi.org/10.1002/chem.201901889>

Publisher's Note Springer Nature remains neutral with regard to jurisdictional claims in published maps and institutional affiliations.

Springer Nature or its licensor (e.g. a society or other partner) holds exclusive rights to this article under a publishing agreement with the author(s) or other rightsholder(s); author self-archiving of the accepted manuscript version of this article is solely governed by the terms of such publishing agreement and applicable law.

Authors and Affiliations

Anastasia S. Kozlenko¹  · Ilya V. Ozhogin¹ · Artem D. Pugachev¹ ·
Maria B. Lukyanova¹ · Islam M. El-Sewify^{1,2} · Boris S. Lukyanov¹

✉ Anastasia S. Kozlenko
anastasiya.kozlenko@gmail.com

¹ Institute of Physical and Organic Chemistry, Southern Federal University, Stachki Prosp., 194/2, Rostov-On-Don 344090, Russia

² Department of Chemistry, Faculty of Science, Ain Shams University, Cairo, Egypt